1341

Université de Neuchâtel
Institut de Physique

Aspects of Quantum Chaos and Disordered Interacting Systems

Tirés à part d'articles composant une forme réduite de la

Thèse

présentée à la Faculté des Sciences
pour obtenir le titre de Docteur ès sciences
par

Philippe Jacquod

Physicien Diplômé de l'Ecole Polytechnique Fédérale de Zürich

Neuchâtel, Mars 1997

Jury :

Prof. J.-P. Amiet	Directeur de thèse
Dr. D. L. Shepelyansky	Codirecteur de thèse
Prof. M. Büttiker	
Prof. J.-P. Derendinger	

IMPRIMATUR POUR LA THÈSE

Aspects of quantum chaos and disordered interacting systems

de M. Philippe Jacquod

UNIVERSITÉ DE NEUCHÂTEL

FACULTÉ DES SCIENCES

La Faculté des sciences de l'Université de Neuchâtel sur le rapport des membres du jury,

MM. J.-P. Amiet (directeur de thèse),
J.-P. Derendinger, M. Büttiker (Genève)
et D.L. Shepelyansky (Toulouse)

autorise l'impression de la présente thèse.

Neuchâtel, le 24 mars 1997

Le doyen:

R. Dändliker

R. Dändliker

Liste des articles inclus en tirés à part:

1. *Evidence for the Validity of the Berry-Robnik Surmise in a Periodically Pulsed Spin System,*
   Ph. Jacquod and J.-P. Amiet, *J. Phys. A : Math. Gen.* **28**, *4799, (1995).*

2. *Hidden Breit-Wigner Distribution and Other Properties of Random Matrices with Preferential Basis,*
   Ph. Jacquod and D. Shepelyansky, *Phys. Rev. Lett.* **75**, *3501, (1995).*

3. *Double Butterfly Spectrum for Two Interacting Particles in the Harper Model,*
   A. Barelli, J. Bellissard, Ph. Jacquod and D. Shepelyansky, *Phys. Rev. Lett.* **77**, *4752, (1996).*

4. *Breit-Wigner Width for Two Interacting Particles In Random Potential,*
   Ph. Jacquod, D. Shepelyansky and O. Sushkov, *Phys. Rev. Lett.* **78**, *923, (1997).*

5. *On the Convergence to Ergodic Behaviour of Quantum Wave Functions,*
   Ph. Jacquod and J.-P. Amiet, accepté pour publication dans *J. Phys. A : Math. Gen., (1997).*

6. *Two Interacting Hofstadter Butterflies,*
   A. Barelli, J. Bellissard, Ph. Jacquod and D. Shepelyansky, accepté pour publication dans *Phys. Rev. B* **55**, *(1997).*

Un exemplaire de la version complète de la présente thèse a été déposé à la bibliothèque de l'Université de Neuchâtel.

NEIP-95-003 March 1995

Evidence for the Validity of the Berry-Robnik Surmise in a Periodically Pulsed Spin System

Ph. Jacquod [1] and J.-P. Amiet[2]

Institut de Physique
Université de Neuchâtel
1, Rue A.L. Breguet
CH - 2000 Neuchâtel

[1]e-mail jack@iph.unine.ch
[2]e-mail amiet@iph.unine.ch

Abstract

We study the statistical properties of the spectrum of a quantum dynamical system whose classical counterpart has a mixed phase space structure consisting of two regular regions separated by a chaotical one. We make use of a simple symmetry of the system to separate the eigenstates of the time-evolution operator into two classes in agreement with the Percival classification scheme [2]. We then use a method firstly developed by Bohigas et. al. [3] to evaluate the fractional measure of states belonging to the regular class, and finally present the level spacings statistics for each class. The level spacings distribution of states belonging to the irregular part of the spectra as well as that of the complete set of levels corroborate the Berry-Robnik surmise [6]. We further present a statistical study of the regular levels. The presence of intermediate states - states which belong to neither class as long as $\hbar$ is finite, phase spatially mixed among the set of regular ones, together with the small fractional measure of regular states strongly affects the corresponding level spacings statistics, resulting in a non negligible deviation from the expected Poisson distribution. We see however the remarkable agreement of the irregular level spacings statistics as a direct confirmation of the Berry-Robnik surmised.

1 Introduction

For more than a decade, the study of quantum mechanical systems whose classical counterpart exhibits chaos has attracted much interest. One motivation for this study is the paradoxical fact that while the correspondence principle, as we understand it, should imply a quantum manifestation of classical chaos, the Schrödinger equation is linear. As a consequence, the time-evolution operator is unitary, and this suppresses any exponential divergence in the time evolution of quantum states. As a spectacular manifestation of this fact, time-reversal invariant models show no lost of memory : reversing the time at a certain moment T brings us back to the initial situation after another time interval T, while this would require infinite precision in a classical chaotic system. Thus a basic manifestation of classical chaos seems to have no place in quantum mechanics.
On the other hand, the destruction of an integral of motion, of a quantum number, has striking effects on the statistical properties of quantum spectras. It is today taken as granted that in a classically integrable system, the levels are uncorrelated, and so have a poissonian level spacings distribution [4] (a remarkable exception being the one-dimensional harmonic oscillator) and that in classically fully chaotic models, the level spacings distribution has a dramatically different shape : it obeys predictions of random matrix theory, i.e. it exhibits level repulsion [1]. The situation in mixed systems, where regular and chaotic regions coexist in the classical phase space, is more intricated. In an old paper Percival [2] classified the eigenfunctions of the Schrödinger equation into two classes belonging to either the regular regions, where the invariant tori are not destroyed, or the chaotic one. This classification was based mostly on the correspondence principle and has been numerically confirmed a few years ago by Bohigas et. al. [3]. While the eigenfunctions that are mostly confined on classically regular regions - we will call them the regular eigenfunctions - tend to concentrate on invariant tori, the irregular ones tend to spread uniformly over the chaotic region as $\hbar \to 0$, as has been rigorously demonstrated by Shnirelman [12]. This picture is assumed to reflect reality in the semiclassical limit $\hbar = 0$. Following this classification, Berry and Robnik postulated that the part of the spectrum that corresponds to regular eigenfunctions, has a poissonian level spacings distribution in opposition to the one corresponding to the irregular eigenstates which exhibits level repulsion [6]. This surmise led them to an expression for the level spac-

ings distribution for mixed systems that has been observed convincingly only recently [7] for the case of the kicked rotator on a torus. As pointed out by Prosen & Robnik and Li & Robnik [8] [13], reasons for this difficulty of observation could be that we are not deep enough in the semi-classical regime. As long as $\hbar$ is finite, a certain number of wave-functions belong neither to the regular nor to the irregular set of eigenfunctions. We may think of states making use of the Heisenberg uncertainty to overlap the frontier between the regular and irregular regions of the classical phase space, or states located on the regular region which, due to the finiteness of the Planck constant, do not yet belong to the set of regular states. Consequently, the Berry-Robnik regime should be observable only in the far semiclassical limit. We will come back to this point later.

In this paper we present a spin model allowing a precise study of a mixed regime. The reasons for this are first that, in a special regime, an approximate simple symmetry of the phase space structure, namely $S_z \rightarrow -S_z$, allows the separation of regular states from the irregular ones, and secondly that the frontier between the regular and the chaotic zones is rather sharp, thus minimizing the number of intermediate eigenstates. This enables us to compute the level spacings statistics independently for the regular and irregular states. We interpret the fact that these statistics obey quite well the poissonian distribution and the GOE respectively as a direct confirmation of the Berry-Robnik surmise.

We study the quantum system defined by the following Hamiltonian [3]:

$$\mathbf{H}_{qm} := \frac{m}{2}((1-z^2)\mathbf{S}_z^2 - z^2\mathbf{S}_x^2) + \kappa \mathbf{S}_z \Delta_T \tag{1}$$

and the corresponding unitary time evolution operator :

$$\mathbf{U}_T := \exp(-\frac{i}{\hbar}\kappa \mathbf{S}_z)\exp(-\frac{i}{\hbar}\frac{m}{2}((1-z^2)\mathbf{S}_z^2 - z^2\mathbf{S}_x^2)T) \tag{2}$$

where $\vec{\mathbf{S}} = (\mathbf{S}_x, \mathbf{S}_y, \mathbf{S}_z) = \hbar(\mathrm{s}_x, \mathrm{s}_y, \mathrm{s}_z) = \hbar\vec{s}$ are spin operators satisfying the usual commutation rules (ϵ^{ijk} is the total antisymmetric tensor of 3^{rd} order):

$$[\mathbf{S}_i, \mathbf{S}_j] = i\hbar\epsilon^{ijk}\mathbf{S}_k \tag{3}$$

[3] We use bold characters in the quantum case in contrast to normal ones which refer to the classical and semiclassical cases : $\vec{\mathbf{S}}$ refers to the quantum spin operator while $\vec{S}$ is either a classical or a semiclassical spin.

$0 \leq \kappa \leq 2\pi$, $\Delta_T := \sum_{n=-\infty}^{+\infty} \delta(t - nT)$, $[m] = \text{energy}^{-1}\ \text{time}^{-2}$ and $0 \leq z \leq 1$. Models of this kind have been extensively studied [11]. They represent a spin which evolves under the influence of a classically integrable Hamiltonian $\mathbf{H}^0_{qm} = \frac{m}{2}((1-z^2)\mathbf{S}_z^2 - z^2\mathbf{S}_x^2)$ during a time T after which the spin undergoes a rotation of angle κ around the z-axis. The regime we consider is defined by $\kappa = 1.1$, $T = \frac{19}{mS}$ and $z^2 = \frac{1}{2}$. Classically there are two regular zones around the north and south poles surrounding a chaotic region which is fairly well symmetric under S_z reflection (Fig.1). In the semiclassical limit which corresponds to $\hbar s = S = \text{constant}$, $\hbar = s^{-1} \to 0$, states which are located on the chaotic region tend to cover it homogeneously according to Shnirelman's theorem [12]. Since this region is symmetric under S_z reflection, the expectation value $< \Psi_{chaos}|\mathbf{s}_z|\Psi_{chaos} >$ of such a state tends to disappear as we approach the semi-classical limit. For small but finite $\hbar$, the distribution of $< \Psi_k|\mathbf{s}_z|\Psi_k >$, where $|\Psi_k >$ is an eigenstate of the operator $\mathbf{U}_T$ defined in (2), will then present a sharp peak around zero corresponding to the irregular states surrounded by two smaller bumps corresponding to regular states (Fig.2). This allows us to separate easily the regular states from the irregular ones, the validity of this selection being confirmed by a numerical semiclassical argument presented in section 3 as well as an extensive study of the Husimi distributions of the selected states [15].
The paper is organized as follows : Section 2 is devoted to a short presentation of the classical model. In section 3 we derive some useful semiclassical quantities such as the density of states and the expression for the action. This will allow us to estimate the number of regular states, and give a check of our selection criterion. In section 4 we present the quantum mechanical model as well as our numerical results for a spin magnitude s=500. All of them were obtained using direct diagonalization techniques. Conclusions and further remarks are given in section 5.

2 Classical model

The unperturbed classical Hamiltonian

$$H^0_{cl} := \frac{m}{2}((1-z^2)S_z^2 - z^2 S_x^2) \tag{4}$$

has one degrees of freedom and is an integral of motion. The trajectories are confined to the intersections of the sphere $|\vec{S}| = S$ with the cones of constant

energy $E = \frac{m}{2}((1-z^2)S_z^2 - z^2 S_x^2)$. The perturbation :

$$H_{cl}^1 := \kappa S_z \Delta_T \tag{5}$$

corresponds to a rotation of angle κ around the z-axis performed at time intervals T. Its addition leads to the destruction of the energy surfaces, and allows more and more trajectories to wander chaotically on the sphere of constant spin magnitude as κ and T grow. Expanding H_{cl}^0 up to the first order in $\delta S_z := S - S_z$ near the poles $S_z = \pm S$,we get a one-dimensional harmonic oscillator of period $T = 2\sqrt{2}\frac{\pi}{mS}$. In particular we have $\delta \dot{S}_z = O(\delta S_z^2)$: in this approximation δS_z is an integral of motion and is furthermore conserved by the perturbation H_{cl}^1 too. It is thus conceivable that the invariant torii near the poles will offer more resistance to the perturbation than those located away from them. We use this property to find a regime in which there are two regular islands around the poles approximately related by the operation $S_z \rightarrow -S_z$ and separated by a chaotic region. This we achieved by setting $\kappa = 1.1, T = \frac{19}{mS}, z^2 = 0.5$ (Fig.1). The regular islands occupy in a good approximation the region $0.22S^2 \leq E \leq E_{max} = 0.25S^2$.

3 Semiclassical approach

We compute the Green function for a trajectory of positive energy and the density of states for the unperturbed case $T = \frac{19}{mS}, z^2 = 0.5$. We follow the lines drawn in [9]. We first write the unperturbed Hamiltonian in canonical variables (S_z, ϕ) for the chosen regime :

$$H_0 = \frac{m}{4}(S_z^2(1+\cos^2(\phi)) - \vec{S}^2\cos^2(\phi)) \tag{6}$$

The action integral for a trajectory of energy E starting at ϕ_0 and ending at ϕ reads ($\vec{S} = \hbar\vec{s}$, $e = \frac{E}{\hbar^2 m}$):

$$\mathcal{S}_\beta(\phi_0, \phi, e) = \hbar\left[\int_{\phi_0}^{\phi^*}\sqrt{\frac{4e + s^2\cos^2(\phi')}{1+\cos^2(\phi')}}d\phi' + n_\beta\int_0^{2\pi}\sqrt{\frac{4e + s^2\cos^2(\phi')}{1+\cos^2(\phi')}}d\phi'\right] \tag{7}$$

where we have set $\phi^* = \phi_0 + (\phi - \phi_0) \bmod 2\pi$, and n_β is the number of complete revolutions accomplished between ϕ_0 and ϕ ($\phi = 2\pi n_\beta + \phi*$). The

sum runs over classical orbits β of constant energy. This leads us to the expression for the corresponding Green function :

$$\begin{aligned} \mathcal{G}(\phi_0,\phi,e) &= -\frac{i}{\hbar}\sum_\beta \sqrt{|\det \mathcal{D}_{1,\beta}(\phi_0,\phi)|}\exp(\frac{i}{\hbar}\mathcal{S}_\beta(\phi_0,\phi,e)-\frac{i\pi}{2}l_\beta) \\ &=: \sum_n \frac{\psi_n^*(\phi)\psi_n(\phi_0)}{(E-E_n+i\epsilon)} \end{aligned} \tag{8}$$

with

$$\det \mathcal{D}_{1,\beta}(\phi_0,\phi) = \frac{1}{m^2}\left(\frac{\partial^2\mathcal{S}_\beta}{\partial\phi\partial\phi_0}\frac{\partial^2\mathcal{S}_\beta}{\partial e^2}-\frac{\partial^2\mathcal{S}_\beta}{\partial\phi\partial e}\frac{\partial^2\mathcal{S}_\beta}{\partial\phi_0\partial e}\right) = \frac{-4}{m^2\sqrt{(4e+s^2\cos^2(\phi_0))(1+\cos^2(\phi_0))(4e+s^2\cos^2(\phi))(1+\cos^2(\phi))}} \tag{9}$$

this result being obtained by partial differentiations of (7). Since this latter value never changes sign, the Maslov index l_β vanishes and so the divergence of the Green function leads to the following semiclassical quantization condition :

$$\int_0^{2\pi}\sqrt{\frac{4e+s^2\cos^2(\phi')}{1+\cos^2(\phi')}}d\phi' = 2\pi M \tag{10}$$

for any integer $0 \le M \le s$. We have then for the averaged density of states (N is the number of states) :

$$\begin{aligned} \overline{\rho}(e) &= -\frac{1}{N\pi}Im\left[\int_0^{2\pi}d\phi\mathcal{G}(\phi,\phi,e)\right] \\ &= \frac{1}{\pi\hbar}\int_0^{2\pi}d\phi\sqrt{|\det \mathcal{D}_{1,\beta}(\phi,\phi)|} \\ &= \frac{2}{\pi\hbar m}\int_0^{2\pi}\frac{d\phi}{\sqrt{(4e+s^2\cos^2(\phi))(1+\cos^2(\phi)))}} \end{aligned} \tag{11}$$

The last equation states in particular that the averaged density of states is proportional to the classical orbit period. Fig. 3 shows the agreement of this semiclassical result with the numerically obtained density of states for the unperturbed quantum model at s=1000. Using (11) we estimate the number of states occupying the regular region of figure 1 :

$$N_{reg} \approx \int_{0.22s^2}^{0.25s^2}\overline{\rho}(e)de \approx \frac{1}{24}(2s+1) \tag{12}$$

The number of states occupying this region in absence of perturbation is $\frac{1}{24}$ times the total number of states. This gives us a first approximation for the number of regular states we must select. A better approximation in presence of perturbation is given using a method developed by Bohigas et. al. [3]. We must evaluate the number N_{reg} of trajectories that satisfy the condition :

$$\sum_{i=0}^{P}\left[\int_{\phi_i^+}^{\phi_i^-} s_z(\phi')d\phi' + s_z(\phi_i^+)\kappa\right] = 2\pi M \tag{13}$$

for some integers M and P, while it nearly closes on itself after the P^{th} kick, i.e. : $s_z(\phi_M^+) \approx s_z(\phi_0^+)$. ϕ_i^- is the angle between the x and the y component of the spin just before the i^{th} kick while ϕ_i^+ refers to the same angle right after this kick.
This condition means that the action integral must still be an integer multiple of 2 π, and that simultaneously, the orbit must be closed. This condition has meaning only on regular regions were the invariant torii are not destroyed, so that the integrals make sense. We transform this condition and compute the number of trajectories satisfying :

$$\frac{\sum_{i=0}^{P}\left[\int_{\phi_i^+}^{\phi_{i+1}^-} s_z(\phi')d\phi' + s_z(\phi_i^+)\kappa\right]}{\kappa P + \sum_{i=1}^{P}\left(\phi_i^- - \phi_{i-1}^+\right)} \approx M \tag{14}$$

for integers M and P, and P sufficiently large. With this we replace two conditions by only one numerically more tractable condition. Since our task is to evaluate the number of regular semiclassical levels, and not to determine them precisely, we believe that condition (14) is sufficient. The number of regular states we numerically estimated with (14) is 50 $\pm$ 4 for s=500, i.e. slightly larger than that estimated with (12). In the next section, we will consider this estimated number of regular states as a check of the validity of our selection criterion.

4 Quantum Model

In this section we study the statistical properties of the spectrum of the quantum Hamiltonian (1) for integer spin magnitude. Since the perturbation term is time-dependent, the energy is no longer a good quantum number,

and we are led to define quasi-energies and quasi-energy eigenstates. The Schrödinger equation leads to the following time evolution from right after a kick to right after the next one:

$$\Psi(T^+) = \mathbf{U}_T \Psi(0^+) = \exp(-\frac{i}{\hbar}\kappa \mathbf{S}_z) \exp(-\frac{i}{\hbar}\mathbf{H}^0_{qm} T)\Psi(0^+) \tag{15}$$

Quasi-energies λ and quasi-energy eigenstates Ψ_λ are then defined by :

$$\mathbf{U}_T \Psi_\lambda = \exp(-i\lambda)\Psi_\lambda \tag{16}$$

Since $\mathbf{U}_T$ is unitary, the λ's are real and defined modulo $2\,\pi$. We introduce two parities :

$$\mathbf{\Pi}|\mu> = |-\mu> \tag{17}$$

$$\mathbf{\Theta}|\mu> = (-1)^{s-\mu}|\mu> \tag{18}$$

We can express the time-reversal operator $\mathbf{T}$ in term of these two parity operators :

$$\mathbf{\Pi} \circ \mathbf{\Theta}|\mu> = \mathbf{T}|\mu> = (-1)^{s-\mu}|-\mu> \tag{19}$$

In the integer spin case the eigenstates $|\Psi>$ of $\mathbf{U}^0_T := \exp(-\frac{i}{\hbar}\mathbf{H}^0_{qm}T)$ satisfy the conditions :

$$\mathbf{\Pi}|\Psi> = \pm|\Psi> \tag{20}$$

$$\mathbf{\Theta}|\Psi> = \pm|\Psi> \tag{21}$$

So $\mathbf{H}^0_{qm}$ and $\mathbf{U}^0_T$ are in particular time-reversible. The perturbation breaks the $\mathbf{\Pi}$-parity but leaves the $\mathbf{\Theta}$-parity unbroken [4]. We will concentrate on the study of even states, i.e. those states satisfying :

$$\mathbf{\Theta}|\Psi> = |\Psi> \tag{22}$$

However partial results obtained for the odd set of states corroborate the results presented here. The key point is now to find a clear quantum manifestation of the approximate symmetry $S_z \to -S_z$ of the classical phase space

[4] In the half-integer spin case, eigenstates of the unperturbed time-evolution operator are eigenstates of the Θ-parity only. The latter is left unbroken by the perturbation we consider.

structure. A practical solution is given by Shnirelman's theorem which states that in the semiclassical limit, the quantum states that are confined on the classically chaotic region of the phase space tend to cover it uniformly. To get an insight in this statement we use the following resolution of unity [14]

$$1 = \frac{2s+1}{\pi} \int d\theta d\phi \sin\theta |\theta, \phi >< \theta, \phi| \tag{23}$$

where we introduced coherent states of the spin $SU(2)$ group :

$$|\theta, \phi >:= \sum_{\mu=-s}^{s} \sqrt{\binom{2s}{s-\mu}} \sin(\frac{\theta}{2})^{s-\mu} \cos(\frac{\theta}{2})^{s+\mu} e^{i(s-\mu)\phi} |\mu >$$

These are states that are centered on the point (θ, ϕ) of the sphere and which minimalize the quantum uncertainty. θ is defined by $S_z = S\cos(\theta)$. Using (22), the symmetry of the chaotical region and Shnirelman's theorem [12] :

$$< \Psi_{chaos}|\theta, \phi > \longrightarrow \begin{cases} 0 & \text{on the regular region} \\ const & \text{on the chaotic region} \end{cases} \tag{24}$$

it is then easy to show that

$$< \Psi_{chaos}|s_z|\Psi_{chaos} > \rightarrow 0 \tag{25}$$

in the semiclassical limit. This translates into Fig.2 where we plotted an histogram of the expectation value of s_z taken over quasi-energy eigenfunctions for s=500, $\kappa = 1.1$, z^2=0.5, and m=1. The central peak clearly reflects our reasoning, while the two smaller bumps surrounding it are mainly due to the regular states that are confined to the classical stability islands. The gap in-between is a consequence of the uniform distribution of irregular states. It is remarkable that this gap overlaps the classical frontier between regular and chaotic region.

We used this property to part the irregular states from the regular ones and then study separately the statistical properties of the spectrums of each class of states. We believe this criterion is justified since the fluctuations

$$\Delta s_z = \sqrt{< s_z^2 > - < s_z >^2} \tag{26}$$

of regular states is much smaller than the "Shnirelman gap" appearing in the histogram of Fig. 2 between the huge central peak and the smaller

bumps. As a consequence only very few regular levels will be selected with the set of irregular ones, while maybe more irregular will be counted with the regular ones. Moreover, the fact that the number of selected regular states is in complete agreement with the numerical semiclassical evaluation given by (14) confirms the relevance of this selection criterion.

We now turn our attention to the study of the spectral properties of the time-evolution operator (16). Due to the Θ-symmetry (18), $\mathbf{U}_T$ belongs to the circular orthogonal ensemble, and not to the circular unitary ensemble as would be expected from the fact that the perturbation breaks the time-reversal symmetry. This situation is similar to the one encountered by Berry & Robnik in certain Aharonov-Bohm billiards [5], or by Delande & Gay in the Hydrogen atom in a magnetic field [10] where the system violates the time-reversal symmetry, but possesses an invariance under a combination of the time-reversal and another symmetry, in our case the $\mathbf{\Pi}$-symmetry. We thus expect a linear repulsion for the part of the spectrum belonging to the irregular states.

The results of our study for a spin magnitude s=500 are plotted in Fig. 4 to 9. Fig. 4 shows a plot of the level spacings statistics for 4233 irregular level spacings computed by diagonalizing ten different evolution matrices for $T = \frac{19}{mS}$ and $1.05 \leq \kappa \leq 1.15$. The solid line is the predicted Wigner distribution. The agreement is excellent. In Fig. 5 we plotted the corresponding cumulative level spacings distribution defined in term of the level spacings distribution [5] $P(\underline{s})$ by

$$W(\underline{s}) = \int_0^{\underline{s}} dt P(t) \tag{27}$$

Also shown are the Poisson and the Wigner distributions. As shown in inset, small deviations from the Wigner distribution appear only around spacings $\underline{s} \approx 2$, but have no significance to our opinion.

Fig.6 and 7 show the level spacings and the cumulative level spacings distribution for 572 regular levels taken from twenty different evolution matrices for $T = \frac{19}{mS}$ and $1.05 \leq \kappa \leq 1.15$. The difficulty here is the relatively small number of regular states (≈ 25). Accordingly, only few intermediate or irregular states can have relatively big effects on the statistics. In a convenient

[5] We have used $\underline{s}$ for the level spacings to avoid confusion with the spin magnitude.

basis, $\mathbf{U}_T$ can be represented by the following matrix :

$$\mathbf{U}_T := \begin{pmatrix} R & K \\ K & C \end{pmatrix} \tag{28}$$

$R = R_i\delta_{i,j}$ is a diagonal $N_{reg} \times N_{reg}$ matrix which corresponds to the N_{reg} regular states, $C = C_i\delta_{i,j}$ is a diagonal $N_{chaos} \times N_{chaos}$ matrix which corresponds to the N_{chaos} irregular states, and $K = O(\hbar)$ couples the two subspaces as long as $\hbar$ is finite. In our picture K disappears in the semiclassical limit, and the R_i and C_i satisfy a poissonian statistics and a GOE statistics respectively. It would be of course a hopeless task to try to determine K for finite $\hbar$. The important point is to recognize that as long as $\hbar$ is finite but small enough, K couples only few regular states with irregular ones, this fact resulting in a deviation from the Berry-Robnik surmise. This deviation is then naturally much more important for the regular part of the spectrum, since it contains much fewer levels than the irregular part. We believe that this is the reason for the deviation of the statistics of the set of levels we have selected as regular from the poissonian predicted behaviour. We must recall that our whole reasoning is based on the assumption of two classically homogeneous stability islands. In such a case, semiclassical wave-function would mimic classical orbits and would therefore fit together as concentric circles. The presence of hyperbolic fixed points or cantori may change this picture, possibly turning regular states into intermediate ones as long as $\hbar$ is finite. The semiclassical wave-function overlap and thus interact at certain regions, and this, in the Pechukas picture [1], modify very sensibly the equations of motions governing the evolution of the quasi-energies λ as κ or T is modified, resulting in the appearance of level repulsion. So some intermediate states are phase spatially mixed among the set of states we have selected as regular and consequently modify the corresponding statistics. Their effect is furthermore enhanced by the small ratio of regular levels. A current investigation of the Husimi densities of the selected regular states corroborates this reasoning [15]. Finally we show in Fig.8 and 9 level spacings and cumulative level spacings statistics for the complete set of levels. We compare our results with the Berry-Robnik prediction for a fractional measure of regular states as approximated by (12). The agreement is amazing, and corroborates our picture. The χ^2-test for both graphs - χ^2=25, i.e. half the number of boxes for Fig.8, and χ^2=1480, i.e. 3.3 times less than the number of levels for Fig.9

- gives full statistical significance to these last graphs. We see them as a good evidence for the validity of the Berry-Robnik surmise in our model.

5 Conclusion

We studied the statistical properties of a quantum spin model whose classical counterpart exhibits a mixed phase space configuration. Due to a simple approximate symmetry, whose effect on the quantum system is drastically enhanced by Shnirelman's theorem, we were able to separate the irregular from the regular levels, thereby confirming implicitely the validity of the Percival classification. We then performed a separated statistical study of these levels. The results confirm the Berry-Robnik surmise : while the irregular set of quasienergies exhibits a clear wigner-like shape, the regular part of the spectrum has a clearly different shape, though its spacings distribution does not follow strictly a poissonian law. This deviation is interpreted as the presence of both irregular and intermediate states among the selected regular ones, their effect being enhanced by the relatively small number of the latter. Nevertheless, due to the small number of regular states we believe that the irregular statistics is much more significant, and see our results as a good confirmation of the validity of the Berry-Robnik surmise in our model.

Acknowledgements

One of us (P.J.) gratefully acknowledges fruitfull discussions with J. Bellissard, C. Rouvinez and D. Shepelyansky , as well as the hospitality of the theoretical physics division of the "Laboratoire de Physique Quantique, Université Paul Sabatier" in Toulouse extended to him during his visit when part of this work has been done. We are grateful to T. Prosen for having drawn our attention on reference [7]. Work supported by the Swiss National Science Foundation.

References

[1] Pechukas P., Phys. Rev. Lett. **51**, 943, (1983)

Bohigas O., Giannoni M.-J. and Shmit C., Phys. Rev. Lett. **52**, 1, (1984)

[2] Percival I.C., J. Phys. B **6**, L229, (1973)

[3] Bohigas O., Tomsovic S. and Ullmo D., Phys. Rev. Lett. **64**, 1479, (1990)

[4] Berry M.V. and Tabor M., Proc. Roy. Soc. A **356**, 375, (1977)

[5] Berry M.V. and Robnik M., J. Phys. A: Math. Gen. **19**, 669, (1986)

[6] Berry M.V. and Robnik M., J. Phys. A: Math. Gen. **17**, 2413, (1984)

[7] Prosen T. and Robnik M., J. Phys. A : Math. Gen. **27**, L459, (1994)

[8] Prosen T. and Robnik M., J. Phys. A : Math. Gen. **27**, 8059, (1994)

[9] Reichl L. E., The Transition to Chaos in Conservative Classical System Quantum Manifestation, Springer, (1992)

[10] Delande D. and Gay J. C., Phys. Rev. Lett. **57**, 2006, (1986)

[11] Nakamura K., Okazaki Y. and Bishop A.R.,

Phys. Rev. Lett. **57**, 5,(1986)

Kus M., Sharf R. and Haake F., Z. Phys. B **65**, 381, (1987)

Kus M., Sharf R. and Haake F., Z. Phys. B **66**, 129, (1987)

Nakamura K., Bishop A.R. and Shudo A., Phys. Rev. B **39**, 12422, (1989)

Kus M., Haake F. and Eckhardt B., Z. Phys. B **92**, 221, (1993)

Schach R., D'Ariano G. and Caves C., Phys. Rev. E **50**, 972, (1994)

Fox R. F. and Elston T. C., Phys. Rev. E **50**, 2553, (1994)

[12] This is a weak convergence. As $\hbar \to 0$, the Husimi density of such a state tends to a constant over the classically irregular region in the sense of a distribution. See the addendum of A.I. Shnirelman in : KAM Theory and Semiclassical Approximations to Eigenfunctions, V.F Lazutkin, Springer (1993).

[13] Baowen Li and Marko Robnik, Preprint CAMTP/94-10 "Separating the regular and irregular energy levels and their statistics in Hamiltonian system with mixed classical dynamics " and Preprint CAMTP/94-11 "Supplement to the paper : Separating the regular and irregular energy levels and their statistics in Hamiltonian system with mixed classical dynamics " , to be published in J. Phys. A : Math. Gen.

[14] Perelomov A., Generalized Coherent States and Their Applications, Springer (1986).

[15] Amiet J.-P. & Jacquod Ph., in preparation.

Figure Captions

Fig.1: Orthogonal projection of the classical phase space on the (S_x,S_y) plane for the case T=$\frac{19}{mS}$, $\kappa = 1.1$ and z^2=0.5.

Fig.2: Histogram of the expectation value of S_z taken over the eigenstates of the unitary time evolution operator defined in (2).

Fig.3: Density of states for the unperturbed Hamiltonian according to (11) (solid line) as compared to numerically obtained datas for tbe case s=1000 (squares).

Fig.4: Level spacings distribution for 4233 irregular level spacings obtained through direct diagonalization of ten evolution matrices in the parameter range $T = \frac{19}{mS}$ and $1.05 \leq \kappa \leq 1.15$.

Fig.5: Cumulative level spacings distribution for the same case as fig.4. In inset : regions of small deviation relatively to the Wigner-distribution.

Fig.6: Level spacings distribution for a set of 472 regular level spacings obtained through direct diagonalization of twenty evolution matrices in the parameter range $T = \frac{19}{mS}$ and $1.095 \leq \kappa \leq 1.105$. The solid line is the predicted Poisson distribution.

Fig.7: Cumulative level spacings distribution for the same levels as Fig.6 compared to the Poisson distribution.

Fig.8: Level spacings distribution for a set of 5000 regular and irregular level spacings obtained through direct diagonalization of ten evolution matrices in the parameter range $T = \frac{19}{mS}$ and $1.095 \leq \kappa \leq 1.105$. The solid line is the predicted Berry-Robnik distribution with fractional measure of regular states $\rho_1 = 0.08$. χ^2=25 is half the number of boxes.

Fig.9: Cumulative level spacings distribution for the same levels as Fig.8 compared to the poissonian and the Berry-Robnik predicted distribution. In inset : Same curve compared to the Wigner distribution. χ^2=1480 is 3.3 times less than the number of levels.

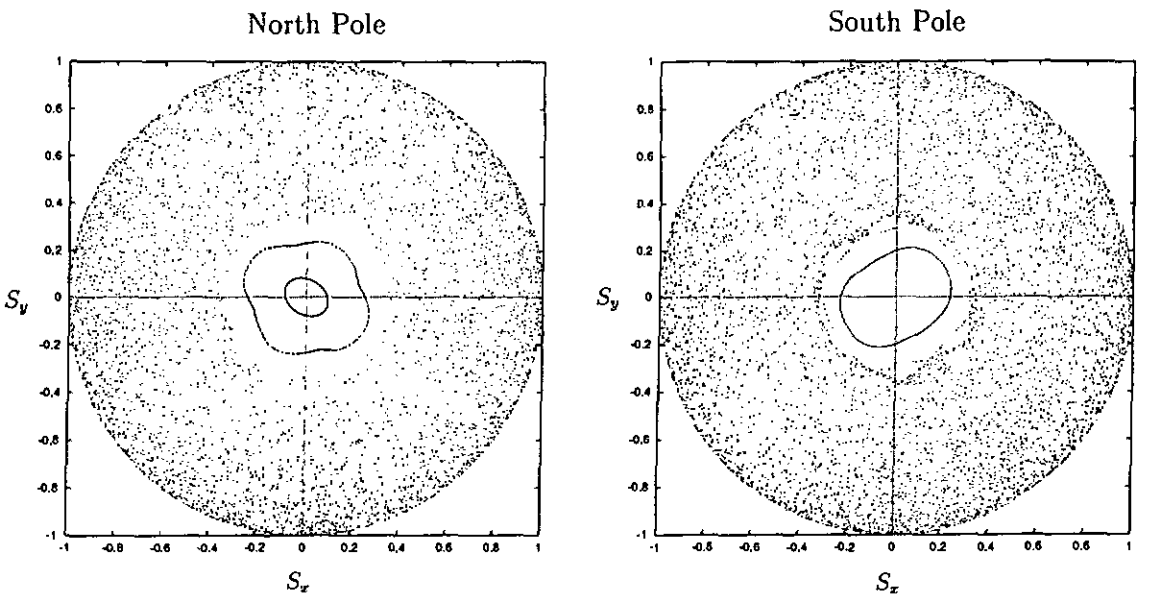

Figure 1

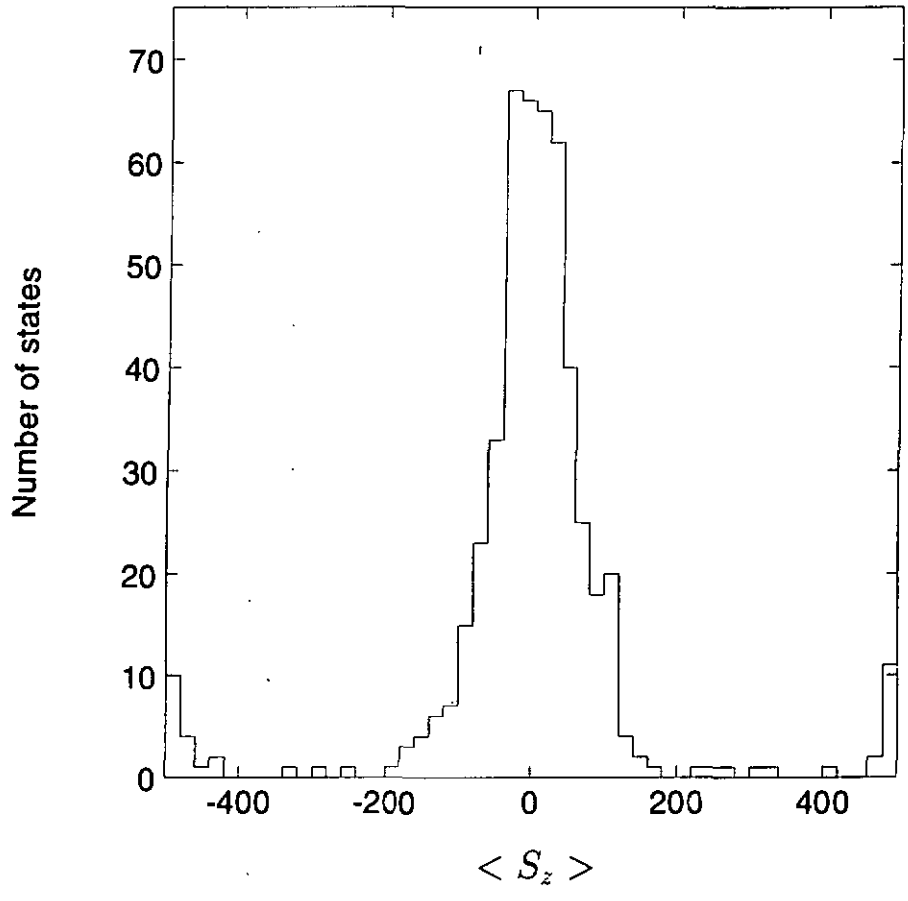
Number of states
70
60
50
40
30
20
10
0
-400
-200
0
200
400
< S_z >
Figure 2

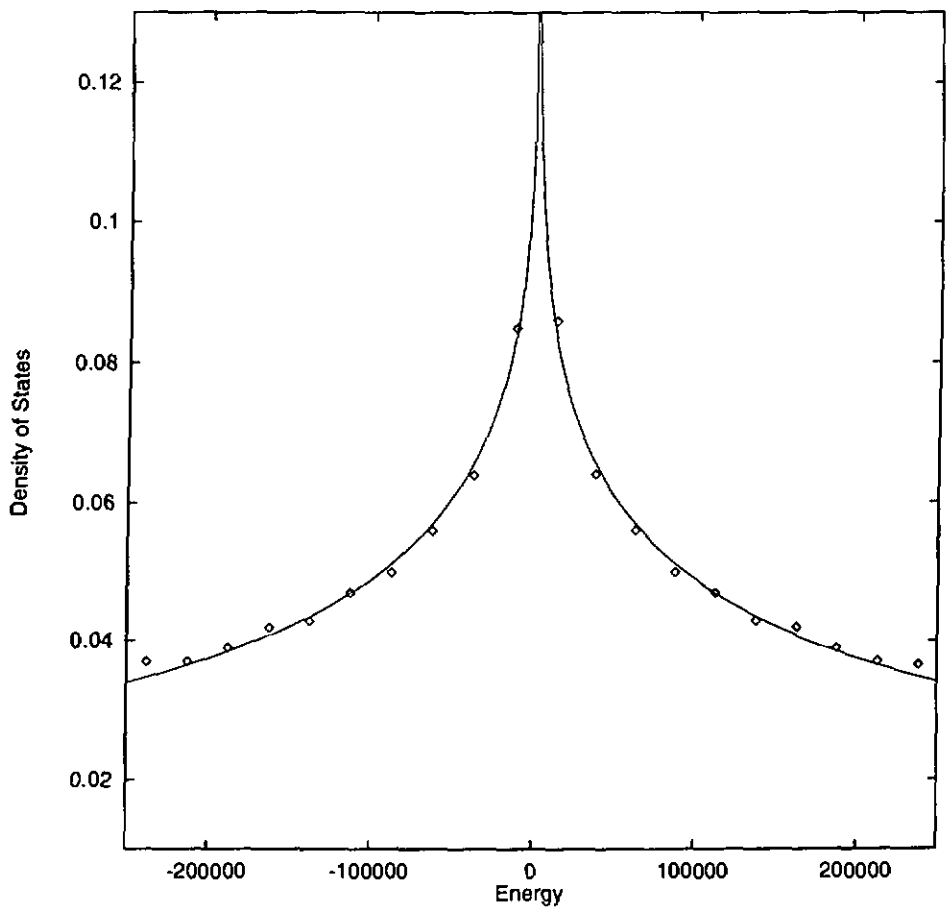
0.12
0.1
0.08
0.06
0.04
0.02
Density of States
-200000
-100000
0
100000
200000
Energy

Figure 3

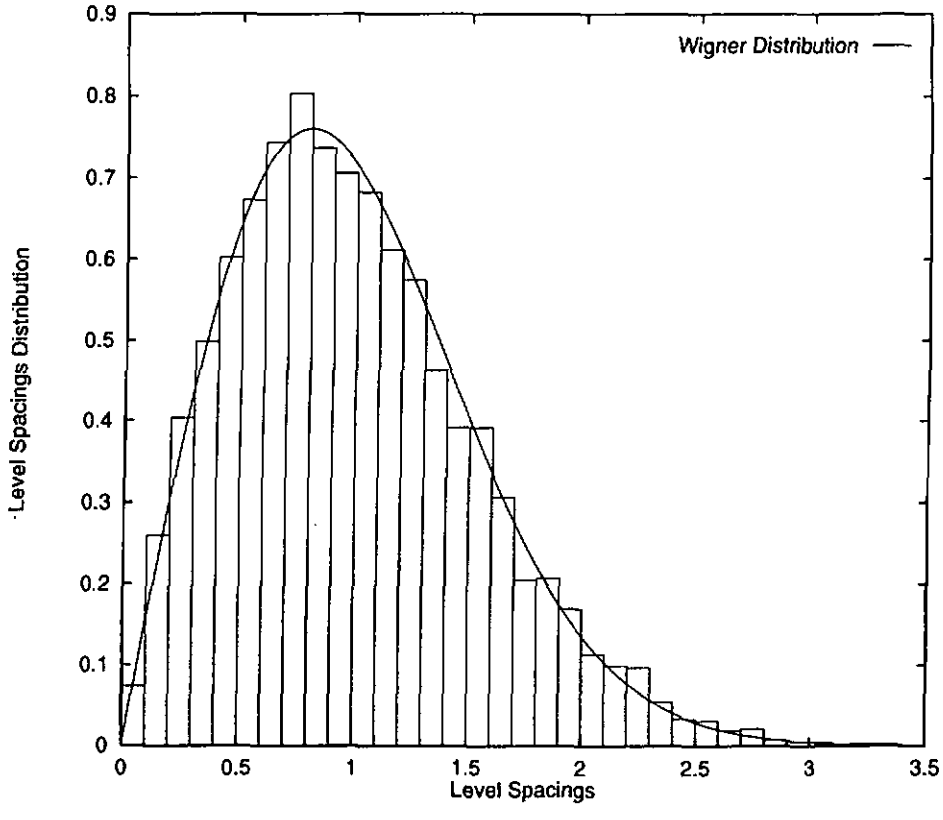
Wigner Distribution
Level Spacings Distribution
Level Spacings
0.9
0.8
0.7
0.6
0.5
0.4
0.3
0.2
0.1
0
0
0.5
1
1.5
2
2.5
3
3.5

Figure 4

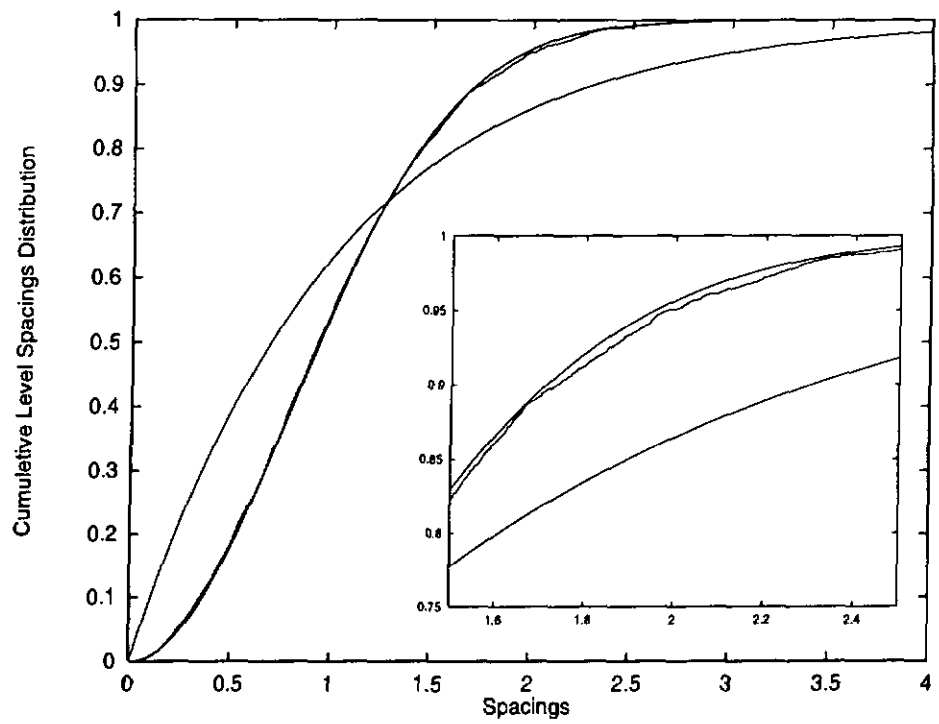
Cumulative Level Spacings Distribution
Spacings
0
0.1
0.2
0.3
0.4
0.5
0.6
0.7
0.8
0.9
1
0
0.5
1
1.5
2
2.5
3
3.5
4
0.75
0.8
0.85
0.9
0.95
1.6
1.8
2
2.2
2.4

Figure 5

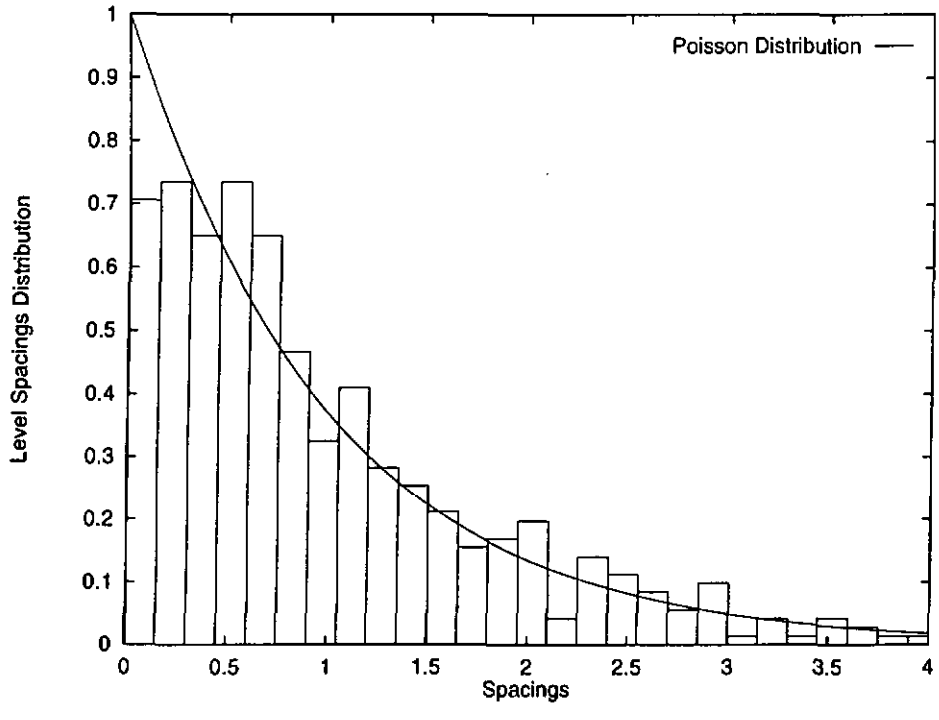
Poisson Distribution
Level Spacings Distribution
Spacings
0
0.1
0.2
0.3
0.4
0.5
0.6
0.7
0.8
0.9
1
0
0.5
1
1.5
2
2.5
3
3.5
4

Figure 6

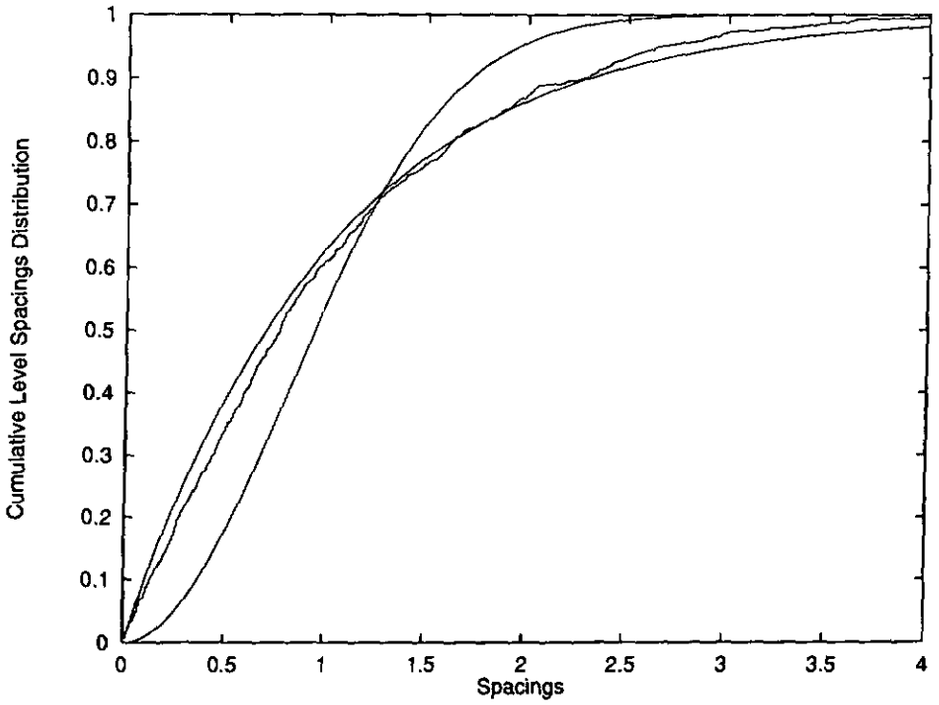
Cumulative Level Spacings Distribution
Spacings
0
0.1
0.2
0.3
0.4
0.5
0.6
0.7
0.8
0.9
1
0
0.5
1
1.5
2
2.5
3
3.5
4

Figure 7

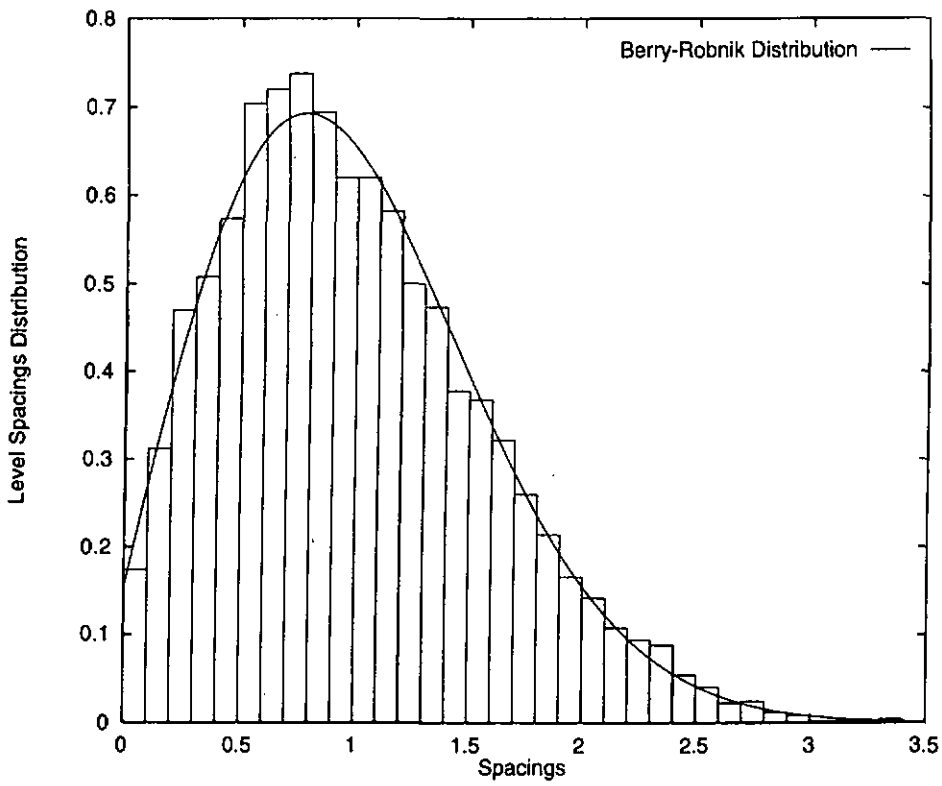
Berry-Robnik Distribution
Level Spacings Distribution
Spacings
0.8
0.7
0.6
0.5
0.4
0.3
0.2
0.1
0
0
0.5
1
1.5
2
2.5
3
3.5

Figure 8

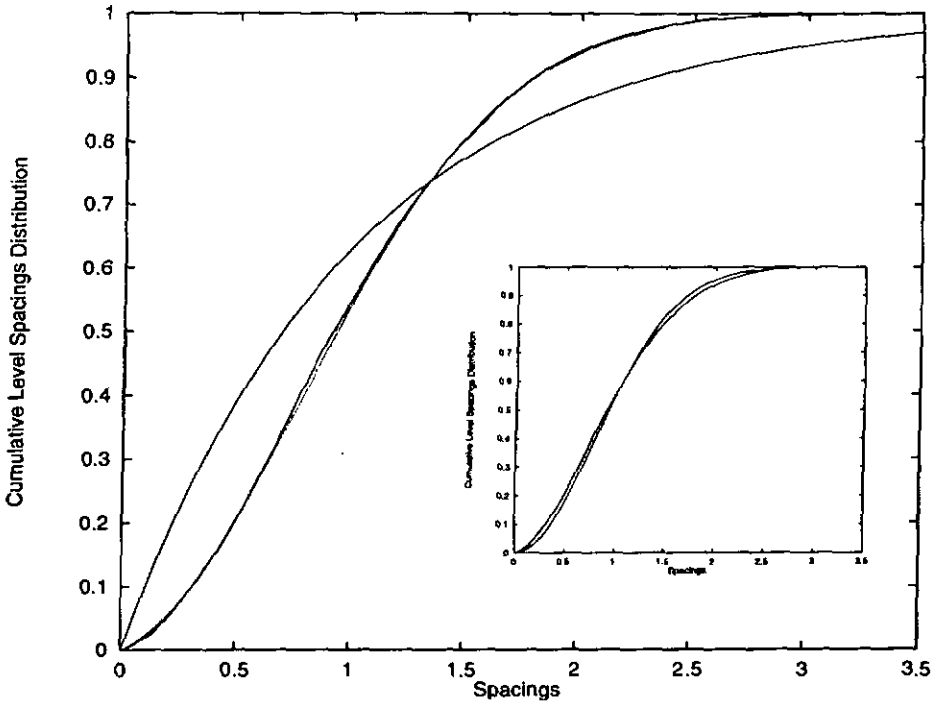
Cumulative Level Spacings Distribution
Spacings
0
0.1
0.2
0.3
0.4
0.5
0.6
0.7
0.8
0.9
1
0
0.5
1
1.5
2
2.5
3
3.5

Figure 9

Hidden Breit-Wigner distribution and other properties of random matrices with preferential basis

Ph. Jacquod[a], D.L.Shepelyansky[b,c]
[a] *Institut de Physique, Université de Neuchâtel, 1, Rue A.L. Breguet, 2000 Neuchâtel, Suisse*
[b] *Laboratoire de Physique Quantique, Université Paul Sabatier, 118, route de Narbonne, 31062 Toulouse, France*
(March 25, 1997)

We study statistical properties of a class of band random matrices which naturally appears in systems of interacting particles. The local spectral density is shown to follow the Breit-Wigner distribution in both localized and delocalized regimes with width independent on the band/system size. We analyse the implications of this distribution to the inverse participation ratio, level spacing statistics and the problem of two interacting particles in a random potential.

PACS numbers: 71.55.Jv, 72.10.Bg, 05.45.+b

Intensive investigations of band random matrices (BRM) have been done during last years [1,2]. Different regimes corresponding to localized and delocalized wave-functions have been studied numerically and analytically and it has been shown that the transition from one regime to another can be described by one scaling function depending on the ratio of the localization length in the infinite system $l \sim b^2$ to the size of the matrix N, where the parameter b determines the size of the band $2b+1$. Similar types of matrices appear in such physical systems as quasi one-dimensional disordered wires and such models of quantum chaos like the kicked rotator that gives additional grounds for investigation of BRM.

The above BRM can be also considered as a reasonable model of one-particle localization in a disordered wire of finite size [1,2]. However recent investigations of two interacting particles (TIP) in a random potential [3] showed that another type of BRM naturally appears in interacting systems. Indeed for interacting particles there is one preferential basis which corresponds to eigenstates without interaction. In this basis, the total Hamiltonian is the sum of a diagonal matrix, with elements given by the sum of one-particle energies, and a BRM, which describes interaction induced transitions between eigenstates of the non-interacting problem. The first investigations of such superimposed BRM (SBRM) allowed to find the dependence of the localization length l_{sb} on the amplitude W_b of large fluctuations on the diagonal and to obtain the localization length l_c for two-particles coherent propagation in a random potential on a distance much larger than one-particle localization length l_1 [3].

While from the TIP model it is clear that matrices with preferential basis should describe interesting physical effects in interacting systems, only few investigations in this direction have been done up to now [4,5]. In this paper we investigate the properties of such matrices in particular the local spectral density and the inverse participation ratio (IPR). Due to the close connection between the SBRM and the TIP problem, the obtained results can also be used for the latter case.

The matrix we study is the sum of a random diagonal matrix and a conventional BRM :

$$H_{n,n'} = \eta_n \delta_{n,n'} + \zeta_{n,n'}/\sqrt{2b+1} \qquad (1)$$

with $-W_b \leq \eta_n \leq W_b$, $-1 \leq \zeta_{n,n'} \leq 1$ for $|n-n'| \leq b$ and $\zeta_{n,n'} = 0$ elsewhere. The connection with the TIP is given by $b \sim l_1^2$ and $W_b \sim 4\sqrt{l_1}V/U$ in terms of the interaction strength U and the one-particle energy bandwidth $4V$, $l_1 \gg 1$. This matrix describes a one-dimensional two-particle Anderson model, with on-site interaction U, in the basis of non-interacting eigenstates. In [3] it was shown that the eigenstates of (1) are localized with localization length $l_{sb} \approx b^2/2W_b^2$ for $1 < W_b \ll \sqrt{b}$. This leads to an enhancement of the length of coherent TIP propagation $l_c = l_{sb}/l_1 \sim l_1^2 (U/V)^2/32$ independent on the sign of interaction.

Our numerical investigations of SBRM (1) show that, in addition to the standard exponentially localized form, the eigenstates are also characterized by large amplitude fluctuations of probability on nearby sites. A typical example of such an eigenstate is presented in Fig.1. The spike eigenstate structure is clearly noticeable. This implies that only certain unperturbed states have strong admixtures into the given eigenstate. Such eigenstate structure is quite different from the case of conventional BRM. For a better understanding of these spiked fluctuations we study the local spectral density ρ_W introduced by Wigner [6] and analyzed in BRM with linearly growing diagonal corresponding to conservative systems [7,8] :

$$\rho_W(E-E_n) = \sum_\lambda |\psi_\lambda(n)|^2 \delta(E-E_\lambda) \qquad (2)$$

The function ρ_W characterizes the average probability $P(|\psi_\lambda(n)|^2) = \rho_W(E-E_n)$ of eigenfunction $\psi_\lambda(n)$ on

site n with energy $E_n = H_{n,n}$, where λ is the eigenvalue index and n marks the original basis. Our numerical investigations in a wide range of parameters ($20 \leq b \leq 2000$, $201 \leq N \leq 4001$ and $1.5 \leq W_b \leq 40$) both in localized ($l_{sb} \ll N$) and delocalized ($l_{sb} \gg N$) regimes show (see Fig.2) that ρ_W is well described by the well-known Breit-Wigner distribution $\rho_W = \rho_{BW}$:

$$\rho_{BW}(E - E_n) = \frac{\Gamma}{2\pi((E-E_n)^2 + \Gamma^2/4)}; \Gamma = \frac{\pi}{3W_b} \quad (3)$$

where Γ is the distribution width. This distribution remains valid in localized and delocalized regimes under the condition that Γ is much less than the energy width $\delta E \approx 1$ of $H_{n,n'}$ at $W_b = 0$. Usually the distribution ρ_{BW} appears in such physical systems as nuclei and complex atoms [8] where due to energy conservation the diagonal term η_n grows linearly with n that corresponds to a finite level density ρ_E. In this case the width is $\Gamma = 2\pi\rho_E < H^2_{n\neq n'} >$ [6,8]. In our case for $W_b \gg 1$ all eigenenergies are homogeneously distributed in the finite interval $[-W_b, W_b]$ and for full matrices with $b = N/2$ we can use the above expression with $\rho_E = N/2W_b$ which gives Γ in (3). For $b \ll N$ according to [3] one should replace ρ_E by the density of directly coupled states $\rho_c = b/W_b$ that leads to the same expression for Γ. The theoretical formula for Γ, independent on b and N, is in a good agreement with our numerical data (Fig.2). The independence of Γ on b and N makes our case quite different from the case of full matrix (1) studied before in [9].

For $W_b \gg 1$ the width of the Breit-Wigner peak is small and therefore according to (3) the probability on nearby levels is a strongly fluctuating spiked function. This spike structure of eigenfunctions can be characterized by the IPR $\xi_\lambda = (\sum_n |\psi_\lambda(n)|^4)^{-1}$ which counts the number of spikes independently on the distance between them. In the case of full matrices with $b = N/2$ the number of spikes can be estimated as the number of states in the interval Γ that gives the average value of IPR $\xi =< 1/\xi_\lambda >^{-1} \sim \rho_E\Gamma \approx N/(2W_b^2)$. The same estimate can be also used in the delocalized regime $l_{sb} \gg N$ with $b \ll N$. Of course this estimate is valid only when the number of states in the width Γ is much larger than one, that implies $\xi \gg 1$ or $W_b \ll \sqrt{N}$.

The numerical results for the dependence of IPR on W_b in the delocalized regime are presented in Fig.3. They demonstrate that for sufficiently large full matrices ($N = 4001$) this dependence approaches to the above estimate. However the convergence is rather slow so that for smaller N values one has approximately $\xi \sim N/W_b^\alpha$ where the exponent α slowly changes with N. For example $\alpha \approx 1.7$ for $N = 2001$. We attribute this very slow approach to the asymptotic value of $\alpha = 2$ to the quite restricted range of W_b variation. Indeed on one side the width of the Breit-Wigner peak should not exceed the width of the energy band for $W_b = 0$ that gives $W_b \gg 1$. On the other side one should have $W_b \ll \sqrt{N}$. Another restriction appears for band matrices with $b < N/2$ namely $l_{sb} \gg N$. The data for this case (Fig.3, full squares) show that for not very large W_b the IPR is close to the regime of full matrices while for large W_b one enters the localized regime $l_{sb} \ll N$ which should be studied separately.

It is interesting to note that in the delocalized regime even for $W_b \gg 1$ many levels are coupled by interaction if $\rho_E\Gamma \approx N/(2W_b{}^2) \gg 1$. Therefore, one would expect that for $W_b < W_b{}^{cr} \approx (N/2)^{1/2}$ the level spacing statistics $P(s)$ will be the same as in the case of Gaussian orthogonal ensemble (GOE) [10]. These expectations are not so evident since the spiked structure of eigenfunctions apparently should lead to a decrease of overlapping matrix elements between eigenfunctions. However, our numerical results for matrices with $N \leq 8000$ show that $P(s)$ remains close to GOE for $1 < W_b < W_b{}^{cr}$. They are also in agreement with the numerical results [11] for full matrices of smaller sizes showing that the transition border in W_b between Poisson and GOE statistics scales as $N^{1/2}$. The question about other statistical properties of levels in the regime $1 < W_b < W_b{}^{cr}$ remains open.

For the localized regime in the above estimate of ξ one should replace N by l_{sb} since only levels in the interval of one localization length can contribute to the IPR. This gives the expression

$$\xi \approx l_{sb}/2W_b{}^{\beta-2} \approx b^2/4W_b^\beta; \quad \beta = 4 \quad (4)$$

which is valid for $\xi \gg 1$ ($1 \ll W_b \ll \sqrt{b}$). The last condition together with $l_{sb} \ll N$ gives strong restrictions for the numerical simulations ($1 \ll W_b \ll N^{1/4}$).

Our results for this localized case are presented in Fig.4. The data can be empirically fitted by $\xi \sim b^2/W_b^\beta$ with $\beta \approx 3$ which differs from the theoretical value $\beta = 4$. We attribute this difference to the fact that we are not far enough in the asymptotic regime of large b and W_b. Indeed, for $W_b > b^{1/2}$ one enters in the perturbative regime and the deviations from a power law becomes evident. We also checked that the probability distribution $P(|\psi_\lambda(n)|^4)$ is proportional to ρ^2_{BW} that gives additional grounds for the theoretical power $\beta = 4$. However, the simulations with large enough values of parameters b, W_b requires too large matrix sizes being beyond our numerical abilities. The numerically found value $\beta > 2$ implies that the number of peaks is smaller than the localization length $l_{sb} \approx b^2/(2W_b^2)$ which determines the asymptotic exponential decay of the eigenstates. It would be desirable to have a more rigorous theoretical derivation of the IPR dependence on parameters in the localized regime.

The above results show that the SBRM (1) has many features similar with the photonic localization in a molecular quasicontinuum [12] as it was remarked in [3]. According to this analogy, the number of levels in one-photon transition (size) is of the order b and the density of coupled states is $b/2W_b$. However, in the photonic

model the levels are ordered in energy in a growing way that leads to a chain of equidistant Breit-Wigner peaks in an eigenstate [12]. For the SBRM (1) all levels are mixed in the energetic interval and the Breit-Wigner peak is hidden.

Let us now discuss the consequences of the result (4) for the TIP model. According to the relation between the parameters of SBRM and TIP given above we obtain from (4) the expression for the IPR ξ_c in the TIP model:

$$\xi_c \sim (U/V)^4 {l_1}^2 > 1 \qquad (5)$$

This result can be also derived directly from the density of states inside the localization length interval l_c ($\rho_E \sim l_1 l_c/V$) and the transition rate $\Gamma_c \sim U^2/(V l_1)$ obtained in [3]. Indeed, the number of levels in the Breit-Wigner peak is $\Gamma_c \rho_E \approx \xi_c$ that gives (5). This result shows that the number of noninteracting eigenstates ξ_c contributing in the eigenfuction is quite large for $U \sim V$ while for $(U/V)^2 l_1 \ll 1$ this number is order of 1. However, the value of ξ_c at $U \sim V$ is much less than the number of unperturbed states ΔN contributing to the TIP eigenfunction in the unperturbed lattice basis. This number determines the IPR $\xi_{max} \approx \Delta N \approx l_c l_1 \sim l_1^3$. The difference between ξ_c and ξ_{max} shows that the noninteracting eigenbasis represents the real eigenfunctions in a much better way. It also stresses the fact that the IPR value is not basis invariant.

From the difference between ξ_c and ξ_{max} it is possible to conclude that the coherent propagation of TIP goes by rare jumps of size l_1 between the states with approximately constant sum of noninteracting energies $E_s = \epsilon_n + \epsilon_{n'}$. The distribution over E_s should have the Breit-Wigner form with the width Γ_c. The length of propagation by such jumps is $l_c \sim {l_1}^2 \gg l_1$. Due to this hidden Breit-Wigner distribution the IPR ξ_c in the basis of noninteracting eigenstates is proportional to ${l_1}^2$ instead of "naive" ${l_1}^3$. For the case of TIP with M transverse channels one should replace l_1 in (5) by $M l_1$ with $l_1 \propto M$ being one-particle localization length.

If one-particle motion is ergodic in a d-dimensional system of size $L < l_1$ then its eigenfunction contains about $N_1 \approx L^d$ components. The matrix element of interaction is then $U_s \sim U/{N_1}^{3/2}$ [3], the density of coupled states $\rho_c \sim {N_1}^2/V$ and the Breit-Wigner width $\Gamma_c \sim {U_s}^2 \rho_c \sim U^2/N_1 V$ for $U < V$ is less than one-particle level spacing $\Delta_1 \approx V/N_1$. Thefore, it is possible that a concept of pairs formed by TIP can be useful even in the ergodic samples with $L < l_1$. In some sense, for $\Delta_2 \ll \Gamma_c \ll \Delta_1$, where $\Delta_2 \approx V/{N_1}^2$ is two-particle level spacing, one can at first average over fast one-particle motion and after that analyse the slow pair dynamics with typical time scale $1/\Gamma_c$. In the ergodic regime $L < l_1$ the IPR is $\xi_c \sim \Gamma_c \rho_c \sim N_1 (U/V)^2 \ll {N_1}^2$ and according to the discussed above properties of $P(s)$ in SBRM and the result [11] the GOE statistics for TIP should be observed for $\xi_c > 1$. For $L \gg l_1$ the strong enhancement of interaction ($\rho_c \Gamma_c \sim {l_1}^d (U/V)^2 \gg 1$) leads to delocalization of the TIP pairs in $d \geq 3$ below one-particle Anderson transition when noninteracting particles are well localized [13].

One of us (P.J.) gratefully acknowledges the hospitality of the Laboratoire de Physique Quantique, Université Paul Sabatier during his stay there and another (D.L.S.) is grateful to the Yale University and the Godfrey Fund at University of New South Wales for hospitality during the process of work on the above problem. We thanks Y.Alhassid, V.Flambaum and O.Sushkov for useful discussions and remarks. Work is supported in part by the Fonds National Suisse de la Recherche.

(c) Also: Budker Institute of Nuclear Physics, 630090 Novosibirsk, Russia

[1] G. Casati, L. Molinari and F.M. Izrailev, Phys. Rev. Lett. **64**, 1851 (1990).
[2] Ya.V. Fyodorov and A.D. Mirlin, Phys. Rev. Lett. **67**, 2405 (1991); **71**, 412 (1993).
[3] D.L. Shepelyansky, Phys. Rev. Lett. **73**, 2607 (1994).
[4] G. Lenz and F. Haake, Phys. Rev. Lett. **67**, 1 (1991).
[5] J.-L. Pichard and B. Shapiro, J. Phys. **4**, 623 (1994); M. Kreynin and B. Shapiro, Phys. Rev. Lett. **74**, 4122 (1995).
[6] E.P. Wigner, Ann. Math. **62**, 548 (1955); **65**, 203 (1957).
[7] G. Casati, B.V. Chirikov, I. Guarneri and F.M. Izrailev, Phys. Rev. E **48**, 1613 (1993); B.V. Chirikov (unpublished 1993).
[8] V.V. Flambaum, A.A. Gribakina, G.F. Gribakin and M.G. Kozlov, Phys. Rev. A **50**, 267 (1994).
[9] V.P.Tatarskii, Sov. Phys. Usp. **30**, 134 (1987); B.V.Chirikov, Preprint INP 87-123, Novosibirsk 1987.
[10] M.L. Metha, *Random Matrices*, Academic Press, New York, (1991).
[11] G. Lenz, K. Zyczkowski and D. Saher, Phys. Rev. A **44**, 8043 (1991).
[12] D.L.Shepelyansky, Physica D **28**, 103 (1987).
[13] D.L.Shepelyansky, unpublished (1994); Y.Imry, preprint (1995); F.Borgonovi and D.L.Shepelyansky, preprint (1995).

FIG. 1. Localized eigenfunction of a SBRM with $W_b = 7$, $b = 100$ and $N = 2001$. The solid line indicates the exponential localization with $l_{sb} \approx 171$ in agreement with results obtained in [3], eq.(3).

FIG. 2. Local spectral density which determines the average probability on a given site $P(|\psi_\lambda(n)|^2) = \rho_W(E - E_n)$ for $b = 100$, $W_b = 5$, $N = 201$ (triangles, 20 realisations of disorder) and $N = 2001$ (squares, 2 realisations of disorder). The solid line gives Breit-Wigner distribution (3) with $\Gamma = 0.21$. The inset shows the dependence of Γ on W_b^{-1} : points are numerical data ($N = 1001, b = 100$), straight line is theory (3).

FIG. 3. IPR ξ normalized with its limit value for the GOE case $N/3$ vs. W_b in the delocalized regime for $N = 2001$, $b = 300$ (full squares), and full matrices with $N = 251$ (open squares), $N = 501$ (open triangles), $N = 1001$ ($\times$), $N = 2001$ (full triangles) and $N = 4001$ (full circles). Dashed line shows the fit for full circles with $\alpha = 1.75 \pm 0.03$; solid lines shows theoretical slope $\alpha = 2$.

FIG. 4. Dependence of ξ/b^2 on W_b in localized regime : $N = 2001$, $b = 50$ (full squares) and $b = 80$ (open squares); $N = 4001$, $b = 50$ (full circles) and $b = 100$ (open circles). Dashed line shows the slope from fit for open circles ($\beta = 3.0 \pm 0.1$) and solid line indicates theoretical slope $\beta = 4$.

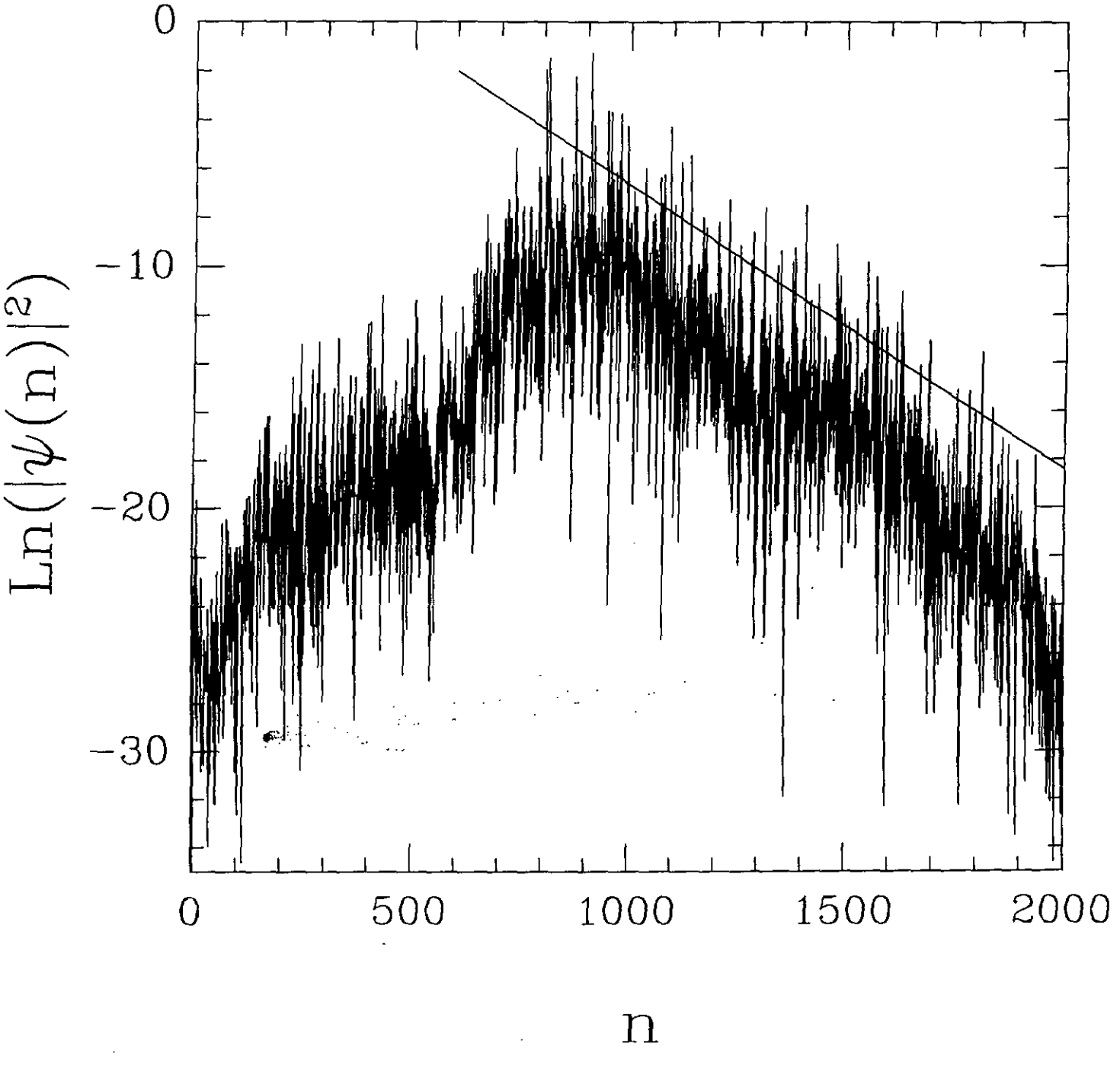
0
−10
−20
−30
Ln(|ψ(n)|²)
0
500
1000
1500
2000
n

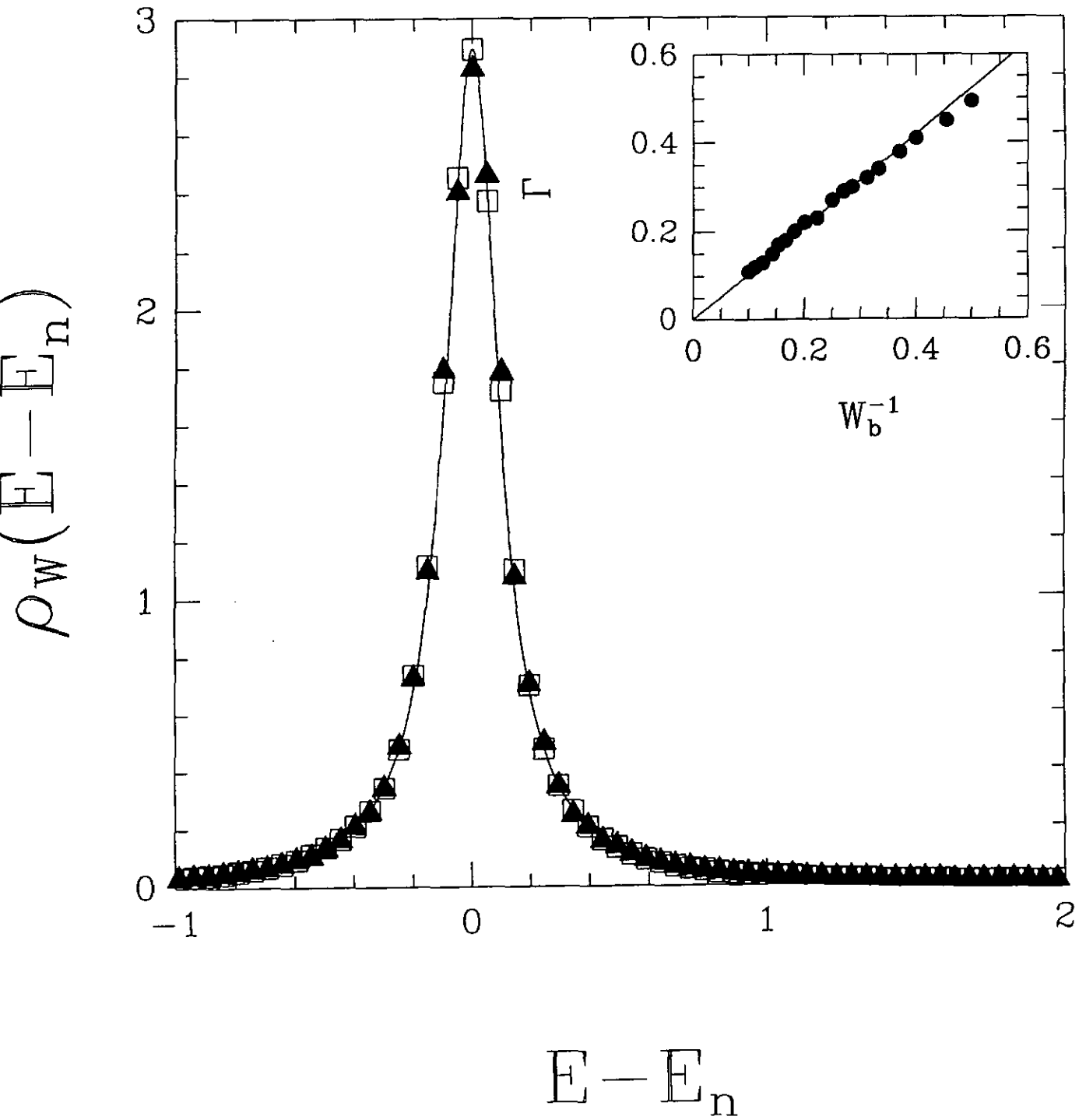
3
2
1
0
−1
0
1
2
$\rho_W(E-E_n)$
$E-E_n$
Γ
0.6
0.4
0.2
0
0
0.2
0.4
0.6
W_b^{-1}

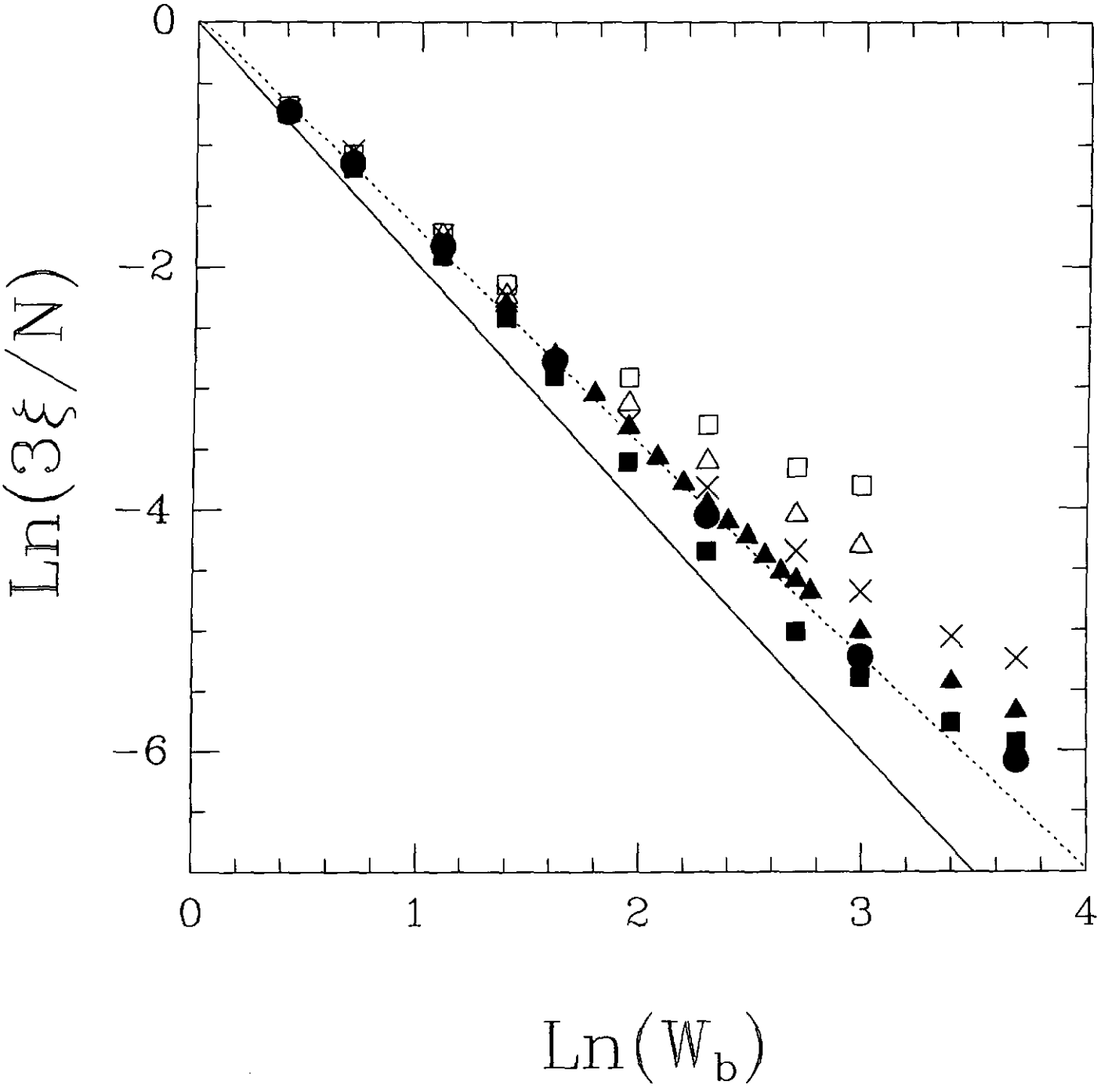
0
−2
−4
−6
0
1
2
3
4
Ln(3ξ/N)
Ln(W_b)

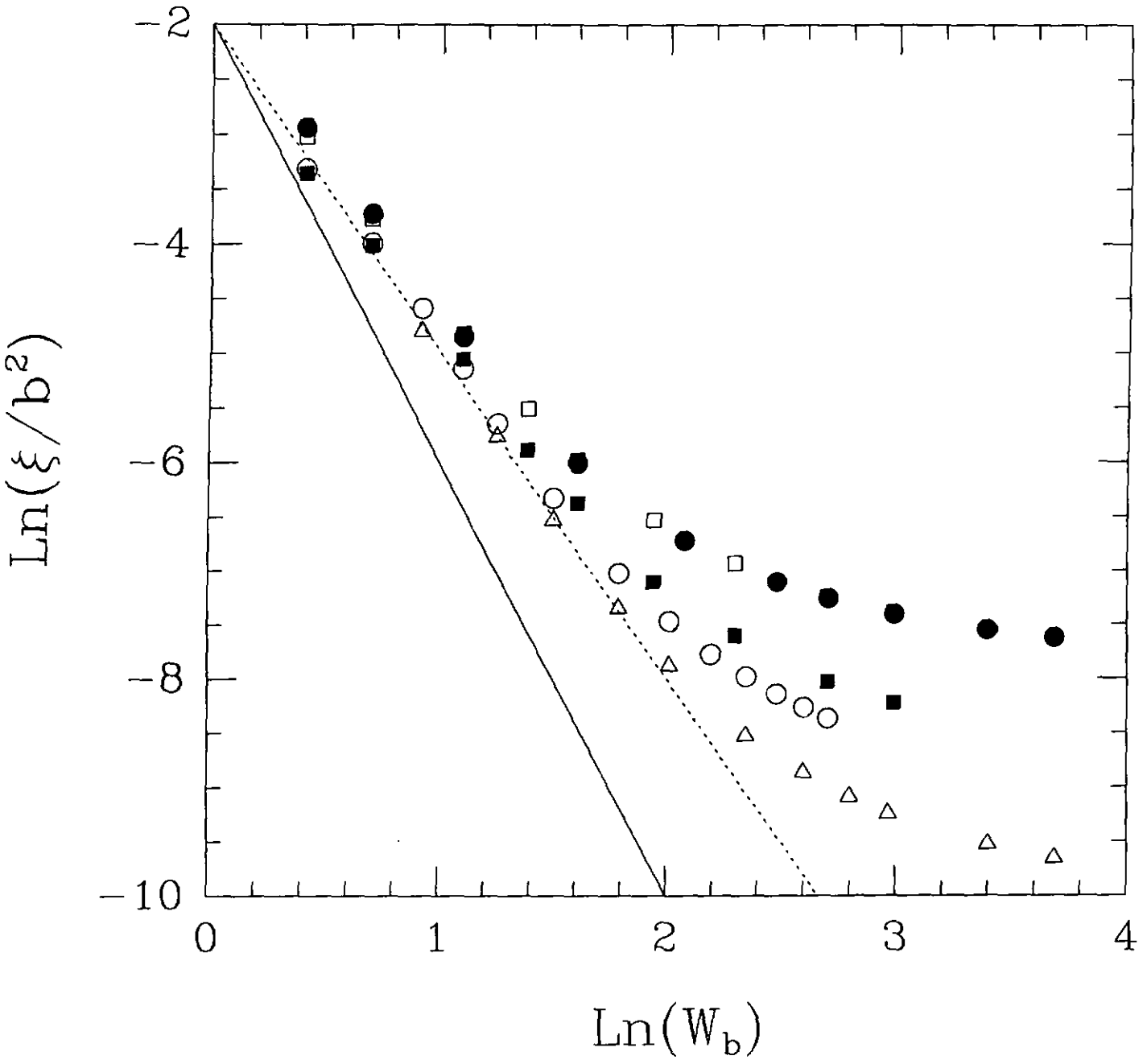
−2
−4
−6
−8
−10
0
1
2
3
4
Ln(ξ/b²)
Ln(W_b)

Double butterfly spectrum for two interacting particles in the Harper model

Armelle Barelli, Jean Bellissard, Philippe Jacquod[a] and Dima L. Shepelyansky[b]
Laboratoire de Physique Quantique, UMR 5626 du CNRS, Université Paul Sabatier, F-31062 Toulouse Cedex, France
[a] *Institut de Physique, Université de Neuchâtel, CH-2000 Neuchâtel, Confédération Helvétique*
(15 September, 1996)

We study the effect of interparticle interaction U on the spectrum of the Harper model and show that it leads to a pure-point component arising from the multifractal spectrum of non interacting problem. Our numerical studies allow to understand the global structure of the spectrum. Analytical approach developed permits to understand the origin of localized states in the limit of strong interaction U and fine spectral structure for small U.

PACS numbers: 05.45.+b, 72.15.Qm, 72.10.Bg

Recently a great deal of attention has been devoted to the investigation of incommensurate systems exhibiting singular continuous spectrum with many interesting multifractal properties (see e.g. [1–3]). Among the physical models, one of the most popular is the Harper model of electrons on a two-dimensional square lattice in the presence of a perpendicular magnetic field [4,5]. This system can be reduced to the study of a rather simple model of particle dynamics on a one-dimensional quasiperiodic lattice. The energy spectrum exhibits multifractal properties and the band spectrum for rational values of magnetic flux looks like a butterfly. In spite of the academic character of such a model, experiments have been performed during the last ten years exhibiting this multifractal butterfly structure. One of the first among them has been performed in 1985 using superconducting networks [6] and more recently experiments with superlattices also allowed to observe the fist hierarchical steps of multifractal butterfly structure [7].

The deep understanding of such an intricate spectral structure attracted interest of mathematicians and physicists who developed new approaches for its investigation such as non commutative geometry [8], pseudo-differential operators [9], functional analysis [10], renormalization group approach [11,12], thermodynamical formalism [13]. All these tools allowed to study the problem on rigorous mathematical ground and to understand the properties of eigenstates. For example using the duality between momentum and spatial coordinate [14], it is possible to prove rigorously the existence of localized or delocalized states [15,16]. It was also found that quantum systems which are chaotic in the classical limit may have quite unusual properties in the presence of underlying quasiperiodic structure [17,1,13].

All the works mentioned above were done for one particle dynamics. However even from the physics of the original Harper model, it is clear that the interaction between electrons on the square lattice in the presence of magnetic flux plays an important rôle. Therefore it is natural to address the question of the influence of interaction on multifractal spectrum. The most simple example of such a case is an interaction between two particles. Recently it has been found that in the case of random potential even such simple model has a number of unexpected properties [18]. For example repulsive/attractive short range interaction leads to appearance of effective pair states in which two particles propagate together on a distance much larger than the one-particle localization length without interaction. Surprinsingly the first numerical studies of interaction effect in a quasiperiodic potential showed an opposite tendency [19]. Namely, repulsive/attractive interaction leads to the appearance of localized states while in the absence of interaction multifractal spectrum generated quasidiffusive spreading of wave packets on the lattice. However, the numerical approach used in [19] allowed to study only the wave packet evolution while the structure of the spectrum itself was not directly accessible. Therefore to understand the spectral structure and the nature of eigenstates we performed numerical simulations by direct diagonalisation based upon Lanczos algorithm.

As a basic model for our investigations we consider the model of two interacting particles (TIP) in the Harper problem described by the following eigenvalues equation

$$(2\lambda\cos(\gamma n_1+\beta_1)+2\lambda\cos(\gamma n_2+\beta_2)+U\delta_{n_1,n_2})\varphi_{n_1,n_2}+ \varphi_{n_1+1,n_2}+\varphi_{n_1-1,n_2}+\varphi_{n_1,n_2+1}+\varphi_{n_1,n_2-1}=E\varphi_{n_1,n_2} \quad (1)$$

where the parameter γ characterizes the quasiperiodic lattice for the one-particle problem. Without interaction, each particle moves in quasiperiodic Harper potential and $\gamma/2\pi=\phi/\phi_0=\alpha$ is the ratio between the magnetic flux within one unit cell of the square lattice and the flux quantum $\phi_0=h/e$. The parameter α plays the role of an effective Planck's constant so that $\alpha\mapsto 0$ corresponds to the semiclassical limit. The two parameters $\beta_{1,2}$ are related to the quasimomentum components in the non interacting problem. The parameter λ characterizes the strength of the quasiperiodic potential and for the case of electrons on a square lattice $\lambda=1$ [5]. However from mathematical point of view it is also interesting to study

the different regimes with $\lambda < 1$ and $\lambda > 1$. Strong analytical and numerical evidence has been given that the spectrum is pure point and the states are localized when $\lambda > 1$ while for $\lambda < 1$ the spectrum is continuous with extended eigenstates [14,10,1,20]. The strength of the short range on-site interaction is characterized by U. We concentrate our investigations on the case $\lambda = 1$, $\beta_{1,2} = \beta$ when for $U = 0$ the spectrum is multifractal for irrational values of $\gamma/2\pi$. We consider only the part of the spectrum corresponding to the symmetric TIP states since antisymmetric configuration is not affected by on-site interaction.

In the absence of interaction, the corresponding two particle spectrum results of the superposition of two one-particle spectra of the Harper model and is shown in Fig. 1 (a). Comparing with the one-particle spectrum (Hofstadter's butterfly), we can remark that the spectrum becomes much more dense near the centers of the bands and subbands but still the gaps in the spectrum survive on all energy scales.

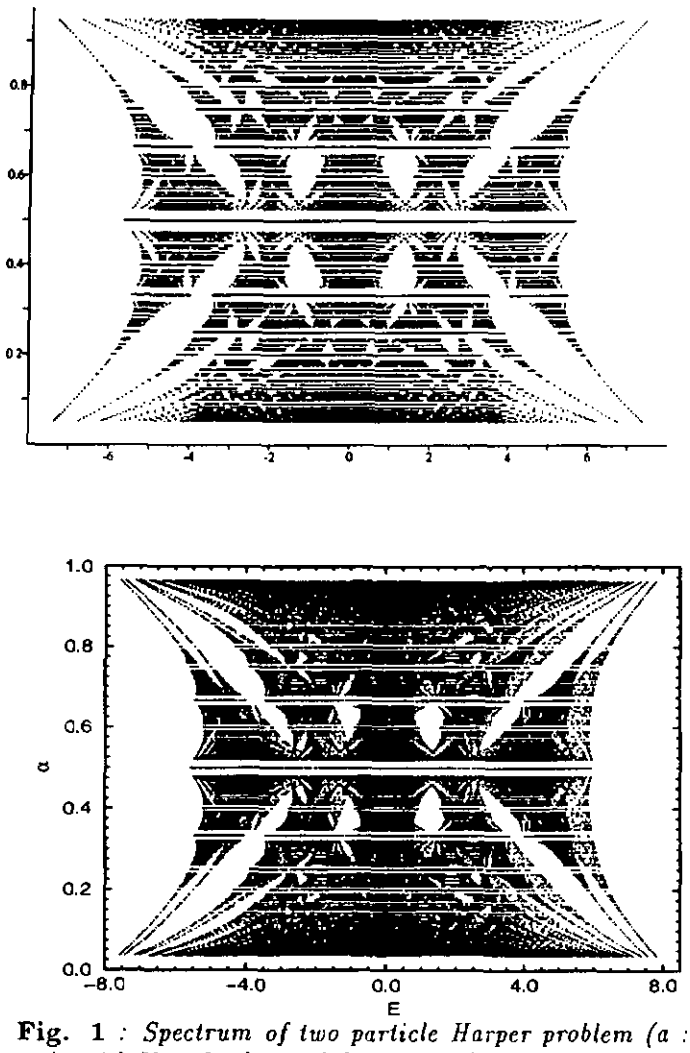

Fig. 1 : *Spectrum of two particle Harper problem (a : up), with $U = 0$ obtained for rational values of $\gamma/2\pi = \alpha = p/q$ with $q \leq 19$; (b : down) with $U = 1$ and $q \leq 23$.*

When increasing the strength of the interaction U, the spectrum is splitted into two butterflies which are slightly shifted one respect to the other. However one of them remains almost at the same place corresponding to the non interacting case of Fig. 1 (a). The shifted butterfly moves to the right since the repulsive interaction $U > 0$ gives global increase of energy. A typical case $U = 1$ of double butterfly spectrum is presented in Fig. 1 (b).

The main features which can be immediately observed in this figure are the smoothness of the edge of the shifted butterfly, the less dense character of its spectrum and the filling of some internal energy gaps (see for example near $\alpha = 0.6$ and $E = -1.5$). However, the gaps in the spectrum still exist on all scales.

The shift of one butterfly and almost unchanged form for the other at moderate values of interaction U can be understood in the following simple way. For that we choose small values of flux $\alpha \ll 1$ and use the perturbation theory in U on the basis of harmonic oscillator functions to get analytical expressions for the Landau sublevels at the spectrum edge. Without interaction, the band edge is given by $E_{\pm}(\alpha) = \pm 8 \mp 4\pi\alpha(m_1 + m_2 + 1) \pm \pi^2\alpha^2\left(2 + (2m_1 + 1)^2 + (2m_2 + 1)^2\right)/4 + O(\alpha^3)$, which is superposition of two Hofstadter butterflies in semiclassical regime [21]. The integers m_1, m_2 are the Landau quantum numbers for oscillator states near the bottoms of potential minima. If two particles are located in different minima, the interaction between them is negligibly small and the energy levels are not shifted by U. These energy states correspond to non shifted butterfly with dense spectrum since there are many states when TIP are separated from each other. If TIP are located in the same potential minimum, the interaction gives energy shift which in the first order of perturbation theory is $\Delta E_{\pm} = U\sqrt{\alpha}$ for $m_{1,2} = 0$ and $m_{1,2} = (0; 1)$ being in good agreement with numerical data for $U < 1$ as can be seen on Fig. 2 (a). This shows that the shifted butterfly corresponds to the case when the two particles are located near each other. The density of such states is smaller than in the case when particles are far from each other and that is why the shifted butterfly is less dense.

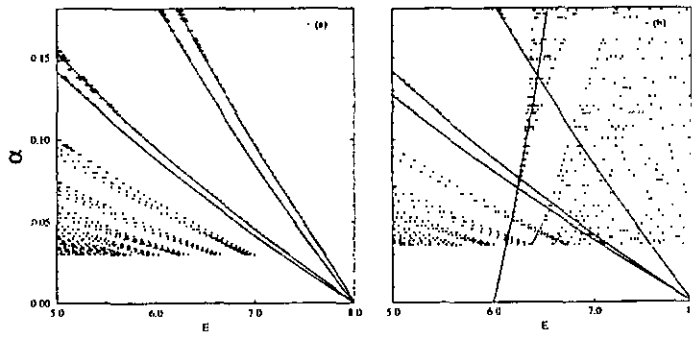

Fig. 2 : *Energy band edges (a) U=0.4, dots are numerical data and solid curves are perturbation theory result. (see text); (b) U=10, dots are data from Fig. 4 and soli*

curves are given by theory described in the text.

Direct analysis of eigenstates for irrational flux values (which are approximated by a continuous fraction expansion) also shows that the states in the shifted part correspond to the situation where two particles stay near each other. However, contrary to the TIP in a random potential, the particles here cannot propagate together and stay exponentially localized near the origin as it can be seen with the typical 3-D plot of Fig. 3.

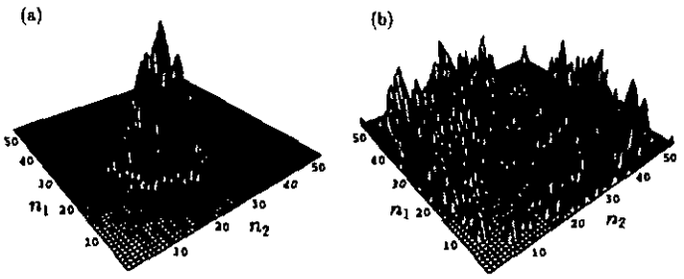

Fig. 3 : *Semilog plot of* $W_{n_1,n_2} = |\phi_{n_1,n_2}|^2$ *for localized* ($E = -1.3376, -10 \leq \ln W \leq -1, \xi = 5.9, \xi_0 = 193$ *(a : left)) and delocalized* ($E = -1.7368, -10 \leq \ln W \leq -3, \xi = 214, \xi_0 = 12.5$ *(b : right)) eigenstates at* $U = 1, \alpha = 34/55, \beta = \sqrt{2}$.

We also investigated the structure of eigenstates in the more dense part of the spectrum (non shifted butterfly). In that case the eigenstates are delocalized and quite similar to those corresponding to the non interacting case. Here the two particles mainly spread quasidiffusively along the quasiperiodic lattice and interaction is not important for them. This structure of localized and delocalized eigenstates is in agreement with the numerical study of wave packet dynamics performed in [19].

The properties of eigenstates can also be analyzed with the help of the inverse participation ratio (IPR) $\xi = (\sum_{n_1,2} W^2_{n_1,n_2})^{-1}$. Its value for different energies is shown in Fig. 4 for $\alpha = 34/55$. In agreement with the above discussion, the localized states with small ξ correspond to the part of the shifted butterfly with less dense spectrum while the unshifted butterfly is associated to large ξ with delocalized states. It is interesting to determine the IPR ξ_0 in the non interacting eigenstates basis. Such approach has been quite useful for TIP in a random potential [22]. It is interesting to note that the situation for TIP in the Harper model is quite different. Namely, the delocalized states have very small value of ξ_0 while the localized ones are delocalized in the non interacting eigenstates basis and have very large ξ_0 (see Fig.3). This result once more shows that delocalized states correspond to almost non interacting particle propagation while localized states appear only due to interaction which can be even repulsive (Fig.3a).

With further increase of U the shifted butterfly goes on moving to the right and becomes more and more deformed. Starting from interaction strength $U \geq 10$, this butterfly is transformed into a spectral band with width two times smaller than the original spectrum at $U = 0$. The center of this band is located at energy $E \approx U$. The typical example of global spectrum is shown in Fig. 5.

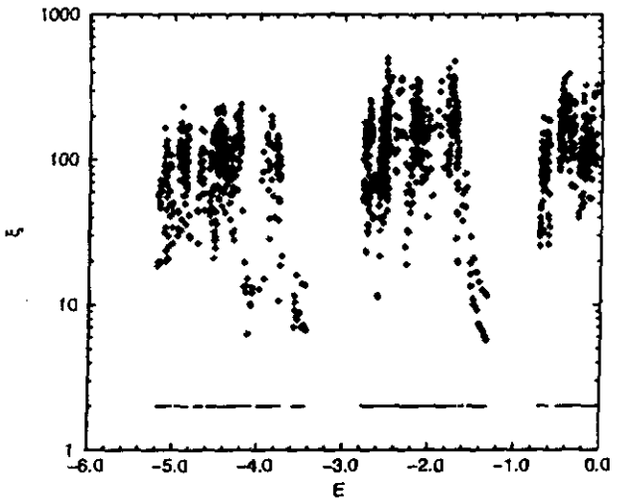

Fig. 4 : *Inverse participation ratios* ξ *vs eigenenergies* E *shown at* $\xi = 2$; $U = 1, \alpha = 34/55, 0 \leq \beta < 2\pi$.

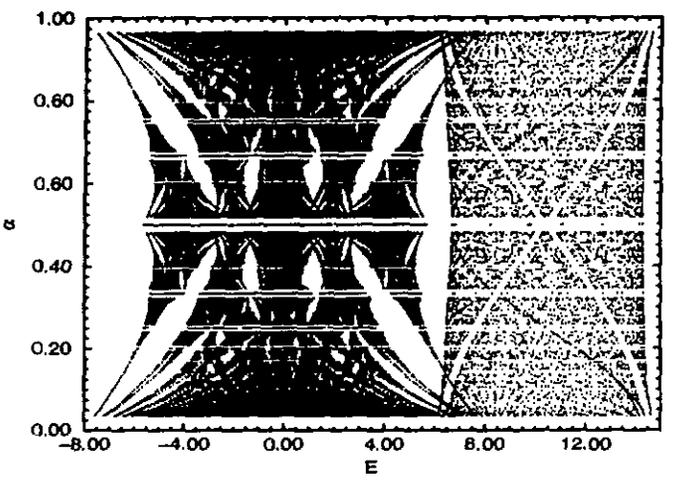

Fig. 5 : *Same as in Fig. 1 with* $U = 10$ *and* $q \leq 28$.

The physical reason for the appearance of such separated spectral band can be understood in the following way. For strong U, there are states for which TIP are localized on the same site so that $n_{1,2} = n$. According to (1) the energy of the states is $E_n = 4\lambda \cos(\gamma n + \beta) + U$. The transition between these states can be obtained with first order perturbation theory in $1/U$ which gives the effective eigenvalue equation :

$$(4\lambda \cos(\gamma n + \beta) + U)\,\phi_n + V_{\text{eff}}\,(\phi_{n+1} + \phi_{n-1}) = E\phi_n \qquad (2)$$

Here V_{eff} is the hopping between such states due to virtual transitions via states with $n_1 \neq n_2$. For $U \gg 1$, the energy difference between diagonal and off-diagonal

states is very large and therefore $V_{\rm eff} \sim 1/U$. The equation for diagonal eigenstates has the form of Harper equation with $\lambda_{\rm eff} = 2\lambda/V_{\rm eff} \gg 1$. Due to that these states are exponentially localized so that particles stay near the origin. In some sense, the interaction renormalizes the constant $\lambda \mapsto \lambda_{\rm eff}$ in the Harper equation for pair of particles. For strong U, the renormalized $\lambda_{\rm eff}$ is much larger than 1 that, according to the Aubry duality [14], leads to localization of TIP pairs in quasiperiodic potential. Our conjecture is that in a sense $\lambda_{\rm eff}$ remains larger than 1 even for moderate values of $U \sim 1$. In a sense interaction breaks Aubry duality leading to appearence of localized TIP phase. However more rigorous analytical confirmations of this conjecture are desirable especially keeping in mind that in a random potential the interaction with $U \sim 1$ leads to delocalization of TIP pair states. The accurate expressions for the TIP energy edges of shifted spectral band can be found using semiclassical analysis at small flux values by methods developed in [8,23]. The details of computations will be given elsewhere [24]. For the case of Fig. 2 (b), they give $E = 6.0 + 0.59 * 2\pi\alpha + O(\alpha^2)$ that is in good agreement with numerical data (Fig. 2 (b)).

For the part of the spectrum represented by unshifted butterfly at $U \gg 1$, the eigenstates become more and more similar to asymmetric TIP configuration i.e. $\phi_{n_1,n_2} = \mathrm{sign}(n_1 - n_2)\left(\chi^{(1)}_{n_1}\chi^{(2)}_{n_2} - \chi^{(1)}_{n_2}\chi^{(2)}_{n_1}\right)/\sqrt{2}$, where χ-s are one-particle eigenfunctions. Due to that, the effective interaction becomes quite small and the unshifted butterfly at large U (TfP are in different wells) looks very similar to the one at $U = 0$. The main difference is the splitting of Landau sublevels which appears due to effective small interaction between particles located in the same well. According to the expression for ϕ_{n_1,n_2}, such splitting can take place only when Landau quantum numbers are different ($m_1 \neq m_2$) so that $\chi^{(1)} \neq \chi^{(2)}$. As the result the first sublevel with $m_{1,2} = 0$ is not splitted. For non interacting part, the edges are given by the same $E_{\pm}(\alpha)$ as for $U = 0$ (see above) while for interacting case, the additional shift is $\delta E(\alpha) = -8\pi\alpha/(U+4)$ (see [24]). These analytical expressions are in good agreement with numerical results as shown in Fig. 2 (b).

In summary, *20 years after* [5] our investigations of spectra and eigenstates for TIP in the Harper model (1) show that repulsive/attractive interaction leads to appearance of localized states. Our conjecture is that due to Aubry duality breaking a localized TIP pair phase appears at arbitrary small interaction strength. At the same time we expect that this breaking is absent for TIP on the 2d-lattice with magnetic flux. However, the later model requires separate investigations [24].

This work is supported in part by the Fonds National Suisse de la Recherche.

---

[b] Also Budker Institute of Nuclear Physics, 630090 Novosibirsk, Russia.

[1] T. Geisel, R. Ketzmerick and G. Petschel, Phys. Rev. Lett. **66**, 1651 (1991); *ibid* **67**, 3635 (1991); *ibid* **69**, 695 (1992).
[2] I. Guarneri, G. Mantica, Phys. Rev. Lett. **73**, 3379 (1994).
[3] F. Piéchon, Phys. Rev. Lett. **76** 4372 (1996).
[4] P.G. Harper, Proc. Phys. Soc. Lond. A **68**, 874& 879 (1955).
[5] D.R. Hofstadter, Phys. Rev. B **14**, 2239 (1976).
[6] B. Pannetier, J. Chaussy, R. Rammal, J.-C. Villegier, Phys. Rev. Lett. **53**, 1845 (1984).
[7] R. Gerhardts, D. Pfannkuche, V. Gudmundsonn, Phys. Rev. B, to appear (1996).
[8] J. Bellissard in *Operator Algebras and Application*, Vol. 2, eds. D.E. Evans and M. Takesaki, Cambridge University Press (1988).
[9] B. Helffer, J. Sjöstrand, Suppl. Bull. Soc. Math. France, Tome 116, Fasc. 4, Mémoire 34 (1988).
[10] Y.Last, Comm. Math. Phys. **164**, 421 (1994).
[11] D.J. Thouless, Phys. Rev. B **28**, 4272 (1983).
[12] M. Wilkinson, J. Phys. A : Math. Gen. **20**, 4337 (1987).
[13] R. Artuso, F. Borgonovi, I. Guarneri, L. Rebuzzini, G. Casati, Phys. Rev. Lett. **69**, 3302 (1992); Int. J. Mod. Phys. B **6**, 207 (1994).
[14] S.Aubry and G.André, Ann. Israel Phys. Soc. **3**, 133 (1980).
[15] J. Bellissard, A. Barelli, in *Quantum Chaos-Quantum Measurement*, eds. P. Cvitanović, I.C. Percival and A. Wirzba (Kluwer, Dordrecht, 1992).
[16] I. Guarneri, F. Borgonovi, J. Phys. A **26**, 119 (1993).
[17] R. Lima, D. Shepelyansky, Phys. Rev. Lett. **67**, 1377 (1991).
[18] D.L.Shepelyansky, Phys. Rev. Lett. **73**, 2607 (1994); Y.Imry, Europhys. Lett. **30**, 405 (1995).
[19] D.L. Shepelyansky, to appear in Phys. Rev. B (1996).
[20] Y. Last, M. Wilkinson, J. Phys. A **25**, 6123 (1992).
[21] R. Rammal, J. Bellissard, J. Phys. France **51**, 1803 (1990).
[22] Ph. Jacquod, D.L. Shepelyansky, Phys. Rev. Lett. **75**, 3501 (1995).
[23] A. Barelli, R. Fleckinger, Phys. Rev. B **46**, 11559 (1992).
[24] A. Barelli, J. Bellissard, P. Jacquod, D.L. Shepelyansky, in preparation (1996).

Breit-Wigner width for two interacting particles in one-dimensional random potential

PH.JACQUOD [a], *D.L.SHEPELYANSKY* [b,d,f] and *O.P.SUSHKOV* [c,e,f]

[a] *Institut de Physique, Université de Neuchâtel,*

1, Rue A.L. Breguet, 2000 Neuchâtel, Suisse

[b] *Institute for Theoretical Physics, University of California*

Santa Barbara, CA 93106-4030

[c] *Institute for Theoretical Atomic and Molecular Physics,*

Harvard-Smithsonian Center for Astrophysics, MS14,

60 Garden Street, Cambridge, Massachusetts 02138

Abstract: For two interacting particles (TIP) in one-dimensional random potential the dependence of the Breit-Wigner width Γ, the local density of states and the TIP localization length on system parameters is determined analytically . The theoretical predictions for Γ are confirmed by numerical simulations.

PACS. 72.15Rn, 71.30+h

Recently, the problem of two interacting particles (TIP) in a random potential has attracted interest of different groups [1, 2, 3, 4, 6, 7]. It has been shown that two repulsive/attracting particles can propagate together on a distance l_c much larger than one-particle localization length l_1 in absence of interaction. The first analytical studies [1, 2] for TIP with on site interaction on a one-dimensional one channel lattice gave the following estimate $l_c/l_1 \sim \Gamma\rho \sim (U/V)^2 l_1$, where U is strength of the interaction, V is intersite hopping matrix element, $\rho \sim l_1^2/V$ is density of the two-particle states coupled by the interaction, and $\Gamma \sim U^2/Vl_1$ is the interaction induced transition rate between these states. The numerical investigations [3, 4] definitely confirmed existence of the strong enhancement of l_c due to interaction. However, a direct verification of the above estimate is quite difficult even for the modern computer facilities due to the strong increase of required basis with l_1. Also the recent numerical results of von Oppen et. al. [4] and Weinmann and Pichard [5] indicate in one-dimensional case almost linear growth of the enhancement factor for l_c with U instead of expected U^2. Due to all these things it would be important to have a more rigorous derivation of the factor l_c/l_1 for this on a first glance quite simple problem, at least in a one-dimensional case. To reach this aim we started from the computation of the rate Γ which also characterizes the spread width of the Breit-Wigner distribution for eigenfunctions in the basis of eigenstates of noninteracting particles[8, 9, 10]. If the parameter dependence of Γ is known then the ratio l_c/l_1 can be determined from the relation $l_c/l_1 \sim \Gamma\rho$ which have been checked in models of superimposed band random matrices [1, 8, 9, 10]. In the present work for calculation of Γ we use the technique developed in [11] which allows to account all orders in the interaction.

We consider one dimensional Hubbard model with Hamiltonian

$$H = -V\sum_{n\sigma}(a^\dagger_{n+1\sigma}a_{n\sigma} + a^\dagger_{n\sigma}a_{n+1\sigma}) + U\sum_n a^\dagger_{n\uparrow}a^\dagger_{n\downarrow}a_{n\downarrow}a_{n\uparrow} \tag{1}$$

Here $a^\dagger_n$ is a creation operator of the particle at the site n, V is hopping matrix element, and U is on site interaction. We assume that particles are distinguishable and denote the type of particle by spin $\sigma = \pm 1/2$. Single particle eigenstate is plane wave $|p\rangle = \frac{1}{\sqrt{L}}e^{ipn}$ with dispersion $\epsilon_p = -2V\cos p$, $-\pi \le p \le \pi$. We set lattice spacing equal to unity. The size of the lattice is denoted by L.

The Breit-Wigner width can be found in the following way. Forward scattering amplitude f for particles with different spins is given by series of diagrams presented at Fig.1. Solid line represents a particle, and wavy line is matrix element of the interaction $\langle p_3p_4|\hat{U}|p_1p_2\rangle = \frac{U}{L}\delta_{p_1+p_2,p_3+p_4}$. Due to optical theorem width of the state $|p_1p_2\rangle = |p_1\rangle|p_2\rangle$ is related to the forward scattering amplitude:

$$\Gamma/2 = -Im\ f. \tag{2}$$

One can easily check the coefficient in this relation considering diagram Fig. 1b which gives usual Fermi golden rule:

$$\begin{aligned}\Gamma \approx -2\ Imf_{1b} &= -2\ Im\sum_{p_3p_4}\frac{\left|\langle p_3p_4|\hat{U}|p_1p_2\rangle\right|^2}{E-\epsilon_3-\epsilon_4+i0} = \\ &= 2\pi\sum_{p_3p_4}\left|\langle p_3p_4|\hat{U}|p_1p_2\rangle\right|^2\delta(E-\epsilon_3-\epsilon_4).\end{aligned} \tag{3}$$

Here E is energy of the initial state $E = \epsilon_1 + \epsilon_2$.

Born term in the amplitude f is given by Fig. 1a and equals $f_{1a} = U/L$. Calculation of the diagram Fig. 1b is also straightforward

$$f_{1b} = \sum_{p_3p_4}\frac{\left|\langle p_3p_4|\hat{U}|p_1p_2\rangle\right|^2}{E-\epsilon_3-\epsilon_4+i0} = \frac{U^2}{L^2}\sum_{p_3}\frac{1}{E+2V\cos p_3+2V\cos(p-p_3)} =$$

$$= \frac{U^2}{L^2}\int_{-\pi}^{\pi}\frac{Ldp_3/2\pi}{[E+2V\cos p_3+2V\cos(p-p_3)]} = \frac{U^2/L}{\sqrt{E^2-16V^2\cos^2 p/2}}, \qquad (4)$$

where $p = p_1 + p_2 = p_3 + p_4$ is total quasi-momentum. Higher orders in Fig. 1 correspond to simple iterations of the box Fig. 1b. Therefore summation of the ladder is reduced to geometrical progression and the result is

$$f(E,p) = \frac{U/L}{1 - U/\sqrt{E^2-16V^2\cos^2 p/2}}. \qquad (5)$$

The scattering amplitude depends only on total energy $-4V \le E \le 4V$ and total momentum $-\pi \le p \le \pi$. The branch of square root should be chosen in such a way that $Im\, f \le 0$.

With amplitude (5) one can easily calculate the Breit-Wigner width using optical theorem (2). But we are interested in the average width at given energy. So we have to average over momentum p. Density of the two particle states is of the form

$$\begin{aligned}\rho(E,p) &= \int_{-\pi}^{\pi}\frac{Ldp_1}{2\pi}\int_{-\pi}^{\pi}\frac{Ldp_2}{2\pi}\delta(p-p_1-p_2)\delta(E+2V\cos p_1+2V\cos p_2) = \\ &= \frac{L^2/(8\pi^2V)}{\sqrt{\cos^2 p/2 - E^2/16V^2}}. \qquad (6)\end{aligned}$$

It is nonzero only if square root is real. After integration over momenta we find

$$\rho(E) = \int_{-\pi}^{\pi}\rho(E,p)\frac{dp}{2\pi} \approx \frac{L^2}{2\pi^2V}\left(\ln\frac{16V}{|E|} + 0.18\frac{|E|}{4V}\right) \qquad (7)$$

The integral in (7) can not be exactly expressed in terms of elementary functions. Presented approximate formula is valid with accuracy better than 1% in the interval $-4V \le E \le 4V$. Now we can find the average Breit-Wigner width.

$$\begin{aligned}\Gamma(E) &= -2\, Im \int f(E,p)\rho(E,p)\frac{dp}{2\pi}\Big/\rho(E) = \\ &= \frac{8Vu^2/L}{(\ln 4/\epsilon + 0.18\epsilon)\sqrt{|u^2-\epsilon^2|(1+u^2-\epsilon^2)}}\cdot F(Z). \qquad (8)\end{aligned}$$

Here $u = |U/4V|$ and $\epsilon = |E/4V|$ is interaction and energy expressed in units of band width: $0 \leq \epsilon \leq 1$. The function $F(Z)$ is defined by

$$F(Z) = \begin{cases} \arctan Z, & \text{for u} \geq \epsilon \\ \frac{1}{2}\ln\frac{1+Z}{1-Z}, & \text{for u} \leq \epsilon \end{cases} \tag{9}$$

$$Z = \sqrt{\frac{|u^2-\epsilon^2|(1-\epsilon^2)}{\epsilon^2(1+u^2-\epsilon^2)}}.$$

At small energy ($\epsilon^2 \ll u^2, 1$) formula (8) can be substantially simplified

$$\Gamma \approx \frac{4\pi V}{L} \cdot \frac{1}{\ln 4/\epsilon} \cdot \frac{u}{\sqrt{1+u^2}}, \tag{10}$$

so that at small interaction ($\epsilon^2 \ll u^2 \ll 1$) it is linear in the interaction. In other limit ($u^2 \ll \epsilon^2$, $(1-\epsilon^2)$) the width (8) is quadratic in the interaction with logarithmic correction:

$$\Gamma \approx \frac{8V}{L} \cdot \frac{1}{(\ln 4/\epsilon + 0.18\epsilon)} \cdot \frac{u^2}{\epsilon} \ln \frac{2\epsilon\sqrt{1-\epsilon^2}}{u} \tag{11}$$

The value of Γ in (10) is significantly larger than in (11) due to the growth of two-particle density of states (7) near the center of the band.

If we now add to the Hamiltonian (1) a single particle random potential $H_{rand} = \sum w_n a^\dagger_{n\sigma} a_{n\sigma}$ with a disorder homogeneously distributed in the interval $-W \leq w_n \leq W$, then one particle eigenstates in infinite lattice become localized with localization length $l_1 \approx 24(V/W)^2\sqrt{1-\epsilon_1^2/4V^2}$, where ϵ_1 is one particle energy. However as soon as $l_1 \gg 1$ the above calculation of the average width remains valid. The reason for this is that $l_1 \gg 1$ is the only condition which we need to formulate scattering problem and to use conventional diagram technique. Distribution of Γ depends on the relation between size of the box L and the localization length l_1. If $L \leq l_1$ all values of Γ are of the order

of the average value given by (8). For $L \gg l_1$ the average value is still given by (8). However in this case Γ vanishes for majority of the states . These are the states in which particles are localized far from each other and practically do not interact. On other hand the width for the states with interparticle distance of the order l_1 is approximately the same as for particles in a box of size $L \approx l_1$ so that Γ is given by eqs.(8),(9) with L replaced by l_1. The two-particle localization length l_c for such states is determined by the relation $l_c/l_1 \sim \Gamma(E)\rho(E)$, with Γ calculated at $L \sim l_1$. This relation is valid if many unperturbed states are mixed by interaction [1, 2] so that $\Gamma(E)\rho(E) > 1$. In the opposite case $\Gamma(E)\rho(E) \ll 1$ the above relation is not valid [8, 9, 10] and the interaction can be treated in a perturbative way. In this regime "Rabi oscillations" between two quasi-degenerate levels play an important role [5].

Above we have considered distinguishable particles. The generalization to identical particles is rather simple: the width Γ vanishes if coordinate wave function is antisymmetric, and it is doubled in comparison with eqs.(8), (9) if coordinate wave function is symmetric.

To check the above theoretical formula for the Breit-Wigner width Γ we studied numerically the model (1) of two identical interacting particles (symmetric coordinate wave function) in the disordered potential on a ring of size L which is less or comparable with one-particle localization length $l_1 \approx 24(V/W)^2$. Using Lanczos technique (see for example [12]) we determined the local density of states for symmetric configurations in the basis of noninteracting eigenstates:

$$\rho_W(E - \epsilon_{m_1} - \epsilon_{m_2}) = \sum_\lambda |\psi_\lambda(m_1, m_2)|^2 \delta(E - E_\lambda) \qquad (12)$$

Here E_λ is the eigenenergy of TIP while $\epsilon_{m_{1,2}}$ are one-particle eigenenergies. The dependence of ρ_W on E is well described by the Breit-Wigner distribution

$$\rho_W(E) = \frac{\Gamma}{2\pi[E^2 + \Gamma^2/4]} \tag{13}$$

an example of which is shown in Fig.2 . The comparison of numerically obtained Γ with theoretical prediction (8), (9) in the regime $\Gamma(E)\rho(E) > 1$ is shown in Figs.3,4 for different energies as the function of interaction. The theory gives good agreement with numerical results for $15 \leq L \leq 300$ and variation of scaled width $\Gamma L/V$ by more than 2 orders of magnitude. For the states with the energy close to the band center ($E \approx 0$) (Fig.3) the dependence of $\Gamma\rho$ on U is almost linear for $U < V$ (see (7), (10)). Therefore, the TIP localization length l_c according to the relation $l_c/l_1 = C\Gamma\rho \approx 2Cl_1(U/V)/\pi$ also varies linearly with U. Here, we took the values of Γ and ρ at $L = l_1$ and introduced the numerical coefficient C to take into account the uncertainty of this choice. According to the numerical results [4] at the center of the band $l_c/l_1 \approx 0.2l_1(U/V)$ which is in good agreement with the above theoretical expression and gives $C \approx 1/4$.

For energies away from the band center and small interaction $|U| \ll |E|$ the enhancement factor according to (7), (11) is $l_c/l_1 \approx l_1U^2\ln(2E/U)/(4\pi^2VE)$ where we have used the above value of C. The dependence on U is almost quadratic in agreement with the first estimate [1, 2]. However, due to the logarithmic correction, to observe clearly the U^2 behavior one should go to really small U values and since the condition $\Gamma\rho > 1$ should be also satisfied this can be reached only for quite large values of l_1 or L. In this respect our numerical approach based on the measurement of Γ is more efficient than the one used in [4]. It allows to see the behavior $U^2 \ln U$ away from the band center in agreement with

the theory (8), (9) (see insert in Fig.4). At moderate $U/V > 0.3$ values in the presence of numerical fluctuations the dependence of Γ on U is hardly distinguishable from a linear one (see normal scale in Fig.4). In our opinion this is the reason why the linear behavior in U had been attributed in [4] also to the states away from the band center. As for the result of Ref. [5] the system size there was too small ($L = 25$) and the main part of the data (Fig. 4 with $U/V < 0.4$) corresponds to the different regime $\Gamma\rho < 1$. In this perturbative case the typical energy scale which determines the change in level statistics is determined by Rabi oscillation frequency in a pair of quasi-degenerate states which is proportional to U [5]. Also, one should keep in mind that the results there are integrated over the whole energy band including the center of the band where the dependence on U is linear even for $\Gamma\rho > 1$.

Turning back to our numerical data (Fig. 4) we would like to mention that there is a significant difference from the theory for negative $U < -1$.. Generally, we should expect such difference for $|U| \gg 1$ when the spectrum is composed from two separated energy bands and the basis of plane wave used for computation of width Γ becomes inadequate. However, we cannot say why this change goes in so asymmetric way for negative and positive U while for $|U| < 1$ the width Γ is independent of sign U in agreement with the theory. We would like to note that such asymmetry for attraction and repulsion away from the band center and relatively strong interaction $U \approx V$ has been seen recently in [4] for the ratio l_c/l_1. Also a change in the behavior of Γ has been observed in [5] for $U > V$.

In summary, taking diagrammatically into account the effects of interaction we have

derived the analytical formula for the Breit-Wigner width Γ which determines the enhancement factor $l_c/l_1 \sim \Gamma\rho > 1$ for TIP in one-dimensional random potential. Our analytical and numerical approaches can be also used for calculation of the TIP width in 2- and 3-dimensional disordered systems where according to Imry estimate [2] interaction between two quasi-particles can strongly affect transport properties.

We acknowledge fruitful discussions with V.V. Flambaum, M.Yu. Kuchiev and P.G.Silvestrov. We also thank the Centro Svizzero di Calcolo Scientifico for allocation of CPU time on their NEC SX-3. One of us (OPS) thanks Laboratoire de Physique Quantique, Université Paul Sabatier for hospitality and financial support during the initial stage of this work. This research was supported in part by the National Science Foundation under Grant No. PHY94-07194, NSF through a grant for the Institute for Theoretical Atomic and Molecular Physics at Harvard University and the Smithsonian Astrophysical Observatory and the Fonds National Suisse de la Recherche.

References

[d] On leave from Laboratoire de Physique Quantique, UMR C5626 du CNRS, Université Paul Sabatier, 31062 Toulouse Cedex, France

[e] On leave from School of Physics, The University of New South Wales, Sydney 2052, Australia

[f] Also : Budker Institute of Nuclear Physics, 630090 Novosibirsk, Russia

[1] D.L. Shepelyansky, Phys. Rev. Lett. **73**, 2607 (1994).

[2] Y. Imry, Europhys. Lett **30**, 405 (1995).

[3] K. Frahm, A. Müller-Groeling, J.-L. Pichard and D. Weinmann, Europhys. Lett. **31**, 405 (1995); D. Weinmann, A. Müller-Groeling, J.-L. Pichard and K. Frahm, Phys. Rev. Lett. **75**, 1598 (1995).

[4] F. von Oppen, T. Wettig and J. Müller, Phys. Rev. Lett. **76**, 491 (1996); F. von Oppen and T. Wettig, Proc. Int. Conf. "Correlated fermions and transport in mesoscopic systems, XXXIst Rencontres de Moriond (1996).

[5] D. Weinmann and J.-L. Pichard, Phys. Rev. Lett. **77**, 1556 (1996).

[6] F. Borgonovi and D.L. Shepelyansky, Nonlinearity **8**, 877 (1995); J. de Phys. I France **6**, 287 (1996).

[7] K. Frahm, A. Müller-Groeling and J.-L. Pichard, Phys. Rev. Lett. **76**, 1509 (1996).

[8] P. Jacquod and D. L. Shepelyansky, Phys. Rev. Lett. **75**, 3501 (1995).

[9] Y. V. Fyodorov and A. D. Mirlin, Phys. Rev. B **52**, R11580 (1995).

[10] K. Frahm and A. Müller-Groeling, Europhys. Lett. **32**, 385 (1995).

[11] O.P.Sushkov, unpublished (1996).

[12] E.Dagotto, Rev. Mod. Phys. **66**, 763 (1994).

Figure captions

Fig. 1: Diagrams for the forward scattering amplitude f in (2) - (5).

Fig. 2: Local spectral density $\rho_W(E)$ computed for the TIP eigenstates in the energy interval $[-0.1, 0.1]$ for the case $L = 150$, $U = 1$, $V = 1$, and $W = 0.4$. The full line gives the best Breit-Wigner fit (13) with $\Gamma = 0.0073$. The theoretical prediction is $\Gamma = 0.0072$.

Fig. 3: Scaled Breit-Wigner width $\Gamma L/V$ as a function of the rescaled interaction $\frac{U}{4V}$ computed in the energy interval $E/V \in [-0.1, 0.1]$. The system size is $L = 15$ ($W/V = 1.$, empty circles), $L = 25$ ($W/V = 1.$, empty squares), $L = 40$ ($W/V = 0.6$, empty diamonds), $L = 60$ ($W/V = 0.5$, full circles), $L = 80$ ($W/V = 0.5$, full squares), $L = 100$ ($W/V = 0.5$, full diamonds) $L = 150$ ($W/V = 0.4$, full triangles up) and $L = 200$ ($W/V = 0.35$, full triangles down). The solid line gives the theoretical prediction (8), (9) multiplied by 2 to take symmetrization into account.

Fig. 4: Scaled Breit-Wigner width $\Gamma L/V$ as a function of the rescaled absolute value of the interaction $\frac{|U|}{4V}$ computed in the energy interval $E/V \in [1., 1.2]$. The system size is $L = 15$ ($W/V = 1.$, empty circles), $L = 25$ ($W/V = 1.$, empty squares and $W/V = 0.5$, empty diamonds), $L = 40$ ($W/V = 0.8$, empty triangles up and $W/V = 0.5$, empty triangles down), $L = 60$ ($W/V = 0.5$, full circles), $L = 80$ ($W/V = 0.5$, full squares), $L = 100$ ($W/V = 0.5$, full diamonds), $L = 100$ ($W/V = 0.5$, negative U, crosses), $L = 150$ ($W/V = 0.4$, full triangles up), $L = 200$ ($W/V = 0.35$, full triangles down) and $L = 300$ ($W/V = 0.25$, full triangles left).

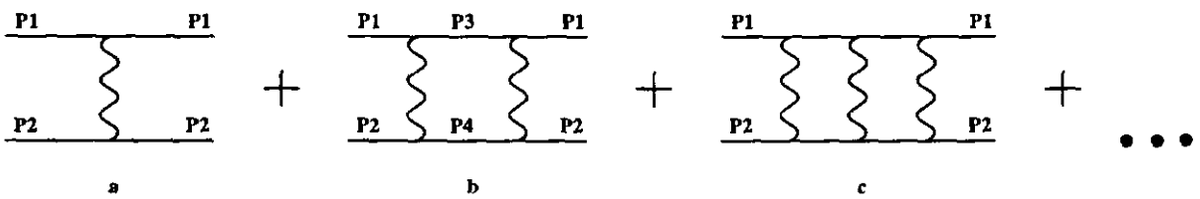

FIG. 1

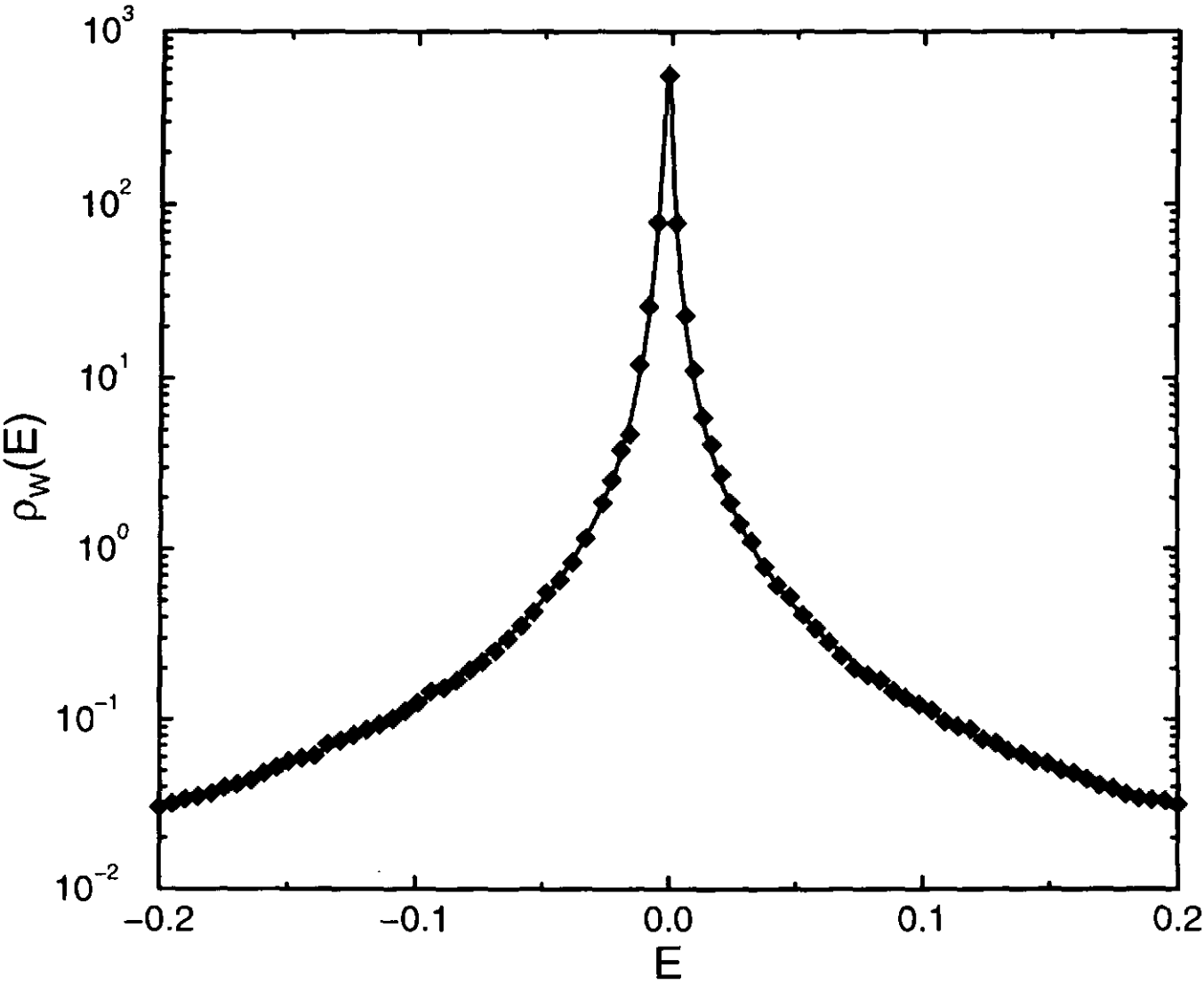
10^3
10^2
10^1
10^0
10^{-1}
10^{-2}
$\rho_W(E)$
−0.2
−0.1
0.0
0.1
0.2
E

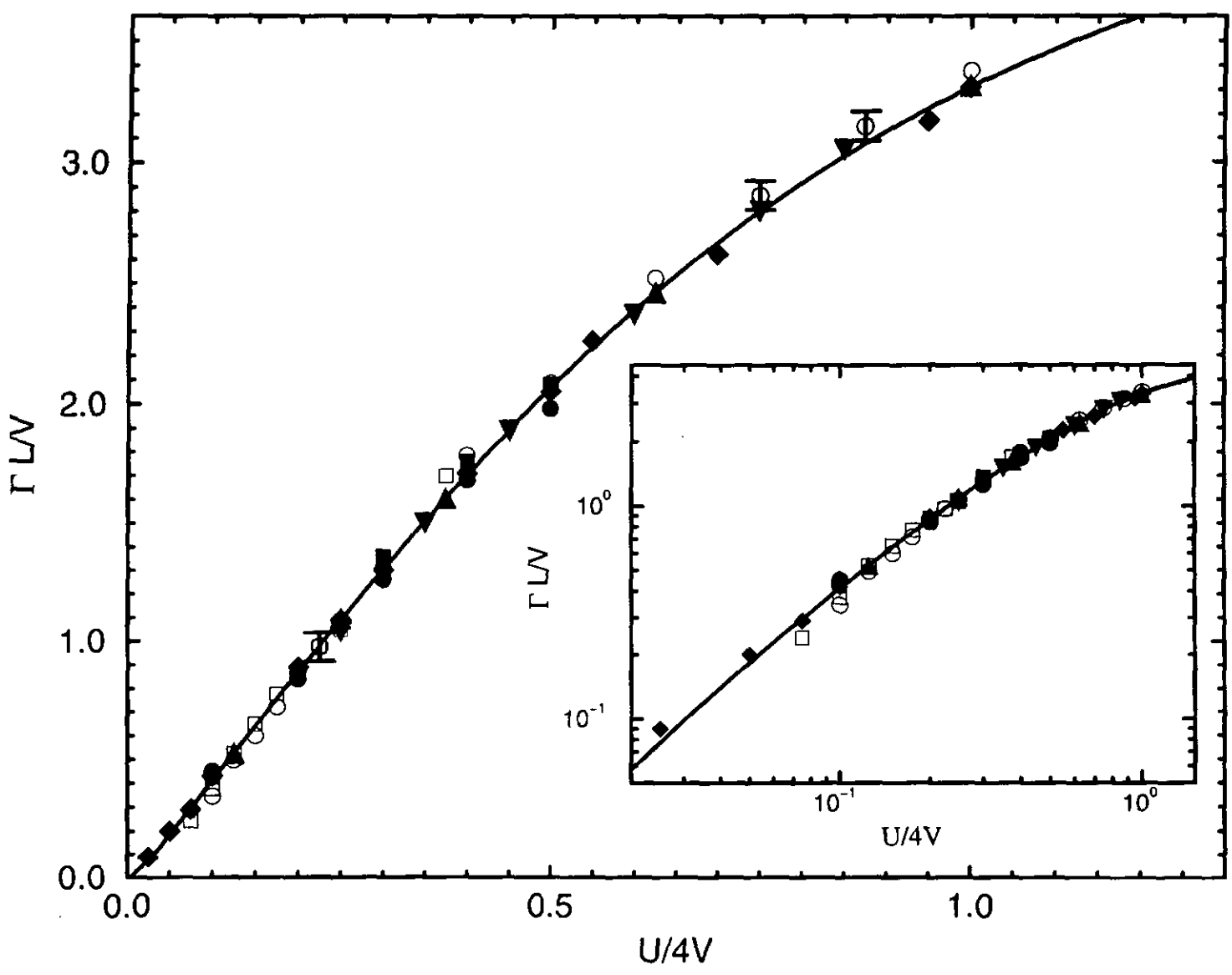
3.0
2.0
1.0
0.0
Γ L/V
0.0
0.5
1.0
U/4V
10^0
10^-1
Γ L/V
10^-1
10^0
U/4V

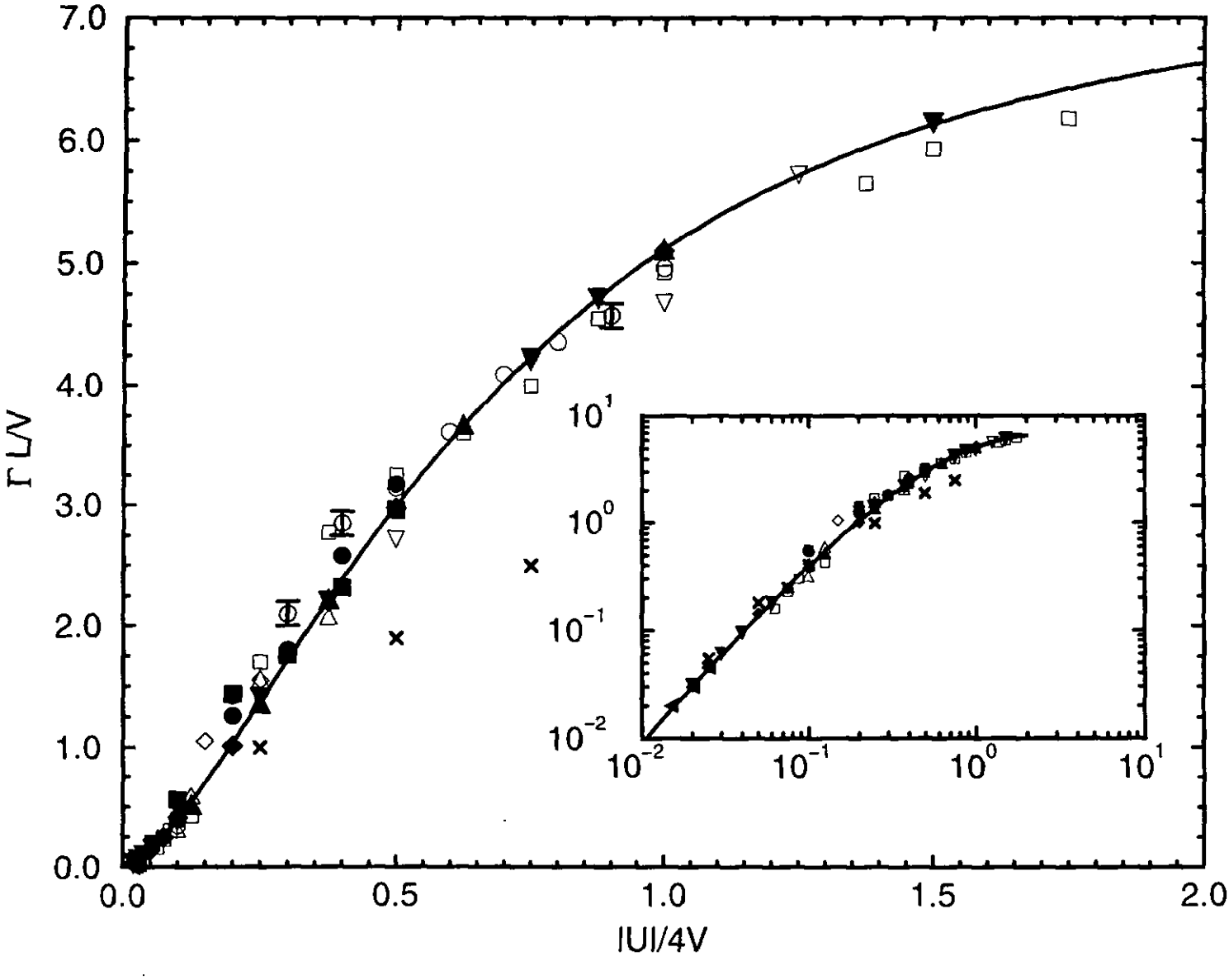
7.0
6.0
5.0
4.0
3.0
2.0
1.0
0.0
Γ L/V
0.0
0.5
1.0
1.5
2.0
|U|/4V
10^1
10^0
10^-1
10^-2
10^-2
10^-1
10^0
10^1

NEIP-96-005 March 25, 1997

On the Convergence to Ergodic Behavior of Quantum Wave Functions

Ph. Jacquod [1] and J.-P. Amiet [2]

Institut de Physique
Université de Neuchâtel
1, Rue A.L. Breguet
CH - 2000 Neuchâtel

Abstract

We study the decrease of fluctuations of diagonal matrix elements of observables and of Husimi densities of quantum mechanical wave functions around their mean value upon approaching the semi-classical regime ($\hbar \to 0$). The model studied is a spin (SU(2)) in a classically strongly chaotic regime. We show that the fluctuations are Gaussian distributed, with a width σ^2 decreasing as the square root of Planck's constant. This is consistent with Random Matrix Theory (RMT) predictions, and previous studies on these fluctuations [1, 2]. We further study the width of the probability distribution of $\hbar$-dependent fluctuations and compare it to the Gaussian Orthogonal Ensemble (GOE) of RMT.

[1] e-mail philippe.jacquod@iph.unine.ch
[2] e-mail amiet@iph.unine.ch

The behaviour of quantum mechanical wave functions in the semiclassical limit has recently attracted much interest. It is motivated by the fact that the spectrum alone cannot contain the whole information on the system. Roughly, one can say that in integrable systems the eigenfunctions condense on classically invariant torii, while in chaotic ones, where such classical structures have been destroyed, they tend to spread uniformly over the whole classically allowed region. Few analytical results have been obtained however in chaotic regimes, the most important of which perhaps is the Shnirelman theorem. One formulation of this theorem would be that in the limit $\hbar \to 0$, almost all the diagonal matrix elements of almost all quantum mechanical observables converge weakly to a constant over the classically chaotic region [3]. A few years ago Feingold and Peres [2] and more recently, Eckhardt et. al. [1] have studied the rate of this convergence for autonomous systems where the semiclassical limit is, according to the Shnirelman theorem, the microcanonical phase-space (i.e. classical) average. As they mentioned, the "almost all quantum mechanical observables" in this formulation exclude projection operators, and in general all operators without smooth classical limit. Moreover, the "almost all diagonal matrix elements" still leave room for scarring of eigenstates by short periodic orbits [4]. For those states, the limit can be dramatically different from the Shnirelman-predicted one. Their conclusion is that in a strongly chaotic system and for a smooth classical observable $A(p,q)$ with which a quantum operator $\hat{A}$, $A_{jk} :=< E_j|\hat{A}|E_k >$, can be associated, the fluctuations of the diagonal matrix elements

$$< F_j^2 >:=< (A_{jj} - \{A\})^2 > \tag{1}$$

around the semiclassical microcanonical average

$$\{A\} = \int A(p,q)\delta(E - H(p,q))d^d p d^d q / \int \delta(E - H(p,q))d^d p d^d q \tag{2}$$

have the same order of magnitude as the mean square of the off-diagonal terms $< |A_{jk}|^2 >$ and decrease proportionally to the inverse of the Heisenberg time $1/T_H \sim \hbar$ upon approaching the semiclassical limit, in agreement with Random Matrix Theory (RMT) predictions. Here $|E_{j,k} >$ are energy eigenstates of the Hamiltonian under consideration, i.e. $H|E_{j.k} >= E_{j,k}|E_{j,k} >$ and $< .. >$ means an average taken over neighboring (in energy) eigenstates. Their arguments are valid provided E_j and E_k are not too distant from each

other, but they do no need to be consecutive eigenvalues. Accordingly, the interval of energy over which the average are taken may or may not overlap. They related the proportionality coefficient to the autocorrelation function of the classical dynamical variable A, $C(t) := \lim_{T\to\infty} \frac{1}{T}\int_0^T A(t+\tau)A(\tau)d\tau$, i.e.

$$< F_j^2 >= \frac{2}{T_H}\int_0^\infty dtC(t) \tag{3}$$

In particular, almost all diagonal elements A_{jj} tend to the semiclassical microcanonical average as $\hbar \to 0$. Eq.(3) states among others that *quantum fluctuations are proportional to classical correlations.* Their argument goes as follows : According to Shnirelman's theorem, the diagonal matrix element

$$< E_j|\hat{A}(t)\hat{A}(0)|E_j > \to C(t) \qquad ; \qquad \hbar \to 0 \tag{4}$$

On the other hand, this matrix element is

$$\begin{aligned} < E_j|\hat{A}(t)\hat{A}(0)|E_j > &= \sum_k \exp\left[i(E_j - E_k)t/\hbar\right]|A_{jk}|^2 \\ &= \sum_{k\neq j} \exp\left[i(E_j - E_k)t/\hbar\right]|A_{jk}|^2 + |A_{jj}|^2 \end{aligned} \tag{5}$$

Thus we have

$$\sum_{k\neq j} \exp\left[i(E_j - E_k)t/\hbar\right]|A_{jk}|^2 \to C(t) - \{A\}^2 \qquad ; \qquad \hbar \to 0 \tag{6}$$

Defining the Fourier Transform of the autocorrelation function $S(\omega) := \int_{-\infty}^{\infty} C(t)\exp(-i\omega t)dt$ we have

$$|A_{jk}|^2 \approx S((E_j - E_k)/\hbar)/(2\pi\rho(E)) = \int_{-\infty}^{\infty}\left[C(t) - \{A\}^2\right]dt \quad ; \quad E_j \to E_k \tag{7}$$

Then, under the assumption that as $E_j \to E_k$, the eigenfunctions $|E_j >$, $|E_k >$ and $|\pm >:= \frac{1}{\sqrt{2}}(|E_j > \pm |E_k >)$ are qualitatively similar, i.e. :

$$\begin{aligned} A_{jk} &\approx < -|\hat{A}|+ > \\ \{A\} &\approx < +|\hat{A}|+ > \approx < -|\hat{A}|- > \end{aligned} \tag{8}$$

we have

$$A_{jk} \approx < -|\hat{A}| + > = \frac{1}{2}(A_{jj} - A_{kk} + A_{jk} - A_{kj}) \tag{9}$$

Finally defining the fluctuations as $F_j := A_{jj} - \{A\}$ and assuming statistical independence of the F_j's, i.e. the average $< F_j^2 >=< F_k^2 >= 2 < |A_{jk}|^2 >$ does not depend on the indices j and k, we get eq. (3). Illustrations of this result on the double rotator model [2], the bakers map and the hydrogen atom in a magnetic field [1] nicely confirmed these predictions. These are to our knowledge the only works that delt with the qualitative description of the approach to ergodicity of quantum mechanical wave functions. Here, we extend these results to a kicked (e.g. non autonomous) system. We will focus on the fluctuations of the Husimi density of the eigenstates, i.e. study the fluctuations of the diagonal matrix elements of the projection operator over coherent states [5]. The Hamiltonian

$$H := \frac{\hbar}{4ST} S_z^2 + \frac{\hbar\kappa}{T} S_y \sum_{n=-\infty}^{+\infty} \delta(t - nT) \tag{10}$$

is expressed in term of the usual SU(2) spin operators S_x, S_y and S_z, while $0 \leq \kappa \leq 2\pi$. Models of this kind have been extensively studied [6] and are usually referred to as "kicked tops". They represent a spin which evolves during a time T under the influence of an integrable hamiltonian after which it undergoes a rotation of angle κ around the y-axis. It thus defines the time evolution (Floquet) operator :

$$U_T := \exp(-i\frac{\kappa}{T} S_y) \exp(-\frac{i}{4S} S_z^2) \tag{11}$$

Previous investigations of this model have illustrated the remarkable agreement of its spectral properties with the GOE/COE of RMT [3]. In this article we will consider fluctuations of expectations values of $SU(2)$ operators taken over eigenstates of the Floquet operator (11). The above argument leading to eq. (3) must be slightly modified in order to apply to the map defined by eq.(10) and eq.(11). Instead of working with energy eigenstates $|E_j >$ of an autonomous Hamiltonian, we deal with quasienergy eigenstates $|\omega_j >$ of

[3] We recall the agreement of GOE and COE (Circular Orthogonal Ensemble) properties in the limit of large matrices $N \to \infty$ [7].

an unitary time evolution operator. As a consequence, the microcanonical average of eq.(2) is replaced by a phase space integral restricted to the corresponding connected chaotic region. In our case and in a strongly chaotic regime eq.(2) reads :

$$\{A\} = \int_{\mathcal{S}^2} A(\theta,\phi)\sin(\theta)d\theta d\phi / \int_{\mathcal{S}^2} \sin(\theta)d\theta d\phi = \frac{1}{4\pi}\int_{\mathcal{S}^2} A(\theta,\phi)\sin(\theta)d\theta d\phi \quad (12)$$

i.e. we integrate over the whole sphere $\mathcal{S}^2$ instead of the energy surface. In the semiclassical limit, the diagonal matrix elements

$$< \omega_j|\hat{A}(t)\hat{A}(0)|\omega_j >= \sum_k \exp\left[i(\omega_j - \omega_k)t/\hbar\right]|A_{jk}|^2 \rightarrow C(t) \quad (13)$$

provided the regime studied is classically strongly chaotic. Moreover, a similar argument as before leads to

$$|A_{jk}|^2 \approx S((\omega_j - \omega_k)/\hbar) \quad (14)$$

and hence we recover eq.(3). Here, we concentrate on the study of the eigenstates of the unitary operator eq.(11) in the regime $T = 50$ and $\kappa = 1.2$. By standard numerical computation of the Liapounov exponent [8] over the whole phase space, we checked that in this regime the classical motion is strongly chaotic. Moreover, we checked that the quantum mechanical operator eq.(11) exhibits the usual characteristics of quantum chaos : its level spacings statistics and spectral rigidity follow the predictions of the GOE/COE of RMT. We stress that even though the perturbation destroys the time-reversibility of the system, a surviving symmetry still persists $\prod|\mu >= |-\mu >$. Because of the existence of this antiunitary symmetry, the model obeys GOE/COE [9].
As mentioned in [1] the Shnirelman theorem leaves room for wave functions to show large deviation from the semiclassical limit value. It only states that the proportion of such wave functions should be negligible, i.e. in the semiclassical limit, they build a subset of zero measure. For "almost all eigenfunctions" then, the variance of these fluctuations should vanish as $\hbar \rightarrow 0$. However, this decay can be substantially perturbed by scarring of eigenfunctions by short periodic orbit [4] : Scarred eigenfunctions are front-line candidates for exceptions to the Shnirelman theorem ! Thus they could significantly - and negatively - affect our results. We must therefore find a way to estimate

and eventually reduce the ratio of such eigenstates and to this purpose we introduce the *level curvature* [10, 11]. The level curvature is a measure of the sensitivity of an eigenvalue to an external perturbation. In our model (10) for instance we can define it as the second derivative of an eigenvalue with respect to κ :

$$K_n = \frac{d^2\omega_n(\kappa, T)}{d\kappa^2} \tag{15}$$

Intuitively, when the studied regime is highly chaotic, the spectrum shows a level repulsive behavior which results in a number of avoided crossings when varying one parameter. In the direct vicinity of an avoided crossing, the curvature of two levels can be huge and therefore the distribution of these values depends very sensitively on the regime studied, i.e. on both κ and T. Scarred eigenstates shift almost linearly in energy when varying one parameter and hence have generally small level curvatures. Consequently, it has been suggested that scarring manifests itself in deviations of RMT predictions in the level curvature distribution [10, 11]. Though not yet rigorously proven, this statement is now widely accepted. This distribution for the model defined by eq.(11) in the regime studied is shown in fig.1. There is a remarkable agreement with the GOE/COE (full curve) prediction [10]

$$P(k) = \frac{1}{2}\frac{1}{(1+k^2)^{3/2}} \qquad k = \frac{K}{\pi\bar{\rho} < (\frac{d\omega_n}{d\kappa})^2 >} \tag{16}$$

Here $\bar{\rho} = 2\pi/(2s+1)$ is the averaged level density. This indicates a small number of scarred eigenstates, an agreement which was already obtained on a similar model in [10]. Therefore, scarring is not likely to influence our study. Let us briefly outline our method. Our goal is to study the behaviour of eigenstates of eq. (11) in the semiclassical limit, i.e. as $\hbar \to 0$, $S \to \infty$ so as to leave the product $\hbar S$ constant. A peculiarity of such systems is that the parameter governing the convergence to the semiclassical limit governs too the number of states $2S+1 \sim 1/\hbar$ and the density of states. In order to determine the implication of this peculiarity on our study, we will therefore check the validity of our results on GOE matrices.
The Husimi density of an eigenstate $|\omega >= \sum_{\mu=-S}^{S} \omega_\mu |\mu >$ of eq.(11) is defined as the projection of this state onto a coherent state $|\theta, \phi >$ of the spin SU(2) group [5] :

$$\Omega_\omega^S(\theta, \phi) := | < \omega|\theta, \phi > |^2$$

$$|\theta,\phi>:=\sum_{\mu=-s}^{s}\sqrt{\binom{2s}{s-\mu}}\sin(\tfrac{\theta}{2})^{s-\mu}\cos(\tfrac{\theta}{2})^{s+\mu}e^{i(s-\mu)\phi}|\mu> \qquad (17)$$

The Husimi density satisfies the assumptions of the Shnirelman theorem [3]. Indeed one formulation of the latter refers to the uniform spreading of eigenstates $|\Psi_{\text{chaos}}>$ over a connected chaotic region of phase space which implies that

$$\Omega_{\Psi}^{S}(\theta,\phi)=|<\Psi_{\text{chaos}}|\theta,\phi>|^2\longrightarrow\begin{cases}0 & \text{on the regular region}\\ \text{const} & \text{on the chaotic region}\end{cases} \qquad (18)$$

Thus in our model, as $\hbar\to 0$, the Husimi density converges weakly to a constant over the whole phase space. The Ω_{ω}^{S} are smooth functions of θ and ϕ and thus can be expanded in a multipole expansion over the basis of spherical harmonics :

$$\Omega_{\omega}^{S}(\theta,\phi)=\sum_{l,m}\sqrt{\tfrac{4\pi}{2l+1}}\Omega_{l,m}^{S}Y_{l,m}(\theta,\phi) \qquad (19)$$

where $l=0,1,2,...2S$ and $m=-l,-l+1,-l+2,...l$ and $|\mu>$ is an eigenstate of S_z, i.e. $S_z|\mu>=\mu|\mu>$. We used the convention to introduce the square root in this expansion. This multipole expansion allows us to interpret the $\Omega_{l,m}^{S}$ in term of magnitude of fluctuations of size $\sim\frac{\pi}{m+1}$ in the ϕ-direction and $\sim\frac{2\pi}{l+1}$ in the θ direction. We will thus get quantitative results on the decrease of fluctuations as a function of their size. Let us recall that the Shnirelman theorem implies that as $\hbar=1/S\to 0$, fluctuations of fixed and non zero l must vanish, i.e. : $\Omega_{\omega}^{S}(\theta,\phi)\to\Omega_{0,0}^{S}$. However it does not say anything about the behaviour of, say, $\Omega_{l(S),m(S)}^{S}$ as $S\to\infty$ when $l(S)$ and $m(S)$ are monotonously increasing functions of S , i.e. investigating such multipoles could lead us to different conclusions than that of [1, 2].
Using the resolution of unity :

$$\mathbf{1}=\frac{2s+1}{4\pi}\int d\theta d\phi\sin\theta|\theta,\phi><\theta,\phi| \qquad (20)$$

the normalization condition reads :

$$\begin{aligned}1\ &=<\omega|\mathbf{1}|\omega>=(2S+1)\Omega_{0,0}^{S}\\ &\Rightarrow\Omega_{0,0}^{S}=\frac{1}{4(2S+1)}\end{aligned} \qquad (21)$$

i.e. the $0^t h$ moment decrease as $1/S \sim \hbar$ on approaching the semiclassical limit. Let us note that this $1/S$ behaviour of the Shnirelman limit $\Omega^S_{0,0}$ is a consequence of the overcompleteness of the coherent states representation which necessitates the $2s+1$ factor in the resolution of unity (20), hence it has no direct physical meaning. In the following, we therefore divide all higher multipoles $\Omega^S_{l,m}$ by $\Omega^S_{0,0}$ to consistantly study their decrease and introduce the notation $\hat{\Omega}^S_{l,m} := \frac{\Omega^S_{l,m}}{\Omega^S_{0,0}}$. On the other hand we have :

$$\hat{\Omega}^S_{l,m} = 4(2S+1) \sum_{\mu=-s}^{s} \omega^*_\mu \omega_{\mu+m} (-1)^{s-\mu} C^{s,s,l}_{s,-s,0} C^{s,s,l}_{\mu+m,-\mu,m} \tag{22}$$

which gives a check of our numerical computation for small S. However, the numerical difficulty for computing the Clebsch-Gordan coefficients $C^{s,s,l}_{\mu+m,-\mu,m}$ for large S leads us to use the following numerically more stable and faster method to compute the multipoles $\hat{\Omega}^S_{l,m}$. We define :

$$M^S_{k,m}(\omega) := 4(2S+1) < \omega | S^k_z S^m_- | \omega > / S^{k+m} \tag{23}$$

It is straightforward to see that there is a linear relation between the $M^S_{k,m}$ and the $\hat{\Omega}^S_{l,m}$: (We use the shorter notation $\gamma = e^{i\phi} \tan(\theta/2)$)

$$\begin{aligned} M^S_{k,m}(\omega) &= \frac{1}{S^{k+m}} Tr \left[|\omega >< \omega| S^k_z S^m_- \right] \\ &= \frac{2S+1}{4\pi S^{k+m}} \int d^2\gamma < \gamma | \omega >< \omega | S^k_z S^m_- | \gamma > \\ &= \frac{2S+1}{4\pi S^{k+m}} \int d^2\gamma \hat{\Omega}^S_\omega(\gamma) \circ (\mathcal{S}_z \circ)^k (\mathcal{S}_- \circ)^m \end{aligned} \tag{24}$$

The curved letters $\mathcal{S}$ stand for classical quantities, and for any function $f(\gamma)$ we have defined the product [12]:

$$f(\gamma) \circ \mathcal{S}_z := (\mathcal{S}_z - \gamma \frac{\partial}{\partial \gamma}) f(\gamma)$$

$$f(\gamma) \circ \mathcal{S}_- := (\mathcal{S}_- + \frac{\partial}{\partial \gamma}) f(\gamma)$$

This allows us to write $< \gamma | \omega >< \omega | S^k_z S^m_- | \gamma >$ as a differential operator acting on $\hat{\Omega}^s_\omega(\gamma)$. The trick is then to partially integrate this expression.

After a little algebra we reach :

$$\begin{aligned} & \frac{2S+1}{4\pi S^{k+m}} \int d^2\gamma \hat{\Omega}^S_\omega(\gamma) \circ (\mathcal{S}_z \circ)^k (\mathcal{S}_- \circ)^m \\ = \; & \frac{(2S+1+m)!}{(2S)! 2^{k+m} 4\pi} \int_0^{2\pi} d\phi \int_{-1}^{1} du e^{-im\phi} (1-u^2)^{m/2} \mathcal{P}^S_{k,m}(u) \hat{\Omega}^S_\omega \end{aligned} \quad (25)$$

where

$$\mathcal{P}^S_{k,m}(u) = ((2S+2+m)u - m - (1-u^2)\frac{d}{du})^k 1 := \sum_{l'=m}^{k+m} p^{l'}_k P^m_{l'}(u) \quad (26)$$

in term of the Legendre polynomials $P^m_{l'}(u)$ and $u = \cos(\theta)$. We finally get :

$$M^S_{k,m}(\omega) \; = \frac{(2S+1+m)!}{(2S)!(2S)^{k+m}} \sum_{l=m}^{k+m} \frac{1}{2l+1} \hat{\Omega}^S_{l,m} p^l_k \quad (27)$$

It is thus possible to obtain the $\hat{\Omega}^S_{l,m}$ through a matrix multiplication of the moments $M^S_{k,m}(\omega)$:

$$M^S(\omega) = \mathcal{M} \hat{\Omega}^S \quad (28)$$

where we defined $(M^S(\omega))_{k,m} = M^S_{k,m}(\omega)$, $(\hat{\Omega}^S)_{l,m} = \frac{(2S+1+m)!}{(2S)^m} \hat{\Omega}^S_{l,m}$ and $(\mathcal{M})_{k,l} = \frac{1}{(2S)!(2S)^k} \frac{1}{2l+1} p^l_k$.

Numerical inversion of this last matrix allows us to get the multipoles $\hat{\Omega}^S_{l,m}$ from the numerical computation of the moments $M^S_{k,m}(\omega)$. The advantage of this method against the direct computation of Husimi densities is the numerical stability. Moreover, if we are interested in the few first multipoles, say up to $l \ll S$, then only the diagonal matrix elements up to $M^S_{l,m}$ are necessary.

Fig.2 shows a plot of a moment distribution $P(\hat{\Omega}^{600}_{1,0})$ obtained through computation of 2404 diagonal matrix elements from 4 unitary matrices defined by eq.(11) [4] close to the regime $T = 50$ and $\kappa = 1.2$. The agreement with the Gaussian fitting is remarkable and allows us to conjecture that the fluctuations of the $\hat{\Omega}^S_{l,m}$ obey the probability distribution

$$P(\hat{\Omega}^S_{l,m}) \propto \exp(-(\hat{\Omega}^S_{l,m} - \hat{\Omega}^\infty_{l,m})^2/(2\sigma^2_{l,m})) \quad (29)$$

[4] We have considered only the projection of (11) on even states, i.e. states which are left invariant by the parity $\Pi|\mu> = |-\mu>$.

where the mean value $\hat{\Omega}^{\infty}_{l,m}$ is the Shnirelman limit. This distribution narrows itself as $\hbar \to 0$, until finally the "almost all" wave functions, i.e. those who obey the Shnirelman theorem, have converged to their Shnirelman limit $\hat{\Omega}^{\infty}_{l,m} = 0$, $l \neq 0$ and $\hat{\Omega}^{\infty}_{0,0} = 1$. In other words, $\sigma^2_{l,m}$ decreases as S increases. This decay follows a power law as shown in Fig.3. We have :

$$\sigma^2_{l,m} \sim S^{-1/2} \qquad \forall l \neq 0 \tag{30}$$

As already mentioned, this law is valid for fixed l and m in the regime l, $m \ll S$.

We further did the same study on GOE matrices. We constructed the M-matrix defined in equation (23) using eigenstates of a GOE matrix instead of the eigenstates $|\omega>$ of the kicked top (11). The result is shown in Fig.4 and indicates a decay of the width of the Gaussian distribution of fluctuations of the Husimi density of the form (29). Let us note at this stage that the relationship between this width and the fluctuations of observables similar to those studied in [1, 2] is :

$$(\sigma^2_{l,m})^2 \sim < F^2_j > \tag{31}$$

Indeed $\sigma^2_{l,m}$ measures the fluctuations of the Husimi density. They are linearly related to the matrix elements of observables according to equations (23) and (27). The fluctuations of these matrix elements are roughly given by their square and hence we get equation (31). We thus get the same $1/S$ decay of the fluctuations as in [1, 2]. In other words, *the Husimi density converges to its semiclassical value with a rate given by the square root of the rate of convergence of diagonal matrix elements of observables.* This rate is independent of the size of the fluctuations. As for the shape of these fluctuations, the diversity of models studied up to date leads us to conjecture that *quantum mechanical systems with strongly chaotic classical counterpart have gaussian distributed fluctuations of their diagonal matrix elements around their microcanonical classical average (Eq.(2) or eq.(12)).* Apparently, the width of this gaussian decays like $\hbar$ as $\hbar \to 0$. This postulate is to be taken with the "almost all" Shnirelman restrictions and excludes of course models like the kicked rotator [15], where quantum interference effects lead to localization of the wave function, thus destroying the ergodicity of the quantum wave function [5]. In the classically strongly chaotic regime we are dealing

[5] However restriction of quantum averages to phase space region smaller than the localization length should lead to a similar behaviour.

with here, the "localization length" in the kicked top exceeds by far the total number of eigenstates $2s+1$, hence no localization effect occurs [13].
Up to now we have shown that our model matches in every respect all the features of a GOE random matrix : its spectrum exhibits level repulsion its level curvature statistics correspond to the RMT predicted distribution and the statistical distribution of the components of its eigenvectors tends to the semiclassical average in the same way, which in its turn implies a decay of the width of the Gaussian distribution of the multipoles $\hat{\Omega}^S_{l,m}$ defined in (19). However as has already been said, there is absolutely no reason to expect a similar decrease when l is not small compared to S. We therefore turn our attention to the behaviour of these multipoles.
We concentrate on the questions :

- Is there a similar power-law decay for $\hat{\Omega}^S_{l(S),m(S)}$ when $l(S)$ and $m(S)$ are increasing functions of S ?
- Are there possibly restrictions on $l(S)$ and $m(S)$ for this power-law to stay valid ?

Answering this questions gives us information on the minimal size $\Delta_{l,m}$ of the relevant fluctuations. From the Heisenberg uncertainty principle, quantum mechanics does not resolve details smaller than $\hbar^d$ in the $2d$-dimensional phase space of a d-dimensional system. Hence we have a lower bound for the fluctuations size $\Delta_{l,m} = \frac{2\pi^2}{(l+1)(m+1)} \gtrsim \hbar \sim 1/S$ and thus an upper bound for l and m : $l, m \lesssim S$. For the sake of simplicity we will restrict ourselves to the study of $m = 0$ multipoles with $l \sim S$ and $\sqrt{S}$ using formula (22) with random eigenfunction components ω_μ which corresponds to the GOE case [6]. We show the result of this study on fig.5 for $l(S) = S/2$, $3S/4$, S and $5S/4$. Obviously, these S-dependent multipoles decay faster than those with fixed l and m. Moreover a S_c is likely to exist for each $l(S)$ above which the magnitude of the corresponding fluctuation decays faster than a power law, possibly exponentially. However this latter conclusion is to be taken carefully because of the restricted S-range of fig.5 [7]. On the other hand the $l = \sqrt{S}$-moment decay as a power law $\sim S^{-3/2}$, at least in the studied range of variation of S.

[6] The ω_μ's are random up to the normalization condition $\sum_{\mu=-S}^{S} |\omega_\mu|^2 = 1$ and the Π-parity : $\omega_\mu \neq 0$ either for $\mu = -S, -S+2, -S+4, \ldots S$ or $\mu = -S+1, -S+3, \ldots S-1$.

[7] This restriction is due to the computation of the Clebsch-Gordan coefficients.

In view of this, we conclude that, in the GOE case, the critical value l_c below which the fluctuations are relevant either tends to a constant, or to infinity slower than S, i.e.

$$l_c \sim S^\alpha \quad 0 < \alpha < 1 \tag{32}$$

On the other hand, previous study of the kicked top emphasized the quasifractal structure of the Husimi density of its eigenfunctions in the chaotic regime [16]. This means that fluctuations in both directions of phase space are present up to the smallest scale allowed by the Heisenberg uncertainty, i.e. up to a size $O(\hbar^{1/2})$, which is consistant with eq. (32) with $\alpha = 0.5$. The fact that the moment $\Omega_{\sqrt{S},0}$ also shown on fig.5 decays more or less as a power-law

$$\Omega_{\sqrt{S},0} \sim S^{-3/2} \tag{33}$$

corroborates this conclusion : multipoles up to $l \sim \sqrt{S}$ are relevant, i.e. $\alpha = 1/2$.

Nevertheless, nothing forces the eigenstates of a quantum chaotical model to match those of a GOE matrix up to the smallest scales. It would therefore be highly desirable to get a condition on α like eq.(32/33) for a quantum chaotical system. This could be achieved by direct computation of $\Omega_{\sqrt{S},m(S)}$ using eq.(22). However, the numerical difficulty associated with the computation of high-order Clebsch-Gordan coefficients renders this task hardly fulfillable, as can be seen on fig.6 where we show results obtained for $\Omega_{\sqrt{S},0}$ through eq.(22) averaged over more than 40000 states for each point. On one hand, the semiclassical randomness of the eigenstates is not attained for small S, while on the other hand, the Clebsch-Gordan coefficients limit the maximal spin magnitude. In other words these two effects dramatically affects fig.6 left and right. Considering the size of our statistics, we attribute to these effects the somehow erratic behaviour of $\Omega_{\sqrt{S},0}$. On fig.6, the solid line indicating a $S - 1.5$-decay is shown as eye-guide, and constitutes in no way a serious result.

In conclusion our study of the Husimi density of eigenstates of the quantum spin system defined by (10) and (11) has confirmed the gaussian shape of fluctuations around the semiclassical limit. These fluctuations decay in size with a rate $\sim 1/\sqrt{S}$ for $l \ll l_c \sim \sqrt{S}$. This rate possibly increases to $1/S^{3/2}$ for l smaller but of the order of l_c. Moreover, this decay results in the same

power law for the decay of fluctuations of diagonal matrix elements of observables as in previous studies [1, 2], indicating perhaps universality. While GOE results tend to confirm the quasifractality proposed in [16], numerical difficulties forbade us to check it for the quantum dynamical system. Investigations to overcome this difficulty are on their way. For the time being, let us just point out that the fact that GOE eigenstates seem to exhibit this quasifractality renders it a direct consequence of the randomness of the states. The maximal randomness is then bounded by Heisenberg's uncertainty, but beside that, the quasifractality of the states seem to contain no physical content.

We thank the Centro Svizzero di Calcolo Scientifico. Work supported in part by the Fonds National Suisse de la Recherche Scientifique.

References

[1] B. Eckhardt, S. Fishman, J. Keating, O. Agam, J. Main and K. Müller, Phys. Rev. E **52**, 5893, (1995).

[2] M. Feingold and A. Peres, Phys. Rev. A **34**, 591, (1986).

[3] See the addendum of A.I. Shnirelman in : *KAM Theory and Semiclassical Approximations to Eigenfunctions, V.F Lazutkin*, Springer (1993).

[4] E. J. Heller, Phys. Rev. Lett. **53**, 1515, (1984).

[5] A. Perelomov, *"Generalized Coherent States and their Applications"*, Springer-Berlin, 1986.

[6] Ph. Jacquod and J.-P. Amiet, J. Phys. A : Math. Gen., **28**, 4799, (1995) and references therein.

[7] M. L. Mehta, *Random Matrices*, 2^{nd} Edition, Academic Press, 1991.

[8] See e.g. A. J. Lichtenberg and M. A. Lieberman, *"Regular and Chaotic Dynamics"* (Second Edition), Springer, 1992.

[9] M. Robnik and M. V. berry, J. Phys. A : Math. Gen. **19**, 669, (1986).

[10] J. Zakrzewski and D. Delande, Phys. Rev. E, **47**, 1650, (1993), and references therein.

[11] T. Takami and H. Hasegawa, Phys. Rev. Lett. **68**, 419, (1992).

[12] J.-P. Amiet and M. Cibils, J. Phys. A : Math. Gen., **24**, 1515, (1991).

[13] For a comparison of the kicked rotator and the kicked top, see e.g. : F. Haake, *"Quantum Signatures of Chaos"*, Springer, 1991.

[14] P. Pechukas, Phys. Rev. Lett. **51**, 943, (1983)

O. Bohigas, M.-J. Giannoni and C. Shmit, Phys. Rev. Lett. **52**, 1, (1984)

[15] D.L. Shepelyansky, Physica **28D**, 103, (1987).

[16] K. Nakamura, Y. Okazaki and A. R. Bishop, Phys. Rev. Lett. **57**, 5, (1986).

Figure Captions

Fig.1: Distribution of level curvatures for the eigenstates of (11) and $S = 200$, $T = 50$ and $\kappa = 1.2$. From the remarkable agreement with RMT predictions we conclude that the ratio of scarred eigenfunctions is very small (see [10, 11]), and should therefore not influence our study.

Fig.2: Moment distribution $P(\hat{\Omega}^S_{1,0})$ as defined in (16) for a spin $S = 600$. The statistics has been computed from 2404 even states of four realisations of (11) taken around $T = 50.$ and $\kappa = 1.2$. The agreement with a gaussian (solid line) is remarkable. On inset we show the same curve on a semi-log plot.

Fig.3: Log-log plot of the width of the gaussiann distribution of multipoles $P(\hat{\Omega}^S_{l,m})$ for model (11), $m = 0$ and $l = 1$ (squares), $l = 3$ (diamonds) and $l = 5$ (triangles) vs. the magnitude of spin S. Inset shows the width of $P(\mathrm{Re}(\Omega^S_{l,m}))$ for $m = 2$ and $l = 2$ (circles), $l = 3$ (squares), $l = 4$ (diamonds) and $l = 5$ (triangles). In both cases, the solid line indicates the $S^{-1/2}$ decay.

Fig.4: Log-log plot of the width of the gaussian distribution of multipoles $P(\hat{\Omega}^S_{l,m})$ for GOE, $m = 0$ and $l = 1$ (circles), $l = 3$ (squares) and $l = 5$ (diamonds) vs. the magnitude of spin S. The solid line indicates the $S^{-1/2}$ decay.

Fig.5: Log-log plot of the width of the gaussian distribution of multipoles $P(\hat{\Omega}^S_{l,m})$ for GOE, $m = 0$ and $l = S/2$ (circles), $l = 3S/4$ (squares), $l = S$ (diamonds), $l = 5S/4$ (triangles) and $l = \sqrt{S}$ (empty diamonds) vs. the magnitude of spin S. The upper and lower solid lines indicate a decay of $S^{-1.5}$ and S^{-36} respectively.

Fig.6: Log-log plot of the width of the gaussian distribution of multipoles $P(\hat{\Omega}^S_{l(S),0})$ for model (11), $l(S) = \sqrt{S}$ and $T = 50.$ and $\kappa = 1.2$, $m = 0$ and $S = \sqrt{S}$ vs. the magnitude of spin S. The solid line indicate a decay of $S^{-1/2}$. We attribute the rather erratic behaviour of the datas to the numerically instable computation of higb-order Clebsch-Gordan coefficients (see text).

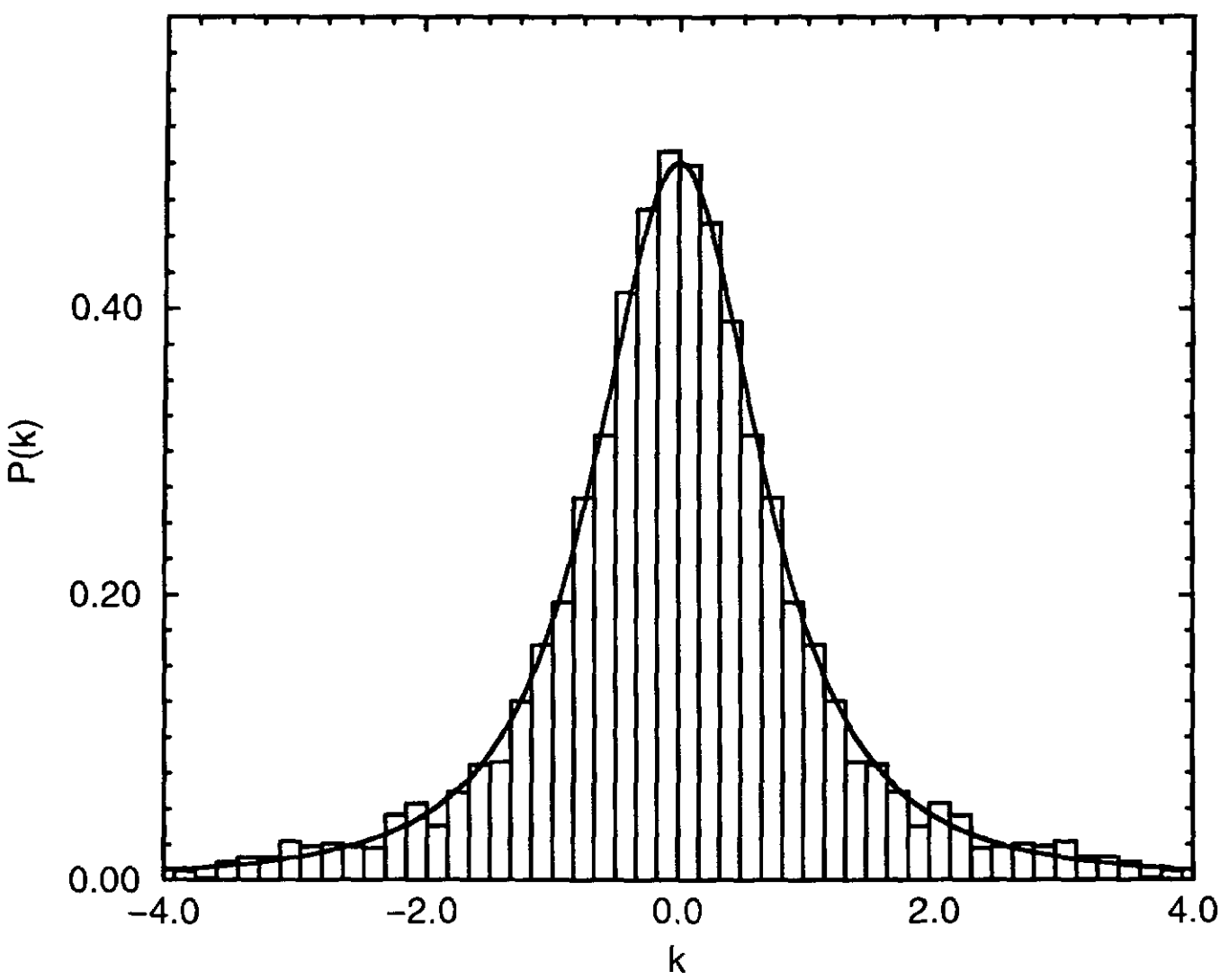
0.40
0.20
0.00
P(k)
−4.0
−2.0
0.0
2.0
4.0
k

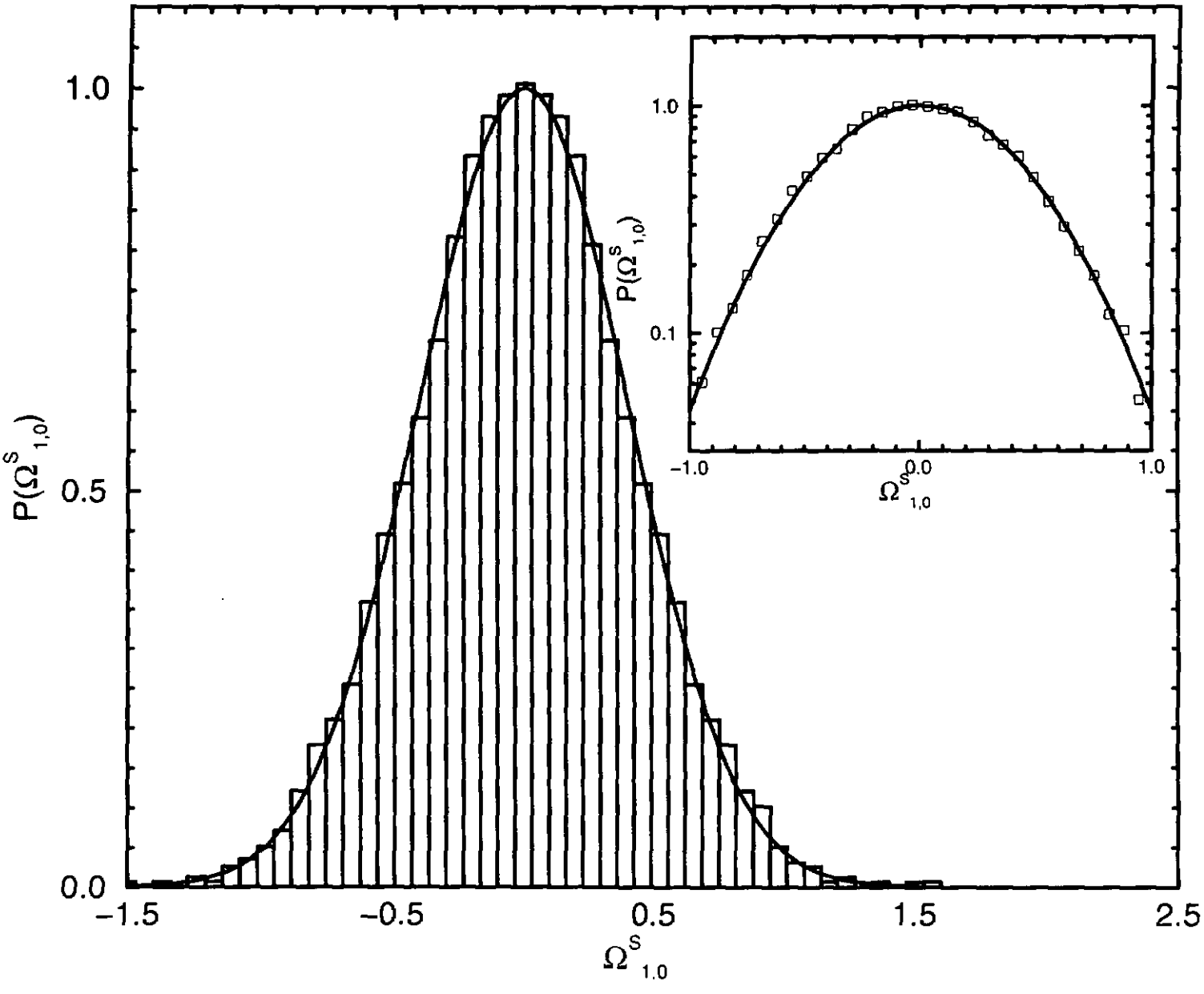
1.0
0.5
0.0
$P(\Omega^S_{1,0})$
−1.5
−0.5
0.5
1.5
2.5
$\Omega^S_{1.0}$
1.0
0.1
$P(\Omega^S_{1,0})$
−1.0
0.0
1.0
$\Omega^S_{1,0}$

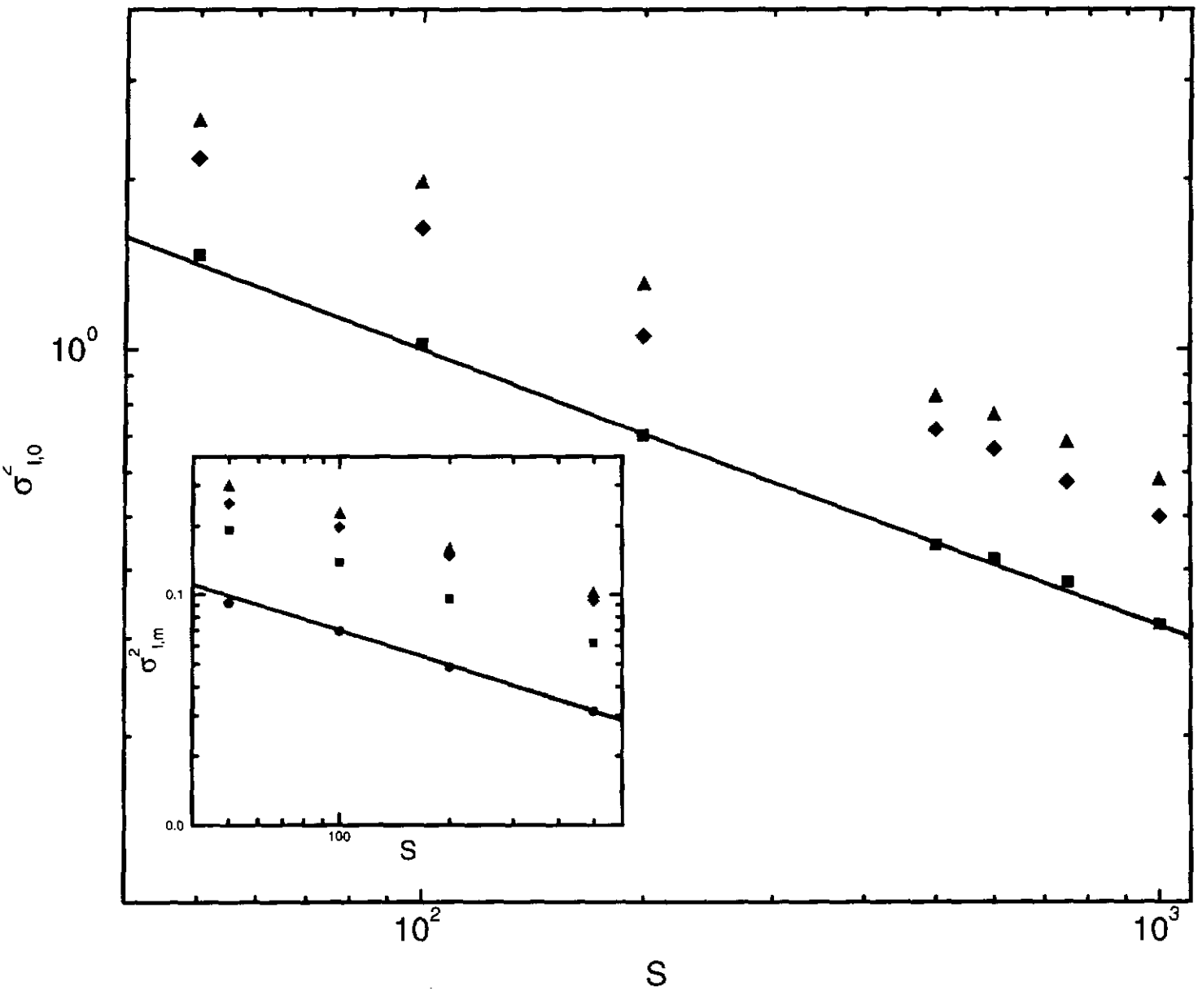
10^0
$\sigma^2_{l,0}$
10^2
10^3
S
0.1
0.0
$\sigma^2_{l,m}$
100
S

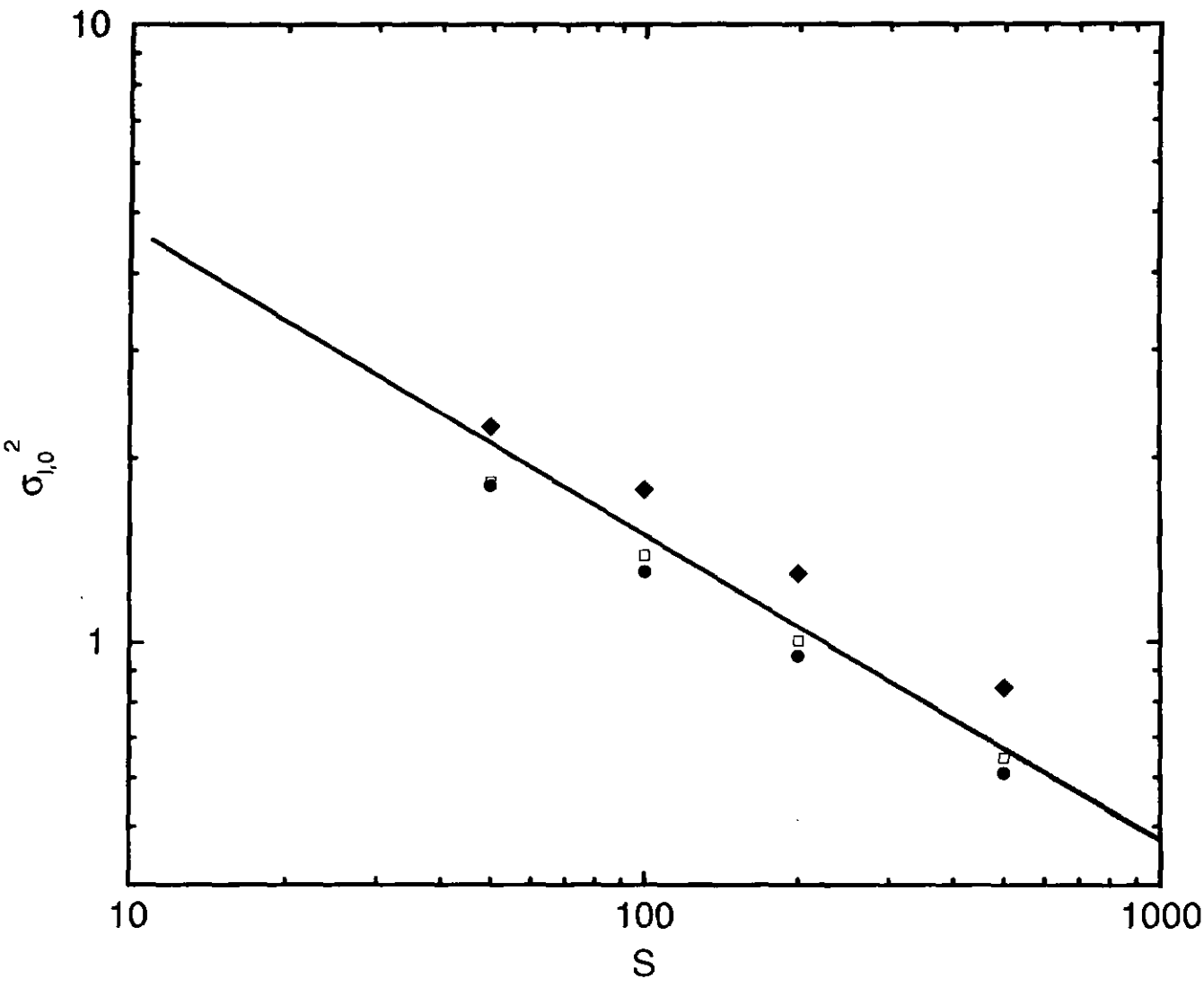
10
1
$\sigma_{I,0}^2$
10
100
1000
S

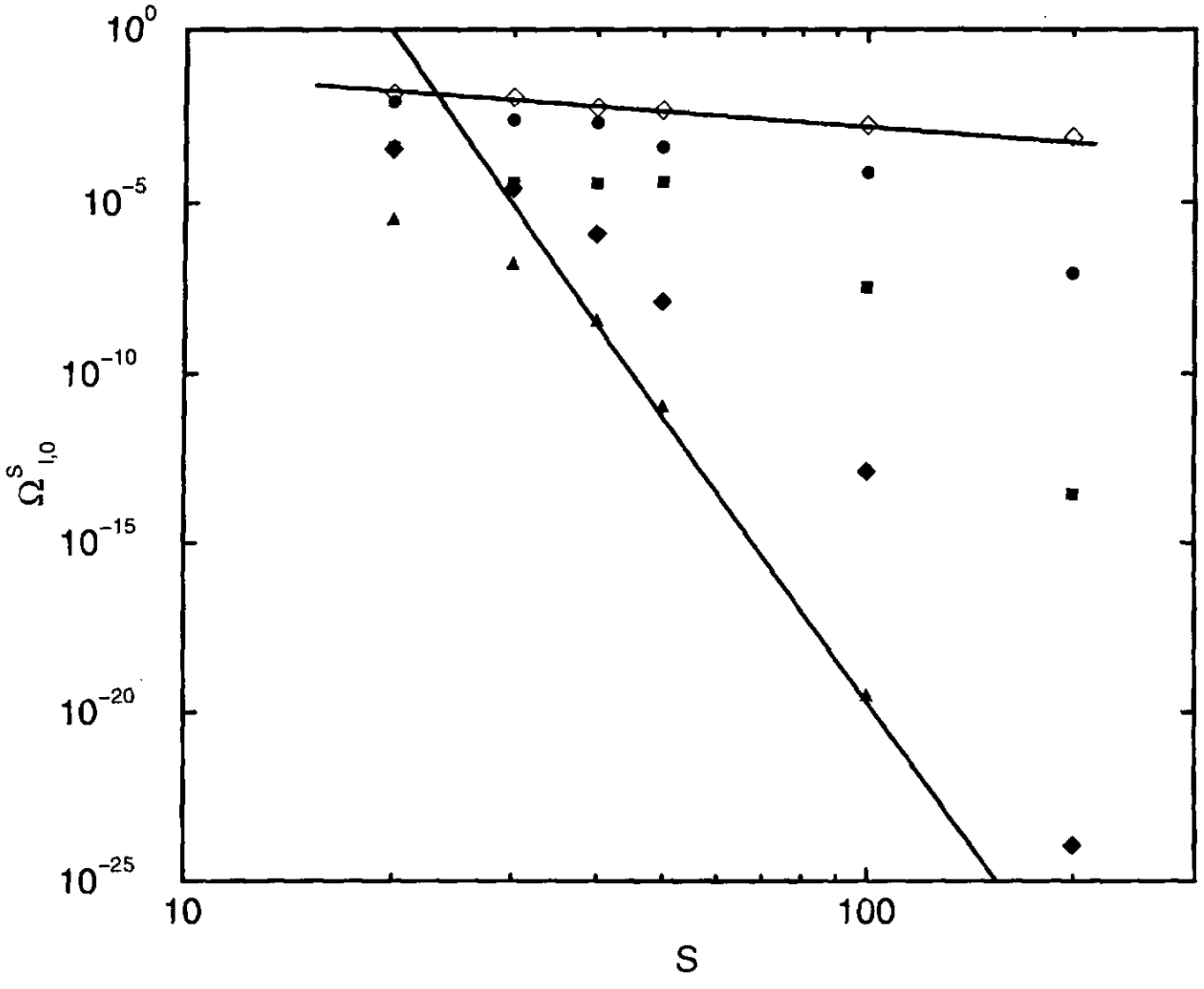
10^{0}
10^{-5}
10^{-10}
10^{-15}
10^{-20}
10^{-25}
$\Omega^{S}_{1,0}$
10
100
S

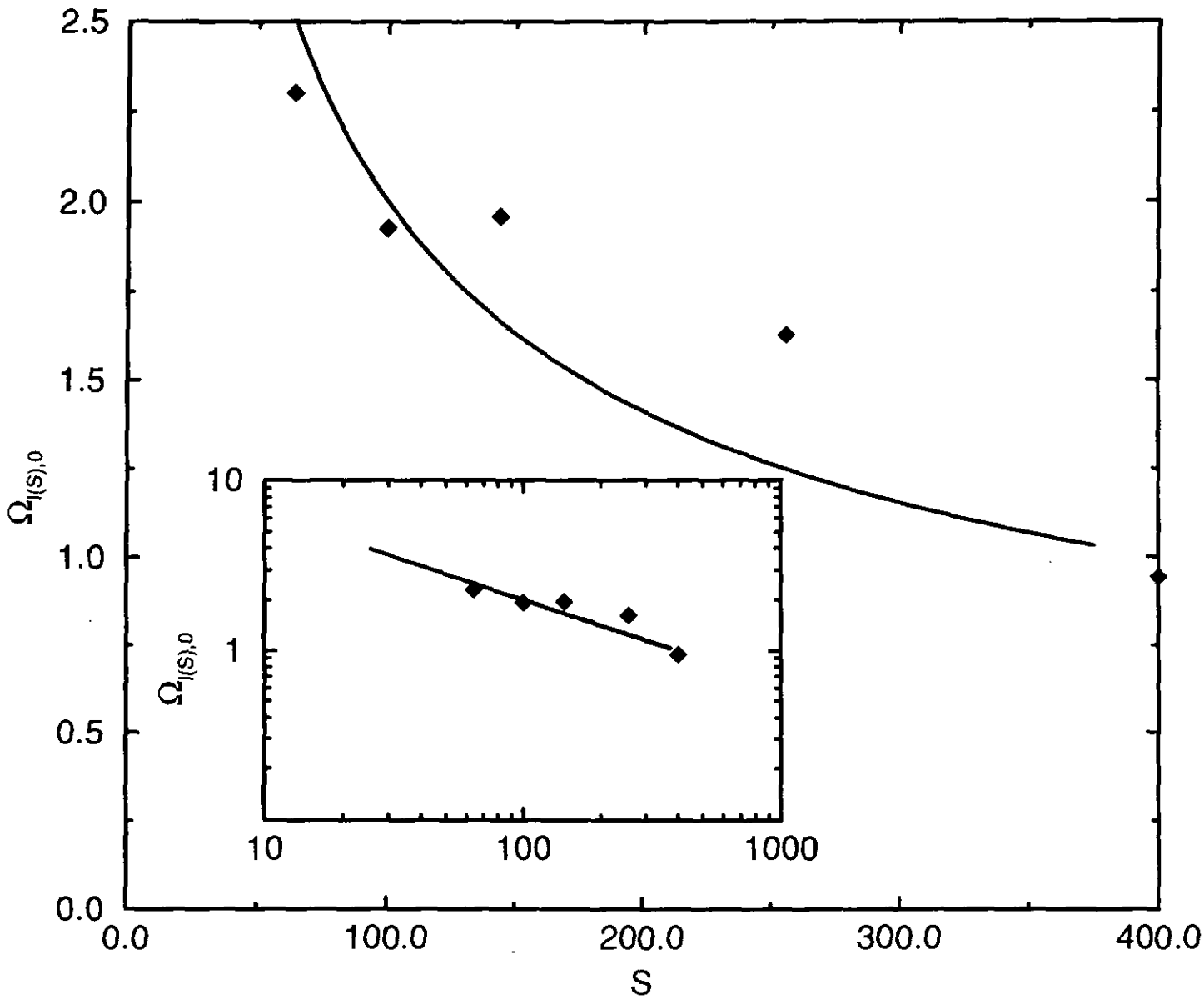
2.5
2.0
1.5
1.0
0.5
0.0
0.0
100.0
200.0
300.0
400.0
S
$\Omega_{I(S),0}$
10
1
10
100
1000
$\Omega_{I(S),0}$

Two interacting Hofstadter butterflies

Armelle Barelli, Jean Bellissard, Philippe Jacquod[a] and Dima L. Shepelyansky[b]
Laboratoire de Physique Quantique, UMR 5626 du CNRS, Université Paul Sabatier, F-31062 Toulouse Cedex, France
[a] *Institut de Physique, Université de Neuchâtel, CH-2000 Neuchâtel, Confédération Helvétique*
(February 18, 1997)

The problem of two interacting particles in a quasiperiodic potential is addressed. Using analytical and numerical methods, we explore the spectral properties and eigenstates structure from the weak to the strong interaction case. More precisely, a semiclassical approach based on non commutative geometry techniques permits to understand the intricate structure of such a spectrum. An interaction induced localization effect is furthermore emphasized. We discuss the application of our results on a two-dimensional model of two particles in a uniform magnetic field with on-site interaction.

PACS numbers: 05.45.+b, 72.15.Qm, 72.10.Bg

I. INTRODUCTION

The study of crystal electrons submitted to a magnetic field has been extensive since the early works of Landau[1] and Peierls[2]. These studies have led to deep insights in the physics of electrons in solids (interpretation of the de Haas van Alphen effect[3], investigation of the Fermi surface...). The number of contributions on the subject between 1950 and 1970 reveals the importance of magnetic field effects. Twenty years ago, Hofstadter numerically computed the spectrum of the Harper model[4] and discovered its fractal structure as a function of the normalized magnetic flux per lattice cell[5] (Fig. 1).

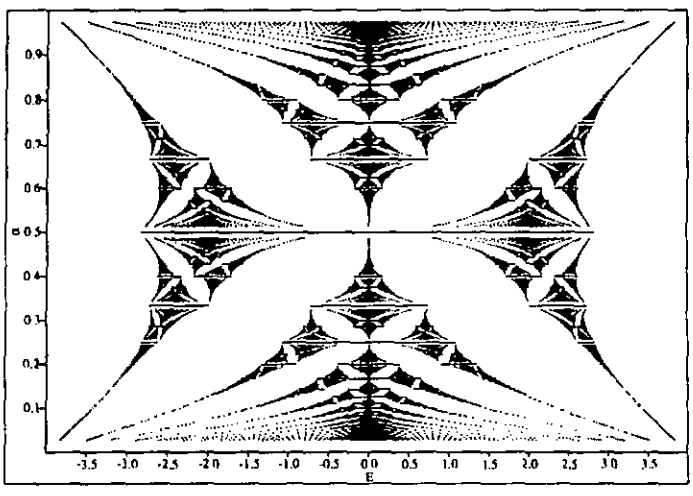

FIG. 1. Hofstadter's butterfly for rational values of $\alpha = p/q$ up to $q = 29$. For each value of the magnetic flux $\alpha = p/q$, we generally have q bands. Near energies equal to ± 4 and zero flux, we observe the emergence of Landau levels.

The problem of a two dimensional electron on a periodic lattice has been of special interest in solid state physics during the last fifteen years : superconducting[6] and normal-metal networks[7]. Harper-like models have been used to describe the quantum Hall effect[8] in organic conductors, in Anyon superconductivity[9] and in flux phases for the Hubbard model[10].

If the lattice is given by the positions of the ions of a metal, the lattice spacing a is of the order of 1 Å, so that even with the highest magnetic fields that can be produced now, namely $B \approx 20T$, we get $\alpha = \gamma/2\pi \approx 0.5 \times 10^{-4}$ which is fairly small and shows that in this situation a "semiclassical" approximation will always be relevant. As a matter of fact, an effective Planck's constant denoted by γ proportional to the applied magnetic field naturally appears as an adjustable variable of the problem. Therefore the weak magnetic field limit $\gamma \mapsto 0$ corresponds to the semiclassical limit $\hbar \mapsto 0$. The corresponding classical phase space at $B = 0$ is the quasimomentum space, namely the Brillouin zone of the corresponding lattice. Topologically it is a 2-torus and the appearance of the magnetic field transforms it into a non commutative 2-torus[11].

Whenever $\gamma = 2\pi p/q$, $(p, q \in \mathbf{N})$ the lattice Hamiltonian H recovers some periodicity and Bloch's theory applies. We shall see then that H can be represented as a self-adjoint $q \times q$ matrix whose entries are periodic functions of the quasimomentum components. Thus, if γ is close to any rational multiple of 2π, it is possible to compute the spectrum using semiclassical methods.

Based on these remarks, many theoretical and mathematical works were published during the last fifteen years using renormalization group analysis[12] and pseudodifferential operators techniques[13]. On the basis of the techniques of non commutative geometry[11], another approach was developed in order to reformulate and extend the semiclassical results[14]. The algebraic semiclassical approach is justified by the simplicity of its application and its efficiency, for example in the computation of Landau levels both in Harper-like models[15] and in a model-Hamiltonian on a triangular lattice[16]. The comparison between semiclassical formulae and exact calculations extracted from the various spectra for $\gamma \in 2\pi\mathbf{Q}$ gives sur-

prisingly accurate agreement even for relatively large γ's (namely $\gamma/2\pi \leq 0.2$).

While in the above formulation of the problem of Bloch electrons in a magnetic field the particles are considered on a two-dimensional lattice, it is possible to map it exactly onto a one-dimensional lattice with quasiperiodic potential. The interesting property of such a lattice is the duality between momentum and spatial coordinates pointed out by Aubry and André[17]. This Aubry duality results in a delocalized structure of the eigenstates characterized by an algebraic decay and a multifractal eigenspectrum. This leads to a quasidiffusive wave packet spreading on such a lattice[18,19].

Recently, numbers of authors have followed a new path in the study of the combined effect of interaction and disorder. The a priori simple problem of two interacting particles in a random potential[20] has indeed revealed an unsuspectly large interaction induced delocalization effect. However, the opposite effect has been discovered in the case of two particles in a quasiperiodic potential. In this case, the interaction leads to the emergence of a pure-point component out of the spectrum of the non interacting problem. These facts have been firmly established by overconvincing numerical and analytical results[21,22]. It is one of the purposes of this paper to again express these arguments in more details.

We shall present in this work analytical and numerical results derived from the two-particle Harper problem with on-site interaction on a one-dimensional lattice. More precisely we devote the second section to the presentation of the algebraic semiclassical approach on the non interacting problem $U = 0$. The corresponding spectrum is somehow an intricate superposition of two Hofstadter butterflies. The aim of section 3 is to study the small interaction regime where usual perturbation theory can be applied. The evolution of the spectrum as a function of the strength of the interaction will be presented. After building the analytical framework in section 4, we apply it to the computation of the levels in the strong interaction regime. We show that for very large U, the spectrum is divided into two parts : one corresponding to the non interacting case and the second one, looking like a Mathieu spectrum corresponding to localized states strongly influenced by the interaction. Based upon Aubry's duality[17], it can be proved that all the wave functions are localized in this regime as far as the Mathieu part of the spectrum is concerned. Finally, we discuss in section 5 the problem of two interacting particles on a two-dimensional lattice submitted to a magnetic flux.

II. NON INTERACTING MODEL

In his 1930's study of the electronic diamagnetism of metals, Landau computed the energy spectrum of a free electron subject to a uniform magnetic field[1]. If B is uniform and parallel to one axis, for example axis 3, the kinetic energy is written as :

$$H_L = \frac{\hbar^2}{2m_e}\left(\tilde{K}_1^2 + \tilde{K}_2^2\right) \tag{1}$$

with $\tilde{K}_\mu = (P_\mu - q_e A_\mu)/\hbar$, $\mu = 1, 2$ and $A = (A_1, A_2)$ is the vector potential satisfying $\mathrm{curl}(A) = B$, q_e is the electron charge. Moreover, the quasimomenta $\tilde{K}_1, \tilde{K}_2$ satisfy

$$[\tilde{K}_1, \tilde{K}_2] = iq_eB/\hbar \tag{2}$$

Let us notice that this commutation rule becomes canonical when replacing $\hbar$ by $q_eB/\hbar$. This new effective Planck constant (divided by 2π) is proportional to the magnetic field B and bebaves as a varying physical parameter, quite naturally.

The spectrum of H_L is $E_n = E_0 h_{\mathrm{eff}}\omega(2\nu + 1)$ with $E_0 = \hbar^2/2m_e$, $\hbar_{\mathrm{eff}} = q_eB/\hbar$ and $\omega = 1$. Therefore :

$$E_\nu = \hbar\omega_c(\nu + 1/2) \tag{3}$$

where $\omega_c = q_eB/m_e$ is the cyclotronic frequency and ν is the Landau quantum number.

When $B = 0$, the electron energy $E(k)$ for each conduction band is given by Bloch's theory, where the quasimomentum components $k = (k_1, k_2)$ are defined modulo the reciprocal lattice such that for a simple square lattice in the tight-binding approximation $E(k) = 2E_0[\cos(k_1a_1) + \cos(k_2a_2)]$ where a_μ is the vector of the Bravais lattice in the μ-direction. The charge carriers energy is calculated by expanding $E(k)$ near its extremum, denoted by k_c, namely :

$$E(k) = E(k_c) + \hbar^2\left(M^{-1}\right)_{ij} k_ik_j/2 + \mathrm{O}\left(|k|^3\right) \tag{4}$$

where M stands for the effective mass matrix such that $M^{-1} = D^2E(k_c)/\hbar^2$.

Thus Landau theory leads to a substitution $k_i \cdot a_i \longmapsto \hat{K}_i = \frac{1}{\hbar}(P - q_eA)\cdot a_i$ when an external magnetic field is applied. We have the following commutation rule :

$$[\hat{K}_i, \hat{K}_j] = iq_eBa_ia_j/\hbar = 2i\pi\phi_{ij}/\phi_0 = 2i\pi\alpha = i\gamma \tag{5}$$

where $\phi_0 = h/q_e$ is the flux quantum, ϕ_{ij} is the magnetic flux through the cell generated by (a_i, a_j) and $\alpha = \phi_{ij}/\phi_0$ is the normalized magnetic flux. For a crystal with periodic spacing, the Peierls operator $\mathcal{P}(k)$ is represented by an effective Hamiltonian[2], namely :

$$\mathcal{P}(k) = \sum_m h_m(\alpha)\mathrm{e}^{im\cdot k}\ , \quad m \in \mathbf{Z}^2 \tag{6}$$

where $h_m(\mathrm{o})$ are smooth functions of o. Thus :

$$H_{\mathrm{eff}}(\hat{K}_1, \hat{K}_2) = \sum_m h_m \mathrm{e}^{im\cdot\hat{K}} \tag{7}$$

If several bands intersect the Fermi level, the interband coupling due to the magnetic field is neglected and therefore :

$$H_{\text{eff}} = 2t\left(\cos\hat{K}_1 + \cos\hat{K}_2\right) \tag{8}$$

where t is physically interpreted as a transfer term corresponding to the required energy for an electron to jump from one site to another (nearest neighbour) of the lattice.

For a wave function $\psi(n_1, n_2)$ defined on the two-dimensional lattice $\ell^2(\mathbf{Z}^2)$, the magnetic field effect can be seen through the magnetic translation operators such that :

$$\begin{aligned}(\mathcal{U}_1\psi)(n_1,n_2) &= \mathrm{e}^{\frac{-iq_e}{\hbar}\int_{(n_1-1,n_2)}^{(n_1,n_2)}\vec{A}\cdot\vec{dl}}\psi(n_1-1,n_2)\\ (\mathcal{U}_2\psi)(n_1,n_2) &= \mathrm{e}^{\frac{-iq_e}{\hbar}\int_{(n_1,n_2-1)}^{(n_1,n_2)}\vec{A}\cdot\vec{dl}}\psi(n_1,n_2-1)\end{aligned} \tag{9}$$

in an appropriate gauge we get :

$$\begin{aligned}(\mathcal{U}_1\psi)(n_1,n_2) &= \psi(n_1-1,n_2)\\ (\mathcal{U}_2\psi)(n_1,n_2) &= \mathrm{e}^{-i\gamma n_1}\psi(n_1,n_2-1)\end{aligned} \tag{10}$$

Because of the presence of the uniform magnetic field, the magnetic translation operators no longer commute, namely in that case

$$\mathcal{U}_1\mathcal{U}_2 = \mathrm{e}^{i\gamma}\mathcal{U}_2\mathcal{U}_1 \tag{11}$$

where γ is the normalized magnetic flux per lattice-cell defined by $\gamma = 2\pi\alpha = 2\pi\phi/\phi_0$, ϕ being the flux per unit cell and $\phi_0 = h/q_e$ the flux quantum.
If we set $\mathcal{U}_1 = \exp\left(i\hat{K}_1\right)$, $\mathcal{U}_2 = \exp\left(i\hat{K}_2\right)$ using the commutation rule (11), we obtain

$$[\hat{K}_1, \hat{K}_2] = \frac{iq_eBa_1a_2}{h} = 2i\pi\frac{\phi}{\phi_0} = 2i\pi\alpha = i\gamma \tag{12}$$

which corresponds to (5) in the particular case $i = 1$ and $j = 2$.

Following Harper[4], the eigenvalue equation is written

$$\begin{aligned}&E_0\left[\psi(n_1+a,n_2)+\psi(n_1-a,n_2)+\right.\\ &\left.+\lambda\mathrm{e}^{iq_eBn_1a/\hbar}\psi(n_1,n_2+a)+\lambda\mathrm{e}^{-iq_eBn_1a/\hbar}\psi(n_1,n_2-a)\right]\\ &\qquad = 2\mathcal{E}\psi(n_1,n_2)\end{aligned} \tag{13}$$

λ represents the strength of the quasiperiodic potential.

Let us assume plane-wave behaviour in one direction, i.e. we set $\psi(n_1, n_2) = \int d\beta \mathrm{e}^{i\beta n_2}\phi(n_1)$ since the coefficients in the previous equation only involve n_1 :

$$\psi(n_1, n_2) = \mathrm{e}^{i\beta n_2}\phi(n_1)$$

and the eigenequation becomes :

$$\begin{aligned}&\phi(n_1+1)+\phi(n_1-1)+2\lambda\cos(2\pi\alpha n_1+\beta)\phi(n_1)\\ &\qquad = \mathcal{E}\phi(n_1)\end{aligned} \tag{14}$$

where we included the additive energy due to the motion in the field direction in the eigenvalue $\mathcal{E}$ and where we changed the origin of n_1.

It is possible to characterize the properties of eigenfunctions from (14) by looking at a special regime, namely $\lambda \ll 1$. Therefore, the hopping term is dominant and we can treat the quasiperiodic potential part of the eigenvalue equation as a perturbation. It is then easy to see that the solutions are given for $\lambda = 0$ by Bloch waves $\phi_k(n) = \exp(ikn)$ with an energy $E = 2\cos k$. For $0 < \lambda \ll 1$, the perturbation theory allows us to perform an expansion of eigenvalues and eigenstates in λ such that

$$\begin{aligned}E(k) &= 2\cos k + \sum_m \lambda^m \epsilon_m(k)\\ \phi_k(n) &= \mathrm{e}^{ikn}\left(1+\sum_m \lambda^m f_m(\gamma n+\beta)\right)\\ &= \mathrm{e}^{ikn}u_m(\gamma n+\beta)\end{aligned} \tag{15}$$

Evaluating the first and second order perturbation theory contributions and replacing the expressions (15) in (14) leads to :

$$\lambda(u_{m+1}+u_{m-1}) + 2\cos(\gamma m+k)u_m = E(k)u_m \tag{16}$$

The previous equation is known as the "almost Mathieu" eigenvalue equation and the argument above is the Aubry duality[17] between momentum and coordinate representations. As far as spectral properties are concerned one can be easily convinced that dealing with Bloch states means that the states are extended. Thanks to this duality, $\lambda \leftrightarrow 1/\lambda$ between (14) and (16), it is quite natural to get localized states for the almost Mathieu Hamiltonian at small λ's. More precisely, it has been proved that the spectrum of the almost Mathieu Hamiltonian is pure-point at small λ's and for almost all β's[23]. Conversely if $\lambda \gg 1$, the almost Mathieu Hamiltonian has purely continuous spectrum for almost all β's[24].

Setting $t = 1$ in formula (8) and using the magnetic translation operators $\mathcal{U}_1$ and $\mathcal{U}_2$ defined on the two-dimensional square lattice by (10), the previous Harper equation can be written as the action of an effective Hamiltonian such that :

$$H_{\text{eff}} = \mathcal{U}_1 + \mathcal{U}_1^{-1} + \mathcal{U}_2 + \mathcal{U}_2^{-1} \tag{17}$$

In order to study the two interacting particles model on a quasiperiodic lattice we transform the previous eigenvalue equation (14) into ($\lambda = 1$)

$$\begin{aligned}&\left[2\cos(\gamma n_1+\beta_1)+2\cos(\gamma n_2+\beta_2)+U\delta_{n_1,n_2}\right]\phi_{n_1,n_2}\\ &+\phi_{n_1+1,n_2}+\phi_{n_1-1,n_2}+\phi_{n_1,n_2+1}+\phi_{n_1,n_2-1}\\ &\qquad = E\phi_{n_1,n_2}\end{aligned} \tag{18}$$

where $\beta_{1,2}$ are related to the quasimomentum components of the non interacting case. Here we chose the form of on-site interaction which only influences the symmetric configurations while the antisymmetric ones remain not affected by U. Due to that, we shall only discuss symmetric configurations in the following.

In the most simple case of non interacting particles ($U = 0$), the spectrum can be computed as before and is shown in Fig. 2.

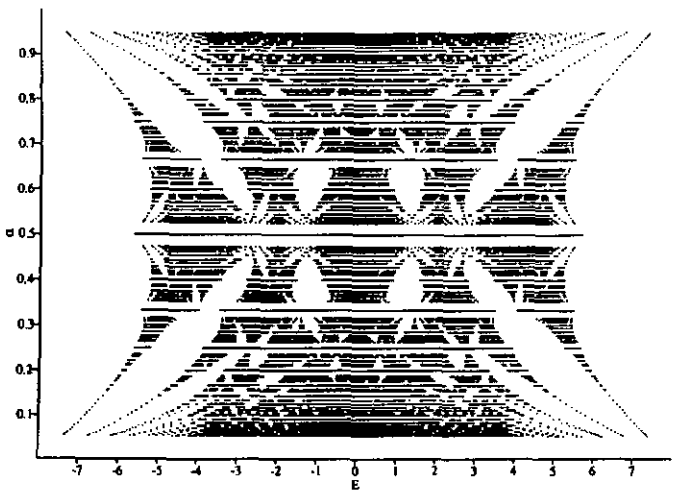

FIG. 2. Spectrum of the two-particle Harper problem with $U = 0$ obtained for rational values of $\alpha = p/q$ up to $q = 19$.

As we pointed out before, $\gamma = 2\pi\alpha$ appears in our problem as an effective Planck constant since the magnetic translation operators $\mathcal{U}_1$ and $\mathcal{U}_2$ obey canonical commutation rules in γ. Therefore, we study the semiclassical limit by letting $\gamma \mapsto 0$. It is also possible to perform calculations near a rational value of the magnetic flux, namely $\gamma' = \gamma - 2\pi p/q \longmapsto 0$. The efficiency and the accuracy of our calculations allow to explain some features of the corresponding spectra.
When $\gamma = 0$, corresponding to $B = 0$, we recover the band function $E(k)$, where $k = (k_1, k_2)$. To study the Landau levels, we expand the classical symbol of the Hamiltonian around an extremum of the band function denoted by k_c :

$$\mathcal{H}(k) = \mathcal{H}(k_c) + \frac{1}{2}\partial_\mu\partial_\nu\mathcal{H}(k_c)k_\mu k_\nu + \cdots \tag{19}$$

The quantization of $\mathcal{H}(k)$ consists in replacing the magnetic translation operators by[14]:

$$\mathcal{U}_j = \exp\left(i(k_{cj} + \sqrt{\gamma}K_j)\right) \ , j = 1, 2 \tag{20}$$

where k_{cj} are the bottom well coordinates and K_j are operators satisfying Heisenberg's commutation relations $[K_1, K_2] = i$. The quantized of $\mathcal{H}$, denoted by H, is written as :

$$H = \sum_m h(\mathrm{m}, \gamma)\mathrm{e}^{i(m\cdot k_c + \sqrt{\gamma}m\cdot K)}$$

with $m \cdot K = m_1K_1 + m_2K_2$. In the weak field limit, one formally expands H in powers of $\sqrt{\gamma}$:

$$H = \sum_m \Big\{ h(\mathrm{m}, 0)\mathrm{e}^{im\cdot k_c} + i\sqrt{\gamma}h(m, 0)\mathrm{e}^{im\cdot k_c}\mathrm{m}\cdot K + \gamma\left[\frac{\partial h}{\partial\gamma}(\mathrm{m}, 0)\mathrm{e}^{im\cdot k_c} - \frac{1}{2}h(m, 0)\mathrm{e}^{im\cdot k_c}(m\cdot K)^2\right]\Big\} + \mathrm{O}(\gamma^{3/2}) \tag{21}$$

which we rewrite as :

$$H = \mathcal{H}(k_c, 0) + \gamma\left(\frac{\partial\mathcal{H}}{\partial\gamma}(k_c, 0) - \frac{1}{2}\partial_\mu\partial_\nu\mathcal{H}(k_c, 0)K_\mu K_\nu\right) + \mathrm{O}(\gamma^{3/2}) \tag{22}$$

The $\partial\mathcal{H}/\partial\gamma$-term takes into account a possible explicit γ-dependence of the classical Hamiltonian whereas $\partial_\mu\partial_\nu\mathcal{H}$ represents the inverse effective mass matrix due to the band function curvature. By a unitary transformation, the quadratic term can be written as $\omega\left(K_1^2 + K_2^2\right)/2$ where ω is related to the determinant of the Hessian matrix $\partial_\mu\partial_\nu\mathcal{H}(k_c, 0)$. We recognize here the harmonic oscillator Hamiltonian. For this reason, the energy levels denoted by E_ν are called "Landau levels" and are equal, to that order in γ, to $\omega(\nu + 1/2)$ leading to :

$$E_\nu(\gamma) = \mathcal{H}(k_c, 0) + \gamma(2\nu + 1)\left(\det\frac{1}{2}D^2\mathcal{H}(k_c, 0)\right)^{1/2} + \gamma\left(\frac{\partial\mathcal{H}(k_c, 0)}{\partial\gamma}\right) + \ldots + \mathrm{O}(\gamma^N) \tag{23}$$

The formula (23) has been checked numerically on several models. To illustrate it, let us consider the two-particle Harper Hamiltonian on the square lattice (18) near the maximum $k_c = (0, 0)$ of the band function. Using (20) and (22) the quantized Hamiltonian is then expressed as an expansion in powers of γ :

$$H = 8 - \gamma\left((K_1^{(1)})^2 + (K_2^{(1)})^2 + (K_1^{(2)})^2 + (K_2^{(2)})^2\right) + \frac{\gamma^2}{3}\left((K_1^{(1)})^4 + (K_2^{(1)})^4 + (K_1^{(2)})^4 + (K_2^{(2)})^4\right) + \mathrm{O}(\gamma^3) \tag{24}$$

where the $K^{(1,2)}$ are quasimomenta for particle 1 and 2 respectively. Finally it gives the Landau levels :

$$E_{\nu_1,\nu_2}(\gamma) = 8 - 2\gamma(\nu_1 + \nu_2 + 1) + \gamma^2\left[(2\nu_1 + 1)^2 + (2\nu_2 + 1)^2 + 2\right]/16 + \mathrm{O}(\gamma^3) \tag{25}$$

where ν_1 and ν_2 are the Landau quantum numbers associated with particle 1 and 2 respectively. To check the accuracy of this formula, we compared it to the datas extracted from the numerical spectrum obtained by exact diagonalization. Fig. 3 shows the accuracy of such a semiclassical expansion in the description of the spectrum of the two-particle Harper model when $\gamma \mapsto 0$.

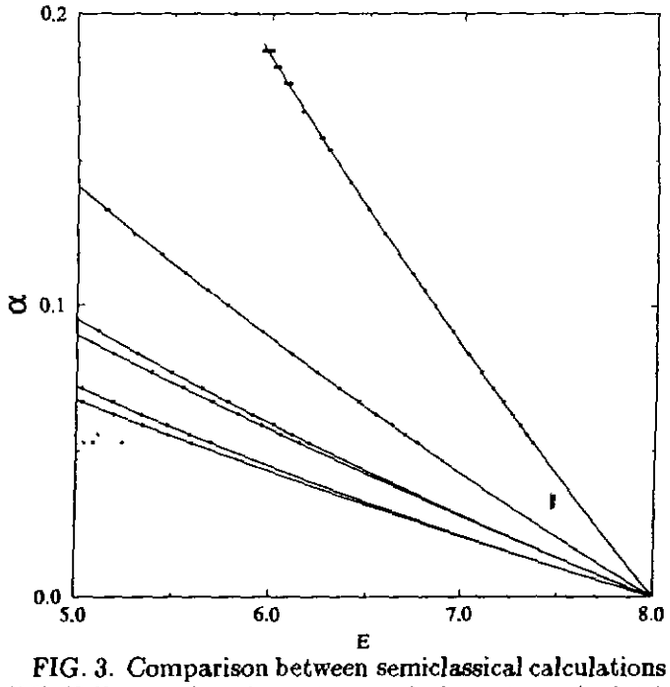

FIG. 3. Comparison between semiclassical calculations (25) (full curves) and exact numerical spectrum (points) for Landau sublevels in the two-particle Harper model on the square lattice when $U = 0$. Datas are extracted in the region of energies corresponding to the maximum $(0,0)$ of the band function.

III. WEAK INTERACTION REGIME

We present here a simple perturbative treatment that enables to implement the already presented results for the weakly interacting case. The first-order contribution allows to understand the splitting of Landau bands at sufficiently weak interaction, and describes it qualitatively well. It moreover enlightens the mechanism through which interaction affects the system. Using the representation defined by (20), we write the unperturbed Hamiltonian as :

$$H_{\text{eff}} = 2\cos(\sqrt{\gamma}K_1) + 2\cos(\sqrt{\gamma}K_2) \tag{26}$$

In the semiclassical limit $\gamma \mapsto 0$ we expand (26) in a power series around a minimum of potential $q_N = \pi/\sqrt{\gamma} + 2\pi N/\sqrt{\gamma}$, $N \in \mathbf{Z}$. Keeping only terms up to the second order in γ we end up with a harmonic oscillator. In this approximation and in the continuous case the one-particle wave functions of the unperturbed Hamiltonian are therefore given by :

$$\psi_\nu(y) = H_\nu(\frac{y}{\sqrt{\gamma}})\exp\left(-\frac{y^2}{2\gamma}\right)/\sqrt{2^\nu \nu! \sqrt{\gamma\pi}} \tag{27}$$

Here, $H_\nu(x)$ is a Hermite polynomial, the index ν refers to the Landau level, $y = x - q_N$ in term of the minimum of potential q_N around which the harmonic approximation has been performed, and x is the spatial coordinate. This expression is of course valid, provided γ and $|x - q_N| \ll 1$, i.e. in the small magnetic field regime, and not too far away from a potential minimum. Extending our expansion to higher powers in γ would allow us to increase the range of validity of this expression. We could indeed write the exact normalized wave functions in an expansion in γ as

$$\varphi_\nu(y) = \exp\left(-\frac{y^2}{2\gamma}\right)(c_0 H_\nu(\frac{y}{\sqrt{\gamma}}) + \gamma c_1 H_\nu^{(1)}(\frac{y}{\sqrt{\gamma}}) + ...) \tag{28}$$

For the purpose of discretization, we introduce a continuous variable $\xi \in \mathbf{R}$ labeling the well, and a discrete one $l \in \mathbf{Z}$ numbering the sites. Then $y = \xi - l\sqrt{\gamma}$ since in the chosen representation, the intersite spacing is $a = \sqrt{\gamma}$. The set $\{\varphi_\nu\}$ builds a quasiorthogonal basis in the sense that for $\xi \neq \xi'$, due to the Gaussian envelop of the states we have :

$$\sum_l \varphi_\nu(\xi - l\sqrt{\gamma})\varphi_\mu(\xi' - l\sqrt{\gamma}) = \mathrm{O}(\exp(-1/\gamma))\delta_{\mu,\nu} \tag{29}$$

These functions are periodic in ξ with period $1/\sqrt{\gamma}$. In the semiclassical limit the norm of φ_ν is :

$$\begin{aligned}\|\varphi_\nu\|^2 &= \sum_{l=-\infty}^{\infty} |\varphi_\nu(\xi - l\sqrt{\gamma})|^2 \\ &= 1/\sqrt{\gamma}\int dy|\varphi_\nu(y)|^2 \\ &= 1/\sqrt{\gamma}\end{aligned} \tag{30}$$

Consequently, to get normalized one-particle wave functions on the discrete lattice $\ell(\mathbf{Z})$ we must multiply the φ's by a factor $\gamma^{1/4}$. We thus can write the symmetrized two-particle unperturbed wave functions as :

$$\begin{aligned}\phi^{\xi,\xi'}_{\nu,\mu}(l,l') = \sqrt{\frac{\gamma}{2}}(\varphi_\nu(\xi - l\sqrt{\gamma})\varphi_\mu(\xi' - l'\gamma) \\ \pm\varphi_\mu(\xi - l\sqrt{\gamma})\varphi_\nu(\xi' - l'\gamma))\left(1 - \delta_{\mu,\nu}(1 - 1/\sqrt{2})\right)\end{aligned} \tag{31}$$

We are now able to compute the first-order correction for the energy. Because of the exponentially localized character of (28), two particles located on different wells have only an exponentially small overlap, and as a consequence do practically not interact. Therefore the first-order interaction induced correction to the energy is non zero only for symmetric wave functions with $\xi = \xi'$. We have :

$$\begin{aligned}\Delta E^{(1)} &= U\sum_l\sum_{l'}(\phi^{\xi,\xi'}_{\nu,\mu}(l,l'))^2\delta(\xi - \xi' + (l' - l)\sqrt{\gamma}) \\ &= U\delta_{\xi,\xi'}\int dy\,(\varphi_\mu(y)\varphi_\nu(y))^2(2 - \delta_{\mu,\nu}) + \\ &\quad + \mathrm{O}(\exp(-1/\gamma))\end{aligned} \tag{32}$$

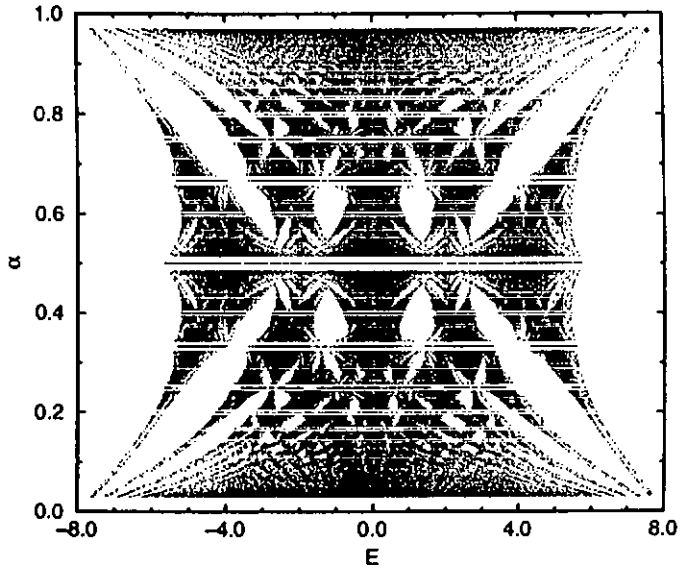

FIG. 4. Spectrum of the two-particle Harper model with on-site interaction at $U = 0.4$ up to $q = 23$.

From (28), the dominant term in the last integral is of order $O(\sqrt{\gamma})$ so that we finally have

$$\Delta E^{(1)} \sim U\delta_{\xi,\xi'}\sqrt{\gamma} \tag{33}$$

The numerical factor can be estimated from the harmonic approximation (27) which leads to :

$$\Delta E_h^{(1)} = U\delta_{\xi,\xi'}\sqrt{\frac{\gamma}{2\pi}} = U\delta_{\xi,\xi'}\sqrt{\alpha} \tag{34}$$

for states with Landau quantum numbers (0,0) and (0,1). This result shows that the interaction primarily acts on two-particle states with high double-site occupancy. In what follows we shall call such states "pair states". States for which the particles are located around different potential minima practically do not feel the interaction. Therefore, switching on the interaction does not modify most of the spectrum as can be seen on Fig. 4.

From (25) and (34) and for small enough interaction, the shifted part of the spectrum is given by :

$$E_{\nu_1,\nu_2}(\gamma) \sim 8 + U\sqrt{\frac{\gamma}{2\pi}} - 2\gamma(\nu_1+\nu_2+1) + \gamma^2\left[(2\nu_1+1)^2+(2\nu_2+1)^2+2\right]/16 \tag{35}$$

The amazing agreement between the numerically computed spectrum obtained by exact Lanczos diagonalization and (35) is shown in Fig. 5 where $U = 0.4$. It is a confirmation of our reasoning : pair states form the shifted part of the spectrum. Because these states are much fewer than states where particles are located in different wells, the shifted spectrum is much less dense. In this sense the interaction splits the butterfly into two parts. One of them is practically not affected by the interaction and corresponds to the states where particles are far from each other. The second one is shifted and relays to the situation where particles form pair states. Here, the interaction results in a global shift of the spectrum. In this way, new states appear in the initial gaps of the non interacting spectrum (see Figs. 4,6 and Fig. 1(b) in[21]). Direct analysis of eigenstates shows that the corresponding states are exponentially localized[21]. We shall come back to this point later on for the case of strong interaction.

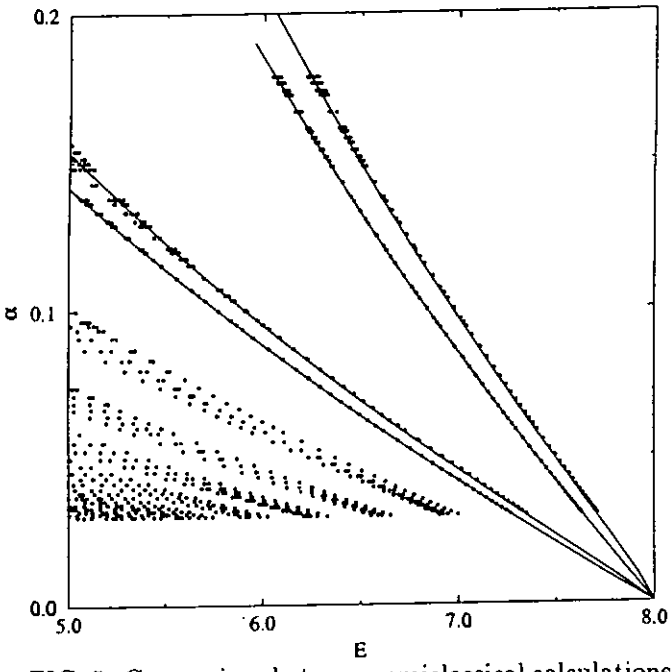

FIG. 5. Comparison between semiclassical calculations extended by perturbation theory (35) (full curves) and exact numerical spectrum (points) for the two-particle Harper model with on-site interaction at $U = 0.4$.

IV. STRONG INTERACTION REGIME

The strongly interacting regime needs a special treatment quite analogous to the one presented in section 2. As we will see, Schur's complement formula can be successfully applied to construct an effective Hamiltonian. The latter is then expanded in a power series in γ to deliver highly accurate formulae. From the weakly interacting regime we learned that particles located on different potential minima do not feel each other : for such pairs the interaction is suppressed by an exponentially small term of order $O(U\exp(-1/\gamma))$. Therefore, this picture remains valid even for large U's, the relevant parameter being the magnetic flux. Pair states on the other hand undergo an energy increase of order $\Delta E \approx U$. Therefore when the strength of the interaction $U > 0$ increases one part of the spectrum is almost not affected. Another

spectral structure appears, initially looking like a shifted butterfly (see Fig. 4 where $U = 0.4$), then evolving to a shifted Mathieu spectrum as the interaction grows bigger and bigger (see Figs. 6, 7 and 8 where $U = 5, 10$ and 20 respectively).

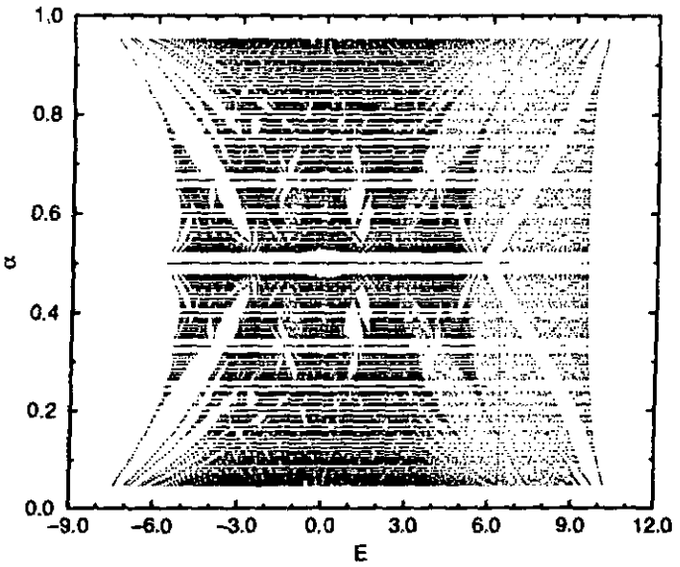

FIG. 6. Spectrum of the two-particle Harper model in the intermediate regime $U = 5$ up to $q = 23$.

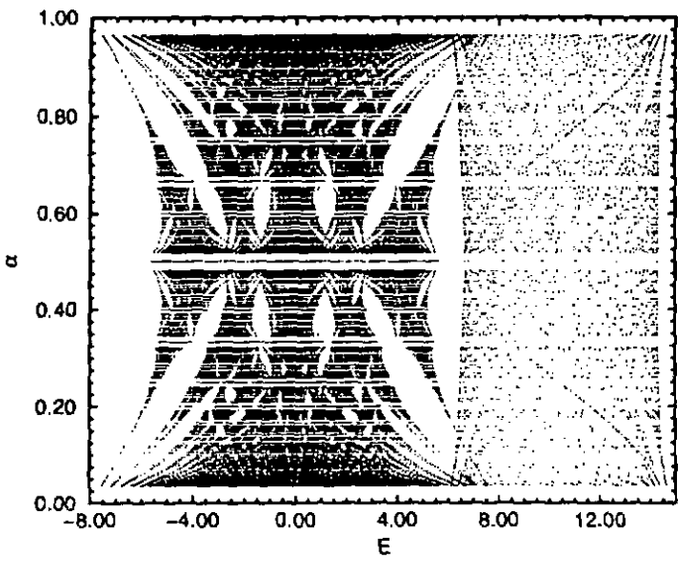

FIG. 7. Spectrum of the two-particle Harper model in the strongly interacting regime $U = 10$ up to $q = 23$.

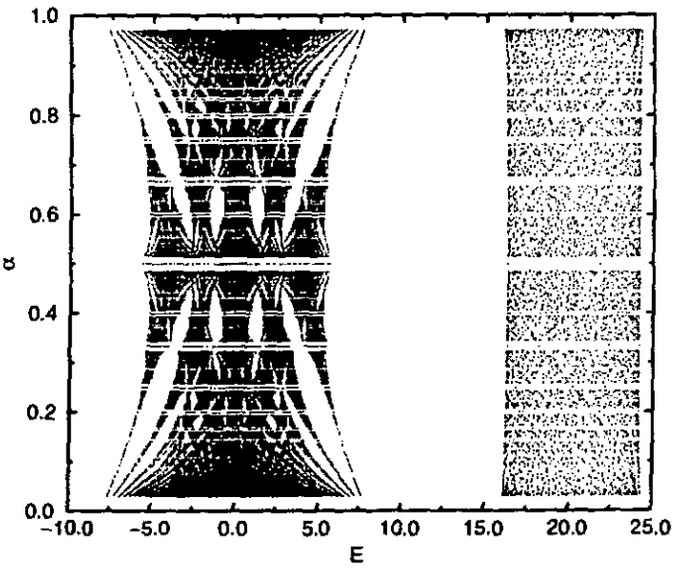

FIG. 8. Spectrum of the two-particle Harper model in the strongly interacting regime $U = 20$ up to $q = 23$.

In this section, we present an analytical approach that allows to understand completely the mechanism driving this evolution of the spectrum. Further details like the splitting of the Landau band $\nu_1 = 0, \nu_2 = 1$ will also be computed, even though the physics is there less transparent (see Fig. 7). We shall concentrate our semiclassical calculation near the band function maximum $k_c = (0, 0)$ corresponding to the energy $z \approx U + 4$ in the spectrum. The two-particle Hamiltonian can be expressed in the following way :

$$\begin{aligned} H_{\mathrm{TIP}} &= \textstyle\sum_{m,n} [2\cos(\gamma m + \beta) + 2\cos(\gamma n + \beta)] \\ &|m \otimes n\rangle\langle m \otimes n| + U \textstyle\sum_m |m \otimes m\rangle\langle m \otimes m| \\ &+ \textstyle\sum_{m \neq n} |m \otimes n\rangle [\langle (m \otimes n + 1| + \langle (m \otimes n - 1| \\ &+ \langle (m + 1 \otimes n| + \langle (m - 1 \otimes n|] \end{aligned} \tag{36}$$

The strategy is based on the so-called Schur complement formula. Our Hamiltonian H_{TIP} is a self-adjoint operator acting on a Hilbert space that can be decomposed as $\mathcal{H} = \mathcal{P} \oplus \mathcal{Q}$. Let P and Q be the orthogonal projections on each subspace of that decomposition, namely :

$$P = \textstyle\sum_m |m \otimes m\rangle\langle m \otimes m|$$

$$Q = \mathbf{I} - P = \textstyle\sum_{m \neq n} |m \otimes n\rangle\langle m \otimes n|$$

In other words, P is the eigenprojection on pair states and Q is its orthogonal. If z is an eigenvalue of H_{TIP} and does not belong to the spectrum of $QH_{\mathrm{TIP}}Q$ then it is also an eigenvalue of the following effective Hamiltonian

$$H^{\mathrm{eff}}_{\mathrm{TIP}}(z) = PH_{\mathrm{TIP}}P + PH_{\mathrm{TIP}}Q\frac{1}{z - QH_{\mathrm{TIP}}Q}QH_{\mathrm{TIP}}P \tag{37}$$

When U is large the dominant term in the effective Hamiltonian given by the Schur complement formula (37) corresponds to the pair states. The semiclassical approach we introduced in section 2 remains valid so that $H^{\rm eff}_{\rm TIP}(z) = H^{\rm eff}_{\rm TIP}(z_0 + \gamma z_1 + \gamma^2 z_2 + O(\gamma^3))$. The implicit equation to be solved is then :

$$H^{\rm eff}_{\rm TIP}(z) = z_0 + \gamma z_1 + \gamma^2 z_2 + O(\gamma^3) \tag{38}$$

with

$$H^{\rm eff}_{\rm TIP}(z) = H^{(0)}_{\rm TIP}(z) + \gamma H^{(1)}_{\rm TIP}(z) + \gamma^2 H^{(2)}_{\rm TIP}(z) + O(\gamma^3) \tag{39}$$

The expansion of the dominant term reads :

$$\begin{aligned} PH_{\rm TIP}P &= U + 4\cos(\sqrt{\gamma}K_2) = U + 4 - 2\gamma K_2^2 \\ &+ \frac{\gamma^2}{6}K_2^4 + O(\gamma^3) \end{aligned} \tag{40}$$

and if we consider U large, z is large too so that :

$$\begin{aligned} \frac{1}{z - QH_{\rm TIP}Q} &= \frac{1}{z} + \frac{QH_{\rm TIP}Q}{z^2} + \frac{QH_{\rm TIP}QQH_{\rm TIP}Q}{z^3} \\ &+ O\left(z^{-4}\right) \end{aligned} \tag{41}$$

Expressing the different contributions in Schur's formula and expanding in powers of γ lead to :

$$\begin{aligned} H^{(0)}_{\rm TIP}(z) &= 4 + U + \frac{8}{z} + \frac{32}{z^2} + \frac{176}{z^3} + O\left(z^{-4}\right) \\ H^{(1)}_{\rm TIP}(z) &= \frac{-2(z^3+8z+64)}{z^3}\left[K_2^2 + \frac{z^2+4z+34}{z^3+8z+64}K_1^2\right] \\ H^{(2)}_{\rm TIP}(z) &= \frac{z^3+8z+256}{z^3}\left[K_2^4 + \frac{z^2+4z+70}{z^3+8z+256}K_1^4\right] \\ &+ 2\frac{z+8}{z^3}\left(K_1^2K_2^2 + K_2^2K_1^2\right) - 8\frac{z+8}{z^3} \\ &+ 16\frac{(z+8)^2}{z^3(z^3+8z+64)}\left(K_1^2 + K_2^2\right) \end{aligned} \tag{42}$$

Finally, we have to solve (38) to get the coefficients z_0, z_1 and z_2. The corresponding equations for those coefficients are at most of degree four. We shall give here the equation that z_0 has to satisfy at the order $O\left(z^{-4}\right)$

$$4 + U + \frac{8}{z_0} + \frac{32}{z_0^2} + \frac{176}{z_0^3} = z_0 \tag{43}$$

In a very similar way used for the computation of z_0, the analytical expressions of z_1 and z_2 can be derived from (38), (42) and (43). The good agreement with the exact numerical spectrum can be seen on Fig. 9 for $U = 50$. Here the numerical values for the sublevels are : for $\nu_{1,2} = 0$, $z(\gamma) = 54.1597 - 0.2826\gamma + 0.0356\gamma^2$, for $\nu_{1,2} = (0,1)$, $z(\gamma) = 54.1597 - 0.8480\gamma + 0.2084\gamma^2$, for $\nu_{1,2} = (1,1)$, $z(\gamma) = 54.1597 - 1.4133\gamma + 0.5539\gamma^2$. A similar computation can be done near the band function minimum $k_c = (\pi, \pi)$ corresponding to the energy $z \approx U - 4$.

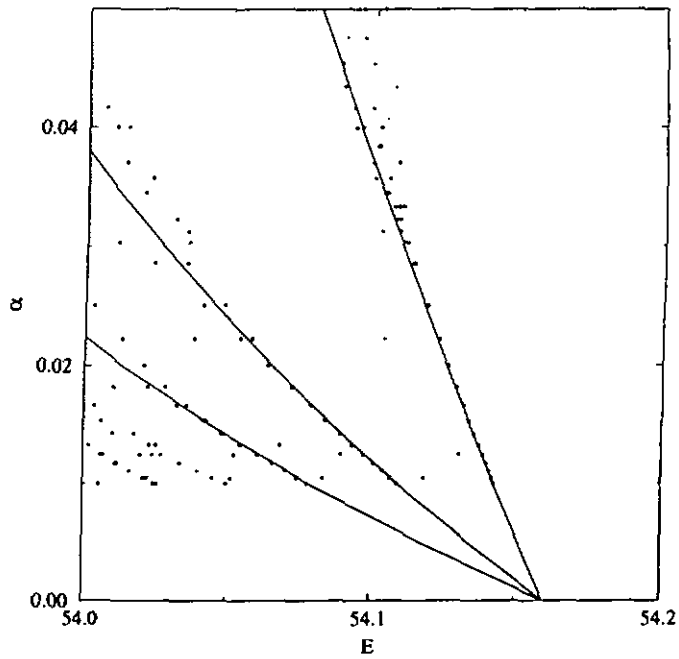

FIG. 9. Comparison between semiclassical calculations (full curves, see text) and exact numerical spectrum (points) for levels in the two-particle Harper model for $U = 50$.

The structure of the pair states for $U \gg 1$ can be understood in the following way : the diagonal term corresponding to the energy of particles located on the same site is $4\lambda\cos(\gamma n + \beta) + U$. The transition amplitude on the diagonal $n_{1,2} = n$ is given by the amplitude of the hopping via virtual states with $n_1 - n_2 = \pm 1$ and energy denominator $1/U$. There are two such paths so that the effective amplitude is $V_{\rm eff} = 2/U$. The same expression can be derived by the Schur formalism (see Sec. IV). After dividing the Hamiltonian by $V_{\rm eff}$ we arrive to the eigenfunctions equation in the form of Harper (14) with λ replaced by $\lambda_{\rm eff} = U \gg 1$. Since $\lambda_{\rm eff} \gg 1$ when $U \gg 1$, the pair states are always within the localized phase of the Harper equation showing exponential localization. In Fig. 10, we show a typical eigenstate of the Mathieu part of the spectrum for $U = 50$ and $\gamma/2\pi = 34/55$. The fact that it is localized confirms the pure-point character of the corresponding spectrum.

Above we showed that in the case of strong interaction, we have $\lambda_{\rm eff} \gg 1$. This explains the appearance of a pure-point component in the spectrum. However, we think that this pure-point component will even appear for small values of the interaction. Our argument is the following : without interaction, the system obeys Aubry's

duality while the presence of the interaction introduces Aubry's duality breaking. Indeed, from (18) it is easy to see that the interaction acts in the coordinate space and the symmetry with momentum space disappears when $U \neq 0$. Formally, this argument is not sufficient to prove the existence of pure-point spectrum at arbitrary small U. However the ensemble of numerical datas we have here and in[22,21] confirms this conjecture.

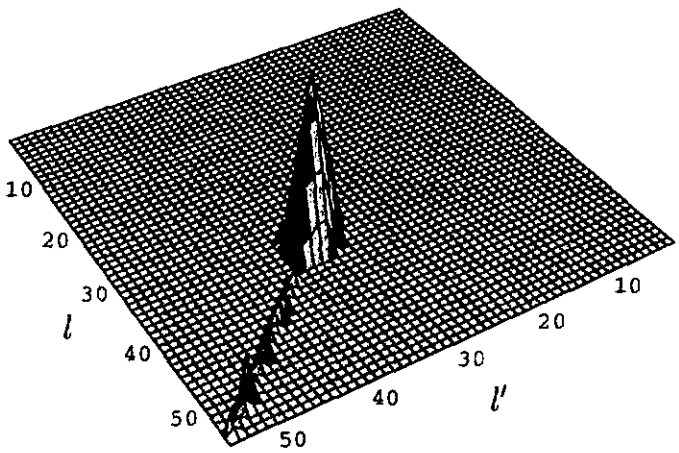

FIG. 10. Semilogplot of $W = |\phi(l,l')|^2$ for a localized state (E=50.25,$-30 \leq \ln W \leq -1$).

When U is large, the unshifted part of the spectrum looks very much like the spectrum at $U = 0$. The main difference can be found by looking carefully at the Landau levels (see Fig. 11). The reminiscence of the existence of the interaction is seen through the appearance of a splitting of Landau sublevels. This splitting only exists when Landau quantum numbers are different $\nu_1 \neq \nu_2$ and the two particles are located in the same well. Such a behaviour is illustrated by Fig. 11. The other sublevels are described by the semiclassical formulae obtained in the case $U = 0$ (25). To derive this splitting using semiclassical analysis, we again apply the Schur complement formula. Dealing with the unshifted butterfly leads us to consider as the dominant term $QH_{\rm TIP}Q$ such that (37) becomes :

$$H^{\rm eff}_{\rm TIP}(z) = QH_{\rm TIP}Q + QH_{\rm TIP}P\frac{1}{z - PH_{\rm TIP}P}PH_{\rm TIP}Q \tag{44}$$

Applying the same scheme as before produces an additional shift from the unperturbed energy given in first order in γ by :

$$|\delta E(\gamma)| = 4\frac{\gamma}{U+4} \tag{45}$$

This shift is valid for the second Landau sublevel ($\nu_1 = 0, \nu_2 = 1$), its accuracy is shown in Fig. 11 and the two splitted subbands are given by : $E(\gamma) = 8 - 4.1666\gamma$ and $E(\gamma) = 8 - 4\gamma$ up to order 1 in γ.

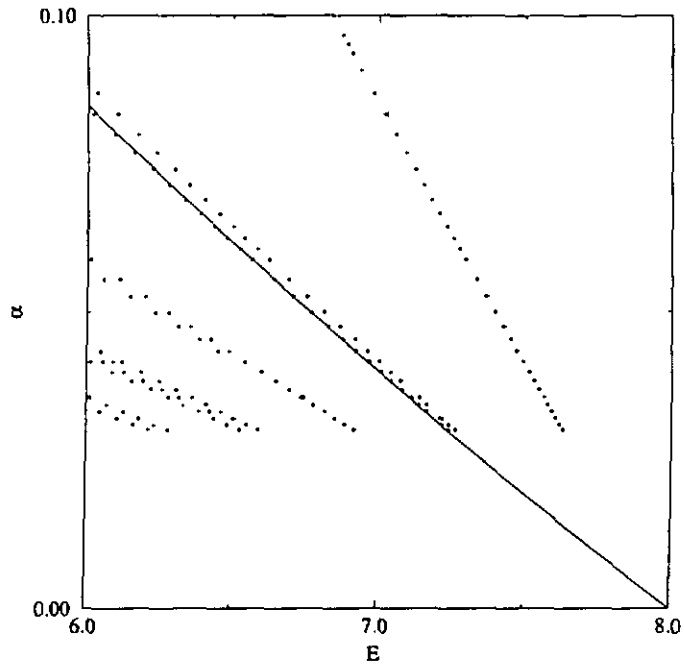

FIG. 11. Semiclassical calculations (full curve) and exact numerical spectrum (points) for the splitting of the $\nu_1 = 0, \nu_2 = 1$ Landau sublevel in the two-particle Harper model for $U = 20$.

V. TWO INTERACTING PARTICLES ON A TWO-DIMENSIONAL LATTICE

Even though the studied model was derived from a model of two-dimensional electrons, its effective dimension is 1 : as we already pointed out, (18) was derived assuming that the particle propagate as plane-wave in one direction. This assumption, though reasonable in the one-particle model, could be violated by interaction induced quantum interferences in the two-particle one. Therefore the question of the survival of interaction induced localization effect for two interacting particles in two dimensions remains an open problem. In this section we would like to discuss briefly this situation. For two interacting particles moving on a two-dimensional square lattice submitted to a uniform magnetic flux, the eigenvalue equation writes :

$$\begin{aligned} &e^{i\gamma y_1}\psi_{x_1+1,y_1,x_2,y_2} + e^{-i\gamma y_1}\psi_{x_1-1,y_1,x_2,y_2} \\ &\quad + \psi_{x_1,y_1+1,x_2,y_2} + \psi_{x_1,y_1-1,x_2,y_2} \\ &+ e^{i\gamma y_2}\psi_{x_1,y_1,x_2+1,y_2} + e^{-i\gamma y_2}\psi_{x_1,y_1,x_2-1,y_2} \\ &\quad + \psi_{x_1,y_1,x_2,y_2+1} + \psi_{x_1,y_1,x_2,y_2-1} \\ &+ \tilde{U}\delta_{x_1,x_2}\delta_{y_1,y_2}\psi_{x_1,y_1,x_2,y_2} = E\psi_{x_1,y_1,x_2,y_2} \end{aligned} \tag{46}$$

where $(x_{1,2}; y_{1,2})$ are integers denoting the positions on the square lattice and $\tilde{U}$ is the on-site interparticle interaction. For $\tilde{U} = 0$, the previous equation can be reduced to the one-dimensional Harper equation we dis-

cussed above (18). With interaction, the same equation (18) can be obtained in the ansatz of plane waves propagating in one direction with renormalized interaction U[22]. While this plane wave approximation is a standard approach for the one-particle Harper problem, it has to be handled with care in the interacting case. Indeed this plane wave ansatz breaks the symmetry of the original problem (46). This symmetry can be seen in the limit of strong interaction $U \gg 1$. In this case, there should be two energy bands : one corresponding to the pair states when particles are located on the same site with energy $E \approx U$ and the other with $E \approx 1$ for the states in which the two particles avoid each other. In the higher energy band, the eigenvalue equation for the pair states up to the terms of order $1/U$ has the form :

$$\frac{2}{U}\left(e^{2i\gamma y}\phi_{x+1,y} + e^{-2i\gamma y}\phi_{x-1,y} + \phi_{x,y+1} + \phi_{x,y-1}\right) + U\phi_{x,y} = E\phi_{x,y} \quad (47)$$

Here the term $2/U$ represents the transition amplitude for pair states. Its derivation is similar to the case of two interacting particles in the one-dimensional Harper model. Indeed if one keeps $x_1 = x_2$ then the hopping term is given by $V_{\text{eff}} = 2/U$ because there are two paths with virtual energy U $(y_{1,2} \to y_{1,2} + 1)$ which contribute to the hopping term in the y- direction. Similarly the hopping in the x-direction is $V_{\text{eff}} = 2e^{\pm 2i\gamma}/U$.

This representation shows that the symmetry between the two directions or the Aubry duality is not broken by the interaction. The main reason is that the symmetry of the interaction is invariant under rotations on the square lattice. In the limit of large U, this property can be seen through equation (47). However the symmetry (Aubry's duality) should also be preserved for small interaction. Due to that, we expect that similarly to the Harper model with $\lambda = 1$, the interaction will not generate pure-point component in the spectrum. However this conjecture has to be directly checked in further analytical and numerical studies.

VI. CONCLUSIONS

In this paper we have emphasized a localizing effect due to the combined action of an on-site interaction and a quasiperiodic potential. Unlike in the random potential case[20], extended unperturbed states are localized by the interaction, and this localization occurs at arbitrarily small attractive/repulsive interaction. We successfully identified the mechanism responsible for this effect as a decoupling of a Mathieu-like model from the original two-particle Harper model in the limit of large interaction. Our conjecture is that a similar mechanism will also work for small U due to an interaction induced breaking of Aubry's duality. This breaking happens in one-dimensional incommensurate models, however in two-dimensional magnetic models, we expect that the interaction will not break the duality and that a pure-point component in the spectrum will not arise. Further verifications of these conjectures are required.

This work has been supported in part by the Fonds National Suisse de la Recherche. One of us (A.B.) wants to thank the Institut de Physique Neuchâtel (Switzerland) for its hospitality.

---

[b] Also Budker Institute of Nuclear Physics, 630090 Novosibirsk, Russia.
[1] L.D. Landau, Z. für Phys. **64**, 629 (1930).
[2] R.E. Peierls, Z. für Phys. **80**, 763 (1933).
[3] W.J. de Haas, P.M. van Alphen, Communications from the Physical Laboratory of the University of Leiden **208d** (1930).
[4] P.G. Harper, Proc. Phys. Soc. Lond. A **68**, 874 (1955); ibid 879.
[5] D.R. Hofstadter, Phys. Rev. B **14**, 2239 (1976).
[6] B. Pannetier, J. Chaussy, R. Rammal, J.-C. Villegier, Phys. Rev. Lett. **53**, 1845 (1984).
[7] B. Pannetier, J. Chaussy, R. Rammal, Phys. Scr. **13**, 245 (1986).
[8] M. Kohmoto, L. Kadanoff, C. Tang, Phys. Rev. Lett. **50**, 1870 (1983).
[9] Y.H. Chen, F. Wilczek, E. Witten, B.f. Halperin, Int. J. Mod. Phys. B **3**, 1001 (1989).
[10] R. Rammal, J. Bellissard, Europhys. Lett. **13**, 205 (1990).
[11] J. Bellissard, in *Operator Algebras and Application*, Vol. 2, D.E. Evans & M. Takesaki Eds., Cambridge University Press (1988).
[12] M. Wilkinson, Proc. Roy. Soc. Lond. A **391**, 305 (1984).
[13] B. Helffer, J. Sjöstrand, Supplément au Bulletin de la Société Mathématique de France, Tome 116, Fasc. 4, Mémoire 34 (1988).
[14] R. Rammal, J. Bellissard, J. Phys. France **51**, 1803 (1990).
[15] A. Barelli, R. Fleckinger, Phys. Rev. B **46**, 11559 (1992).
[16] J. Bellissard, C. Kreft, R. Seiler, J. Phys. A **24**, 2329 (1991).
[17] S. Aubry, G. André, Ann. Isr. Phys. Soc. **3**, 133 (1979).
[18] T. Geisel, R. Ketzmerick and G. Petschel, Phys. Rev. Lett. **66**, 1651 (1991); *ibid* **67**, 3635 (1991); *ibid* **69**, 695 (1992).
[19] M. Wilkinson, E.J. Austin, Phys. Rev. B **50**, 1420 (1994).
[20] D.L.Shepelyansky, Phys. Rev. Lett. **73**, 2607 (1994); Y.Imry, Europhys. Lett. **30**, 405 (1995).
[21] A. Barelli, J. Bellissard, P. Jacquod, D.L. Shepelyansky, cond-mat 9609135 (1996).
[22] D.L. Shepelyansky, to appear in Phys. Rev. B (1996).
[23] J. Bellissard, R. Lima, D. Testard, Commun. Math. Phys. **88**, 207 (1983); Ya.G. Sinai, J. Stat. Phys. **46**, 861 (1987); V. Chulaevsky, Ya.G. Sinai, Commun. Math. Phys. **125**, 91 (1989); J. Fröhlich, T. Spencer, P. Wittwer, Commun. Math. Phys. **132**, 5 (1990).
[24] W. Chojnacki, Commun. Math. Phys. **143**, 527 (1992).

Remerciements

Je tiens à remercier particulièrement les personnes suivantes sans l'aide desquelles la tâche d'écrire cette thèse aurait été bien plus ardue.

Michel Droz grâce à qui l'enseignement de la physique dans les collèges valaisans se passera de moi quelques années encore...

Jean-Pierre Amiet qui fut un directeur de thèse des plus disponibles tout en me laissant une liberté d'action et de mouvement des plus agréables...

Armelle Barelli grâce à qui mes contacts avec la "ville rose" se sont noués...

Dima Shepelyansky qui a essayé de faire de moi un pur produit de l'école russe ! J'espère qu'il y est parvenu au moins partiellement...

Jean Bellissard pour sa recette du foie gras poëlé et ses théories du matin au cours desquelles la physique du vingtième siècle était décortiquée...

Markus Büttiker et Jean-Pierre Derendinger pour avoir accepté de figurer dans mon jury de thèse...

Hans Beck, troisième professeur de physique théorique à l'institut de Neuchâtel, dont la voix de stentor m'a tiré plus d'une fois d'un sommeil coupable...

Philippe "Ce Bon Monsieur" Page sans qui j'ignorerais toujours que Marat est né à Boudry...

Peter Bamert chef organisateur des rencontres de Lauenen...

Claudio Lucchesi qui m'aura donné l'occasion de délassements intellectuels à de nombreuses reprises...

Raymond Frésard pour son introduction à la transition de Mott-Hubbard, sa lecture attentive de l'introduction au chapitre deux de cette thèse et son optimisme communicatif...

Christophe Rouvinez pour m'avoir mis sur une bonne piste à plus d'une reprise...

Tous mes collègues tant à Neuchâtel qu'à Toulouse et qui ont souhaité garder l'anonymat pour des raisons bien compréhensibles...

Mes parents pour m'avoir forcé à faire ce que j'avais envie de faire...

Mireille enfin qui n'aura bien souvent eu qu'à subir le contrecoup du stress engendré par l'écriture de cette thèse.

Qu'ils reçoivent tous ici l'expression de ma gratitude.